

INVESTIGATION OF "HIDDEN" POLISHING  
PARAMETERS IN MAGNETIC FLOAT POLISHING  
(MFP) OF SILICON NITRIDE ( $\text{Si}_3\text{N}_4$ ) BALLS

By

KOK-LOONG LEE

Bachelor of Science

Oklahoma State University

Stillwater, Oklahoma

2000

Submitted to the Faculty of the  
Graduate College of the  
Oklahoma State University  
in partial fulfillment of  
the requirements for  
the Degree of  
MASTER OF SCIENCE  
May, 2005

INVESTIGATION OF “HIDDEN” POLISHING  
PARAMETERS IN MAGNETIC FLOAT POLISHING  
(MFP) OF SILICON NITRIDE (Si<sub>3</sub>N<sub>4</sub>) BALLS

Thesis Approved:

Dr. Ranga Komanduri

---

Thesis Advisor

Dr. HongBing Lu

---

Dr. C. E. Price

---

Dr. A. Gordon Emslie

---

Dean of the Graduate Collage

## SUMMARY

Over the past decade, Magnetic Float Polishing (MFP), a batch polishing process, had been successfully used for finishing small batches of Grade 10C silicon nitride ( $\text{Si}_3\text{N}_4$ ) balls for hybrid bearing applications. This was done in combination with (1) the concept of MFP, (2) the studies of polishing parameters, and (3) the methodology of MFP. However, it was not proof to finish a larger batch of Grade 10C  $\text{Si}_3\text{N}_4$  balls (46 balls of  $\frac{3}{4}$  in. diameter) by this process to specifications, especially the roundness of the balls. In order to improve the roundness of balls, a groove was formed on the bevel of the polishing cup during polishing was required. Subsequently, it was required to machine the groove in order to improve the surface finish. Hence, there are additional polishing parameters, the so-called, “hidden polishing parameters” that play an important role in MFP process, but have not been investigated. This is accomplished in this thesis by a purposely designed polishing set-up, namely, “Critical Polishing Condition.”

The first objective of this thesis is to identify the hidden polishing parameters of MFP process through “Critical Polishing Condition” polishing set-up. The second objective of this thesis was to reduce the total consumption of

expensive magnetic fluid. The final objective of this thesis is to recover the used abrasives for recycling or to re-sell for other applications.

The original small batch polishing apparatus (inside chamber of 2 in. diameter) was not suitable for the purpose of this investigation, to reveal and investigate the hidden polishing parameters of MFP process. Hence, a new aluminum polishing chamber (inside chamber of 4 in. diameter) was built. Another new stainless steel polishing cup (3 in. outside diameter and 0.5 in wall thickness) was made. A batch of larger  $\text{Si}_3\text{N}_4$  balls (10 balls of 0.9 in. diameter) was chosen in this investigation to create the polishing set-up of “Critical Polishing Condition”, with the newly made polishing chamber and polishing cup. Of course, a larger permanent magnet base (55 pieces of rectangular magnets: 0.45 x 0.45 x 1 in.) was needed to compensate the larger polishing chamber.

Consider the MFP apparatus set-up as a commercial ball bearing and you are the ball bearings manufacturer. Will the design and fabrication (if possible) a ball bearing that consists of 10  $\text{Si}_3\text{N}_4$  balls of 0.9 in diameter with a 4 in. diameter of the outer sleeve and a 2 in. diameter of the inner ring? The answer is definitely “No”. This is because the balls inside the bearing would not roll and rotate properly. This means the “Critical Polishing Condition” polishing set-up is not the optimum polishing condition for MFP process.

Surprisingly, this “Critical Polishing Condition” set-up successfully revealed and studied the roles and effects of the hidden polishing parameters in the MFP process. They are:

- 1) The groove formed on the bevel of the polishing cup during polishing
- 2) The magnetic fluid patterns formed during polishing
- 3) The gap/spacing among the balls
- 4) The uniformity of the as-received workmaterial ( $\text{Si}_3\text{N}_4$  balls)
- 5) The evaporation of magnetic fluid during polishing

Following are the results and discussions of the above hidden polishing parameters that were observed in this thesis.

At the roughing stage, a re-machined slope on the bevel of the polishing cup is used initially to improve the roundness and diameter of a batch of  $\text{Si}_3\text{N}_4$  balls (10 balls of 0.9 in. diameter) with initial average roundness of 26.59  $\mu\text{m}$ . The groove formed on the bevel of the polishing cup is removed after each polishing run. Poor average roundness of 1.43  $\mu\text{m}$  (0.78 – 2.72  $\mu\text{m}$ ) was found after four polishing runs (Run 1 – 4). On the other hand, the uniform geometry of the balls (0.9013 in. diameter) has already been obtained.

Then, a groove formed on the bevel of the polishing cup during polishing (in Run 4) was maintained and used in Run 5. An average roundness of 0.94  $\mu\text{m}$  (0.70 – 1.12  $\mu\text{m}$ ) was found and the uniform geometry of balls (0.8996 in. diameter) was also maintained. Hence, a proper formed groove on the bevel of the polishing cup during polishing plays an important role in improving the roundness of the balls.

Again, in Run 6, the groove formed on the bevel of the polishing cup during Run 5 was removed. Surprisingly, a slightly better average roundness of 0.86  $\mu\text{m}$  (0.63 – 1.15  $\mu\text{m}$ ) was found. From the previous observation, without a

groove or properly formed groove on the bevel of the polishing cup, poor average roundness would result. But, it is not. Hence, another important hidden polishing parameter of MFP process that is not easily revealed and studied by the ordinary MFP apparatus, was found.

With the understanding of the above hidden polishing parameters, a groove on the bevel of the polishing cup further improve the roundness of the balls. It is also believed that with or without a groove on the bevel of polishing cup no damage on the roundness of the balls occurs, as long as other polishing parameters (e.g. optimum polishing speed, load and time) and polishing set-up (e.g. the alignment of polishing apparatus) are maintained.

Another, helpful hidden polishing parameter which was found very useful and easy to apply in MFP process, is the magnetic fluid pattern formed during polishing (magnetic fluid pocket and magnetic fluid bubbles). The formation of a “magnetic fluid bubbles” pattern during polishing is a positive sign of the MFP process. It means an effective polishing run is taking place. Hence, the roundness of  $< 1 \mu\text{m}$  is guaranteed. The formation of “magnetic fluid pocket” pattern during polishing is a bad sign of the MFP process. It means an ineffective polishing run is taking place. Hence, it will damage the roundness of the balls.

A vibration monitoring system (Vibroport 41) was added to the newly built polishing chamber to clarify the “doubt”, why there were two different magnetic fluid patterns formed during polishing and only the “magnetic fluid bubbles” pattern would guarantee a better roundness of the balls. It was found that the “magnetic fluid bubbles” pattern generated low vibration amplitude at  $\sim 200 \text{ Hz}$

excitation frequency ( $0.06 \text{ m/s}^2$ ) and only one dominant frequency spectrum was observed. In contrast, the “magnetic fluid pocket” pattern generated higher vibration amplitude at  $\sim 200\text{Hz}$  excitation frequency ( $0.13 \text{ m/s}^2$ ). Hence, the low amplitude of the excitation frequency ( $\sim 200 \text{ Hz}$ ), which is an analogy to the vibrating behavior of a good commercial ball bearing, indicated the “magnetic fluid bubbles” pattern during MFP process is a good sign.

Uniform roundness of a single  $\text{Si}_3\text{N}_4$  ball proved difficult to obtain when the size of the balls is larger (0.9 in. diameter). A total of 3 measurements were taken per ball with each measurement  $90^\circ$  apart to give the average roundness of a single ball.

In order to achieve the uniform roundness of a single  $\text{Si}_3\text{N}_4$  ball of 0.9 in. diameter, a batch of  $\text{Si}_3\text{N}_4$  balls (8 balls of 0.9 in. diameter) instead of (10 balls of 0.9 in. diameter) was polished. This means the gap/spacing among the balls has increased. Thus, the balls can roll around the polishing chamber freely and rotate more efficiently. In this way, each ball was uniformly polished. The average roundness of a batch of 8  $\text{Si}_3\text{N}_4$  balls was improved to  $0.51 \mu\text{m}$  ( $0.45 - 0.60 \mu\text{m}$ ).

After identifying and studying those transient (hidden) polishing parameters of MFP process, they are ready to be implemented in the normal polishing apparatus or a larger new polishing apparatus.

Non-uniformity of the workmaterial ( $\text{Si}_3\text{N}_4$  balls) can affect the roundness and diameter of a single ball. The non-uniform workmaterial (only appear near the ball surface) is due to imperfections in the workmaterial and the consequence of the hot isostatically pressed (HIP) process. This non-uniform workmaterial

(Si<sub>3</sub>N<sub>4</sub> balls) can be effective polishing by MFP process through further reducing the diameter of the balls (if the final diameter is allowed).

In order to reduce the consumption of expensive magnetic fluid (water-based, W-40), a sealed-polishing was used to study the effect of MFP process. An 8-hour of a single polishing run was carried out with no sign of magnetic fluid “dry-out”. The loss of water through evaporation from the heated magnetic fluid during polishing would drop back to the chamber by condensation. However, the average roundness of the balls was adversely effect. Hence, this polishing condition is only suitable for the roughing stage where higher material removal rate is the only concern.

Finally, through revealing, investigating and understanding of the hidden polishing parameters in this thesis, the polishing mechanism of MFP process is apparent.



## **ACKNOWLEDGMENTS**

I would like to express my heartfelt thanks to my advisor, Dr. R. Komanduri, for his guidance, encouragement, advice, and valuable discussions throughout my master program. I would like to show my sincere appreciation to Dr. H. B. Lu and Dr. C. E. Price for serving on my graduate advisory committee.

This project has been supported by a grant (DMI-0000079) from the Manufacturing Processes and Machines Program of the Division of the Design, Manufacture, and Industrial Innovation (DMII) of the National Science Foundation. The author thanks Drs. W. Devries and G. Hazelriggs for their interest and support of this work.

Special thanks to Dr. N. Umehara, Dr. R. Makaram, Dr. Z. B. Hou, and Mr. A. Lakshmanan for their helpful advice, discussions, and visits. Thank is also due to Dr. M. Jiang for long distance discussions and suggestions. Friendly thanks to Mr. G. Robert, Mr. K. Tejas, Mr. T. Rishid, Mr. U. Anand, and Mr. R. V. Hariprasad for working together in an exciting and wonderful polishing research group. Thanks are also due to Mr. Dale Jerry, Mr. K. L. Choo, and Mr. R. Madhan for additional supports of this work.

I am indebted to my parents, Mr. K. C. Lee, Mrs. N. L. Chong, two brothers, Mr. K. S. Lee, Mr. K. W. Lee, and sister, Miss Y. N. Lee who were always encouraging me. Without them, I would have not come this far. Above

and beyond, I am genuinely thankful to my wife, Mrs. H. M. Soo, who has been always wonderfully encouraging and supporting me through out this work.

## TABLE OF CONTENTS

Chapter	Page
1. Introduction.....	1
1.1 Hot Isostatically Pressed Silicon Nitride ( $\text{Si}_3\text{N}_4$ ) balls.....	1
1.2 Magnetic Float Polishing (MFP) Process.....	8
1.3 Abrasives – Boron Carbide, Silicon Carbide, Cerium Oxide.....	11
1.4 Magnetic Fluid.....	16
2. Magnetic Float Polishing Literature Review.....	18
3. Problem Statement.....	36
4. Approach.....	38
4.1 Design of the “Critical Polishing Condition” MFP apparatus.....	38
4.2 Alignment of MFP apparatus.....	41
4.3 Six experimental approaches.....	45
4.4 List of the balls’ characterization instruments.....	52
5. Results and Discussions.....	53
5.1 First experimental approach: Reveal and study the roles of groove formed on the bevel of the polishing cup during MFP process.....	53

5.2	Second experimental approach: Clarify the formation of the two distinctive magnetic fluid patterns during MFP process.....	67
5.3	Third experimental approach: Reveal and study the roles of Gap/Spacing among the balls during MFP process.....	70
5.4	Fourth experimental approach: Found poor uniform roundness of a single Si <sub>3</sub> N <sub>4</sub> ball due to the non-uniform workmaterial.....	79
5.5	Fifth experimental approach: Reveal and study the roles and effects of the prevention of magnetic fluid during MFP process...	80
5.6	Sixth experimental approach: Reveal and study the beneficial of the after-polishing abrasives.....	83
6	Conclusions.....	84
7.	Future Work.....	88
	References.....	91

## LIST OF FIGURES

Figure		Page
Figure 1.1.1	Rolling elements of $\text{Si}_3\text{N}_4$ material.....	2
Figure 1.1.2	Silicon nitride of jets, nozzles and valves.....	3
Figure 1.1.3	$\text{Si}_3\text{N}_4$ cutting tool inserts.....	3
Figure 1.1.4	Schematic of solution-precipitation mechanism in HIP'ed $\text{Si}_3\text{N}_4$ material.....	4
Figure 1.1.5	TEM image of HIP'ed hexagonal $\beta$ - $\text{Si}_3\text{N}_4$ grains.....	5
Figure 1.1.6	SEM image of 3D view of "Rod-like" $\text{Si}_3\text{N}_4$ grains.....	5
Figure 1.1.7	SEM micrograph of $\text{Si}_3\text{N}_4$ grains.....	6
Figure 1.1.8	SEM micrograph of showing the elongated $\beta$ - $\text{Si}_3\text{N}_4$ grains (that resists or change the crack direction) were responsible for the high toughness of $\text{Si}_3\text{N}_4$ material.....	6
Figure 1.1.9	The commercial fabrication process of $\text{Si}_3\text{N}_4$ balls.....	7
Figure 1.1.10	Photograph of the as-received (semi-finishing) $\text{Si}_3\text{N}_4$ balls used in this investigation.....	7
Figure 1.2.1	Schematic of magnetic float polishing apparatus.....	8

Figure 1.2.2	Schematic view of magneto-hydrodynamic behavior of magnetic fluid.....	9
Figure 1.2.3	The schematic view of magneto-hydrodynamic behavior of magnetic fluid on non-magnetic abrasives.....	9
Figure 1.2.4	(a) The magnetic fluid profile (without the present of magnetic field), (b) the magnetic fluid profile (with the present of the permanent magnet base that used in this investigation), and (c) the non-magnetic abrasives, acrylic float and the $\text{Si}_3\text{N}_4$ balls are floated or elevated in the magnetic fluid by the magneto-hydrodynamic behavior of magnetic fluid (only the balls were shown).....	10
Figure 1.3.1	SEM micrographs of (a) $\text{B}_4\text{C}$ (500 grit) 500 and (b) $\text{SiC}$ (600 grit) abrasives, respectively.....	12
Figure 1.3.2	SEM micrographs of (a) $\text{B}_4\text{C}$ (1500 grit) and (b) $\text{SiC}$ (1200 grit) abrasives, respectively.....	13
Figure 1.3.3	SEM micrographs of $\text{SiC}$ (10,000 grit) abrasives.....	14
Figure 1.3.4	SEM micrographs of $\text{CeO}_2$ abrasives, (a) lower magnification (2000x) and (b) higher magnification (4000x)..	15
Figure 2.1	Diagram of the “Magnetic Fluid Grinding” apparatus.....	18
Figure 2.2	Schematic view of magnetic float polishing of $\text{Si}_3\text{N}_4$ balls.....	19
Figure 2.3	Variation of grinding loads with clearance showing the effective of the float .....	20

Figure 2.4	Variation of sphericity with grinding time showing improvement in sphericity using a float .....	20
Figure 2.5	Effect of polishing time against the stock removal.....	22
Figure 2.6	Effect of polishing load against the material removal rate.....	23
Figure 2.7	Effect of polishing speed against the material removal rate.....	23
Figure 2.8	Variation of material removal rate with abrasives grain size	24
Figure 2.9	Effect of abrasives concentration against the material removal rate.....	24
Figure 2.10	Schematic view of MFP model: (a) first model of MFP and (b) modified model of MFP.....	25
Figure 2.11	TalySurf 250 surface roughness profile of finished $\text{Si}_3\text{N}_4$ balls surface.....	30
Figure 2.12	SEM micrograph of finished $\text{Si}_3\text{N}_4$ balls surface.....	31
Figure 2.13	Roundness of $\text{Si}_3\text{N}_4$ balls: (a) as-received: 200 $\mu\text{m}$ and (b) final roundness: 0.15 $\mu\text{m}$ .....	31
Figure 2.14	Vibration monitoring system to the polishing chamber.....	32
Figure 2.15	Variation of frequency spectrum against the time and corresponding roundness of $\text{Si}_3\text{N}_4$ balls.....	33
Figure 2.16	Photograph of a self-aligned large batch polishing apparatus used to finish larger $\text{Si}_3\text{N}_4$ balls (46 balls of 3/4 in. diameter).	34

Figure 2.17	(a) Front view and (b) the side view of the self-alignment large batch polishing apparatus.....	35
Figure 4.1.1	(a) Newly built MFP chamber that purposely designed and developed for this investigation to reveal and study the roles and effects of the hidden polishing parameters, named, the “Critical Polishing Condition” chamber for finishing larger Si <sub>3</sub> N <sub>4</sub> balls (10 balls of 0.9 in. diameter). Instead, it was more suitable for finishing a batch of smaller Si <sub>3</sub> N <sub>4</sub> balls (20 balls of ½ in. diameter) as shown in (b).....	39
Figure 4.1.2	(a) Newly made polishing chamber with two accelerometers attached, (b) the polishing cup, (c) top-view and (d) front-view of the permanent magnets base.....	40
Figure 4.1.3	Overview of the MFP apparatus used in this thesis.....	40
Figure 4.2.1	Alignment system of MFP apparatus for the present study.....	42
Figure 4.2.2	(a) – (f) First alignment of the polishing apparatus.....	43
Figure 4.2.3	(a) – (d) Second alignment of the polishing apparatus.....	44
Figure 4.4.1	First experimental approach, used to reveal and study the roles and effects of the groove formed on the bevel of the polishing cup during polishing.....	46



Figure 4.4.2	Second experimental approach, used to clarify the magnetic fluid patterns formation that observed in the first experimental approach.....	47
Figure 4.4.3	Third experimental approach, used to further improve the average roundness of the Si <sub>3</sub> N <sub>4</sub> balls and the uniform roundness of a single ball, namely, the gap/spacing among the balls during MFP process.....	48
Figure 4.4.4	Fourth experimental approach, used to find the non-uniform roundness of a single non-uniform workmaterial (the Si <sub>3</sub> N <sub>4</sub> balls).....	49
Figure 4.4.5	Fifth experimental approach, used to study the possibility of saving or reduced the consumption of the expensive magnetic fluid in MFP process.....	50
Figure 4.4.6	Sixth experimental approach, used to study the possibility of recycling and used it as (1500 grit) abrasives or for other applications, in order to bring down the overall cost of MFP process.....	51
Figure 5.1.1	Average roundness improvement of a batch of Si <sub>3</sub> N <sub>4</sub> balls (10 balls of 0.9 in. diameter) after 4 polishing runs.....	54
Figure 5.1.2	Ball diameter reduction and shape improvement of a batch of Si <sub>3</sub> N <sub>4</sub> balls (10 balls of 0.9 in. diameter) after 4 polishing runs.....	55

Figure 5.1.3	Variation of average roundness for different balls with the groove (Run 5) and re-machined groove (Run 4) on the polishing cup .....	56
Figure 5.1.4	Variation of average roundness for different balls with the re-machined groove (Run 6) and groove (Run 5) on the polishing cup .....	57
Figure 5.1.5	(At roughing stage, Run 1 - 7) the average roundness of the balls was greatly improved with maintaining the groove throughout the runs.....	60
Figure 5.1.6	(At semi-finishing stage, Run 8 - 11) the average roundness of the balls was further improved with maintaining the groove throughout the runs.....	61
Figure 5.1.7	(a) – (c) TalyRond roundness profile of a single non-uniform workpiece ( $\text{Si}_3\text{N}_4$ ball) at three different axis measurements ( $90^\circ$ apart).....	63
Figure 5.1.8	MRR comparison between the groove formed on the bevel of the polishing cup and re-machined surface on the bevel on the polishing cup.....	64
Figure 5.1.9	(a) With the present of the groove formed on the bevel of the polishing cup, rougher surface finish of the balls was observed with SiC (10,000 grid), $R_a \sim 0.47 \mu\text{m}$ and $R_t \sim 0.3501 \mu\text{m}$ . (b) Without the groove, very smooth surface finish was found, $R_a \sim 97 \text{ nm}$ and $R_t \sim 739 \text{ nm}$ .....	66

Figure 5.2.1	Two different type of magnetic fluid patterns formation during polishing, namely, (a) “Magnetic Fluid Pocket” and (b) “Magnetic Fluid Bubbles” patterns.....	67
Figure 5.2.2	Average vibration amplitude of the “Magnetic Fluid Bubbles” pattern at ~ 200 Hz, excitation frequency, was ~ 0.06 m/s <sup>2</sup> .....	68
Figure 5.2.3	Average vibration amplitude of the “Magnetic Fluid Pocket” pattern at ~ 200 Hz, excitation frequency, was ~ 0.13 m/s <sup>2</sup> .....	69
Figure 5.3.1	Non-uniform roundness of a single Si <sub>3</sub> N <sub>4</sub> ball, Example 1 and Example 2.....	73
Figure 5.3.2	(a) Good gap/spacing among the balls, a batch of 8 Si <sub>3</sub> N <sub>4</sub> balls, and (b) Poor gap/spacing among the balls, a batch of 10 Si <sub>3</sub> N <sub>4</sub> balls.....	74
Figure 5.3.3	Low-amplitude vibration behavior of a “good gap/spacing among the balls” polishing run. The average amplitude was ~ 0.06 m/s <sup>2</sup> at ~ 200 Hz excitation frequency throughout the polishing run.....	74

Figure 5.3.4	Vibration behavior (at ~ 200 Hz excitation frequency) of a batch of a “poor gap/spacing among the balls” polishing run. (a) High amplitude (also means the formation of the “Magnetic Fluid Pocket” pattern) was observed, ~ 0.20 m/s <sup>2</sup> for the first 2 - 2½ hours of the run. (b) Low amplitude (also means the formation of the “Magnetic Fluid Bubbles” pattern) was observed, ~0.06 m/s <sup>2</sup> till the end of the run. (c) Gradually increased amplitude (~ 0.25 m/s <sup>2</sup> or higher) was observed, if the polishing run was not stopped before the magnetic fluid started drying-up.....	75
Figure 5.3.5	Poor roundness was observed; if the magnetic fluid was severely dry-out at the end of the run.....	76
Figure 5.3.6	(a) Poor uniform roundness of Si <sub>3</sub> N <sub>4</sub> balls, after Run 12 with 10 balls. (b) – (c) Good uniform roundness of Si <sub>3</sub> N <sub>4</sub> balls, after Run 13 and 14, respectively, with 8 balls.....	78
Figure 5.4.1	Two geometry measurements with micrometer were carried out on a non-uniform workmaterial.....	79
Figure 5.5.1	Photographs of sealed-polishing chamber.....	80
Figure 5.5.2	(a) – (b) Photographs showing evaporation and condensation of magnetic fluid during polishing. (c) A view at the end of a sealed-chamber polishing run.....	82
Figure 5.6.1	SEM images of: (a) After-polished 500 grit B <sub>4</sub> C abrasives and (b) fresh 1500 grit B <sub>4</sub> C abrasives.....	83

Figure 7.1.1 A simple modification and inexpensive design of cooling system to the newly built polishing chamber that used in this thesis..... 89

## LIST OF TABLES

<b>Tables</b>	<b>Page</b>
Table 1.1.1 Properties of Silicon Nitride.....	2
Table 1.1.2 Chemical composition of Si <sub>3</sub> N <sub>4</sub> balls.....	7
Table 1.3.1 Abrasives used in this investigation.....	11
Table 1.4.1 Characteristics of the water-base magnetic fluid (W-40)*.....	16
Table 2.1 Polishing result of finished ball and compare to the as-received ball.....	21
Table 2.2 Polishing results of Si <sub>3</sub> N <sub>4</sub> balls using MFP process by several researchers.....	26
Table 2.3 ASTM standard specification for Si <sub>3</sub> N <sub>4</sub> bearing ball, μm (μin.) for individual ball.....	27
Table 2.4 ASTM standard specification for Si <sub>3</sub> N <sub>4</sub> bearing ball, μm (μin.) for lots of balls.....	27

Table 2.5	Methodology of MFP process, which successfully finished a batch of $\text{Si}_3\text{N}_4$ balls that meet the ASTM standard specifications for $\text{Si}_3\text{N}_4$ bearing balls.....	29
Table 2.6	Surface finish of $\text{Si}_3\text{N}_4$ balls that finished using the methodology of MFP.....	30
Table 5.1	Details of the polishing conditions from Run 1 to Run 4 (prior each polishing run the groove formed on the bevel of the polishing cup was removed).....	54
Table 5.2	Detail of polishing conditions in Run 4 and 5.....	56
Table 5.3	Details of polishing conditions from Run 1 to 7.....	59
Table 5.4	Details of polishing conditions from Run 8 to 11.....	59
Table 5.5	Polishing conditions of Run A and B.....	65

# Chapter 1

## Introduction

### 1.1 Hot Isostatically Pressed Silicon Nitride ( $\text{Si}_3\text{N}_4$ ) balls

In late 1980s, silicon nitride ( $\text{Si}_3\text{N}_4$ ) received consideration attention as a potential material for structural applications, such as rolling elements for hybrid ceramic bearings (see Figure 1.1.1), jets, nozzles and valves (see Figure 1.1.2), cutting tools (see Figure 1.1.3), turbo-charger rotors, gas turbines, spark plugs, crucibles, and extrusion dies [Budinski and Budinski, 2002]. The  $\text{Si}_3\text{N}_4$  has many attractive properties, as listed below and shown in Table 1.1.1.

- High toughness (no loss of strength in air at high temperatures, 1800°C)
- High Hardness
- High wear-resistance
- High thermal conductivity
- High elastic modulus
- Excellent thermal shock resistance
- Low thermal expansion coefficient
- Low density (one-third of the weight of steel)
- Chemically resistant



Table 1.1.1 Properties of Silicon Nitride [Lee and Rainforth, 1994]

	<i>HPSN</i>
Theoretical density ( $\text{g cm}^{-3}$ )	3.2–3.9
Material density (% theoretical)	95–100
Hardness (GPa)	14–18
Fracture toughness $K_{Ic}$ ( $\text{MPa m}^{1/2}$ )	3.4–8.2
Thermal expansion coeff. 0–1000°C ( $10^{-6} \text{K}^{-1}$ )	2–3
Elastic modulus (GPa)	280–320
RT bend strength (MPa)	400–1000
Thermal conductivity at RT ( $\text{W m}^{-1} \text{K}^{-1}$ )	15–50



Figure 1.1.1 Rolling elements of  $\text{Si}_3\text{N}_4$  material [Lee and Rainforth, 1994]



Figure 1.1.2 Silicon nitride jets, nozzles and valves  
[<http://www.ceradyne.com>]

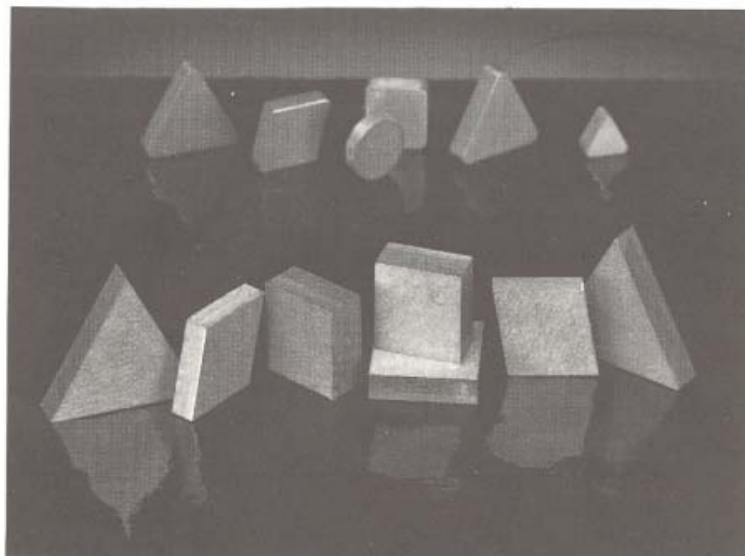
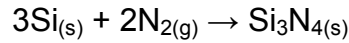


Figure 1.1.3 Si<sub>3</sub>N<sub>4</sub> cutting tool inserts [Lee and Rainforth, 1994]

The commercially available  $\text{Si}_3\text{N}_4$  powder (used for making  $\text{Si}_3\text{N}_4$  products) are produced by the reaction of silicon powder with nitrogen gas at 1250 to 1400°C (as shown below) and generally consists of a 90:10 mixture of  $\alpha$  -  $\text{Si}_3\text{N}_4$  and  $\beta$  -  $\text{Si}_3\text{N}_4$  phases [Lee and Rainforth, 1994].



As shown schematically in Figure 1.1.4  $\text{Si}_3\text{N}_4$  powder is densified by hot-pressing at a pressure of 15 – 30 MPa in graphite dies at 1550 – 1800°C for 1 – 4 hours under a nitrogen atmosphere, in order to prevent decomposition of the  $\text{Si}_3\text{N}_4$ . Figures 1.1.5 – 1.1.8 show the microstructures of  $\text{Si}_3\text{N}_4$ . Figure 1.1.9 shows the commercial fabrication process of  $\text{Si}_3\text{N}_4$  balls. Figure 1.1.10 and Table 1.2.1 show the initial condition and chemical composition of  $\text{Si}_3\text{N}_4$  balls (10 balls of 0.9 in. diameter) that is used in this investigation.

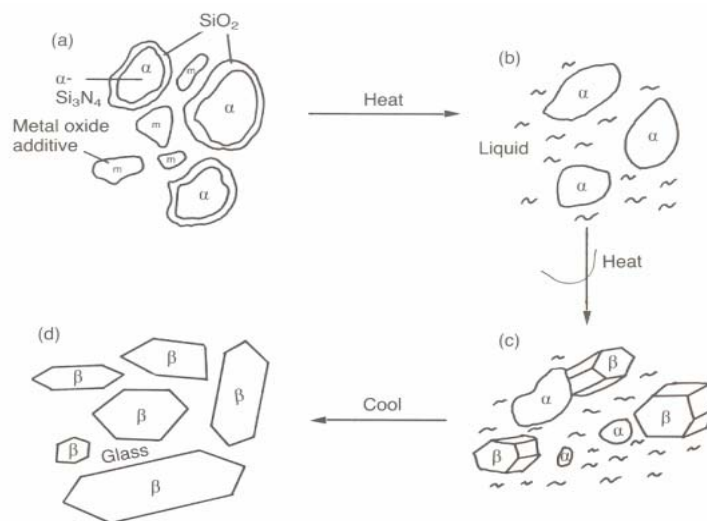


Figure 1.1.4 Schematic of solution-precipitation mechanism in HIP'ed  $\text{Si}_3\text{N}_4$  material. (a) The starting powders, with certain ratio of  $\alpha$  -  $\text{Si}_3\text{N}_4$  and  $\beta$  -  $\text{Si}_3\text{N}_4$  phases and metal oxide additive. (b) Silicate and metal oxide additives were melted. (c) At high temperature, precipitation of  $\beta$  -  $\text{Si}_3\text{N}_4$ . (d) After cooling, the final hexagonal  $\beta$  -  $\text{Si}_3\text{N}_4$  grains were formed within a glassy matrix. [Lee and Rainforth, 1994]

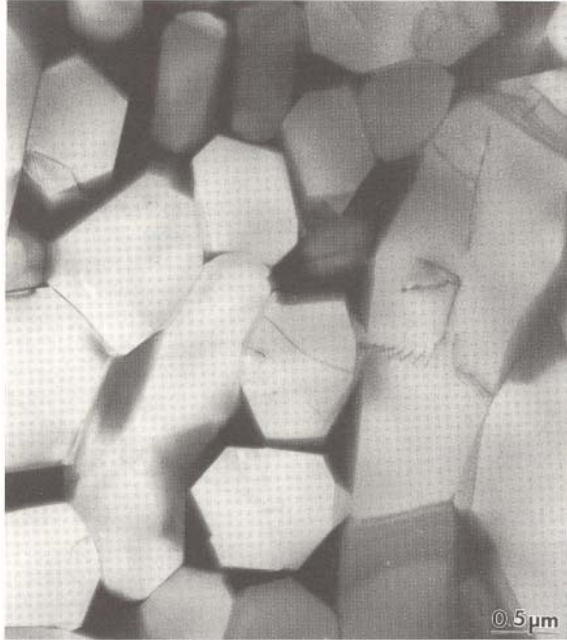


Figure 1.1.5 TEM image of HIP'ed hexagonal  $\beta$  -  $\text{Si}_3\text{N}_4$  grains [Lee and Rainforth, 1994]

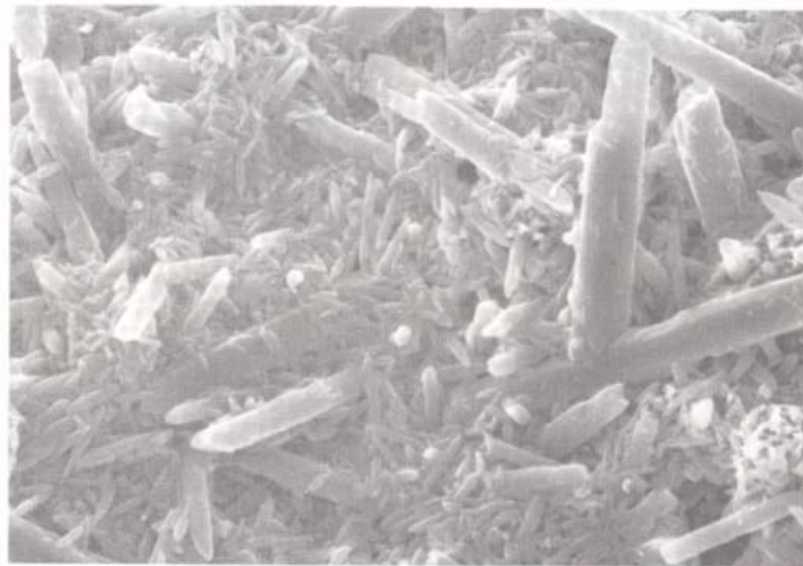


Figure 1.1.6 SEM image of 3D view of "Rod-like"  $\text{Si}_3\text{N}_4$  grains [Chiang et al., 1997]

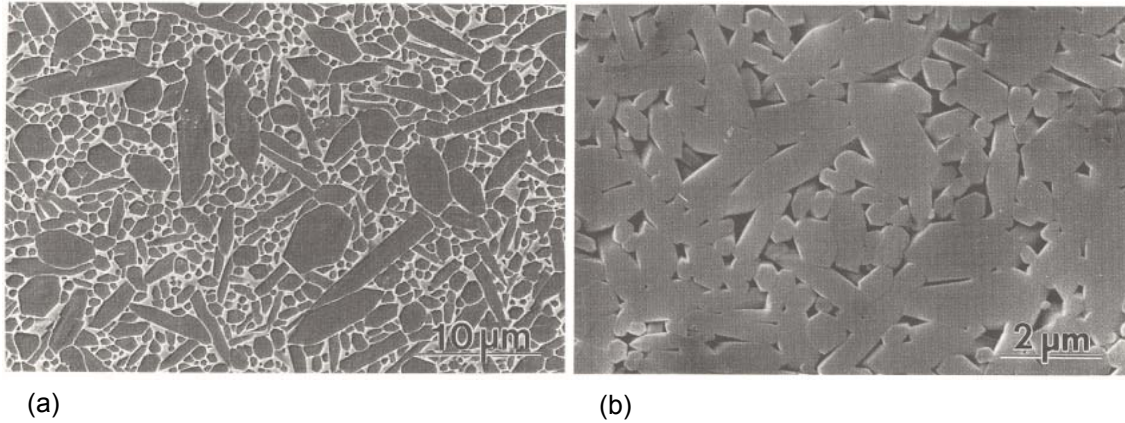


Figure 1.1.7 SEM micrographs of  $\text{Si}_3\text{N}_4$  grains: (a) after plasma-etching and (b) after etching the glassy grain boundaries [Lee and Rainforth, 1997]

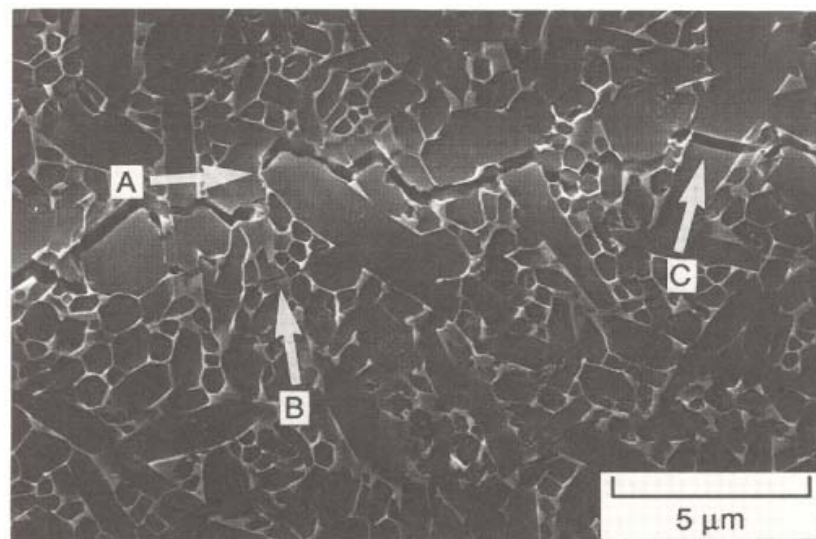


Figure 1.1.8 SEM micrograph showing the elongated  $\beta$  -  $\text{Si}_3\text{N}_4$  grains (that resist or change the crack direction) responsible for high toughness of  $\text{Si}_3\text{N}_4$  material [Lee and Rainforth, 1997]



Figure 1.1.9 (In general) Commercial fabrication process for producing Si<sub>3</sub>N<sub>4</sub> balls [<http://www.cerbec.com/>]



Figure 1.1.10 Photograph of the as-received (semi-finishing) Si<sub>3</sub>N<sub>4</sub> balls used in this investigation

Table 1.1.2 Chemical composition of Si<sub>3</sub>N<sub>4</sub> balls [Jiang, 1998]

Mg	Al	Ca	Fe	C	O	Si <sub>3</sub> N <sub>4</sub>
0.6 - 1.0	≤0.5	≤0.04	≤0.17	≤0.88	2.3 - 3.3	94.1 - 97.1

## 1.2 Magnetic Float Polishing (MFP) Process

During the past decade, Magnetic Float Polishing (MFP) technique (as shown in Figure 1.2.1) had been well-developed, fully-studied, and well-understood as an extremely effective batch polishing process for finishing silicon nitride ( $\text{Si}_3\text{N}_4$ ) balls.

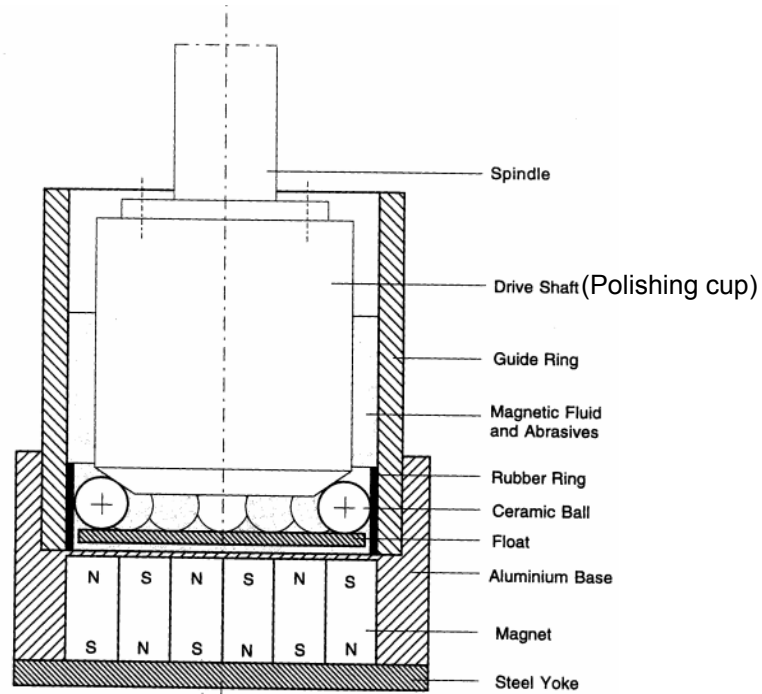


Figure 1.2.1 Schematic of the magnetic float polishing apparatus [Jiang, 1998]

This well-known MFP technique is based on the concept of magneto-hydrodynamic behavior of magnetic fluid, a stable colloidal suspension of extremely fine (100 to 150 Å) iron oxide particles, usually magnetite ( $\text{Fe}_3\text{O}_4$ ). Figures 1.2.2 and 1.2.3 show the magneto-hydrodynamic behavior of magnetic fluid after Umehara and Kato (1990). When a magnetic field (a block of permanent magnets) is placed in a container that is filled with magnetic fluid and

non-magnetic object, levitation is created when the fine iron particles attracted down toward the area of higher magnetic field (bottom of container) and an upward buoyant force is exerted on all the non-magnetic objects in the opposite direction.

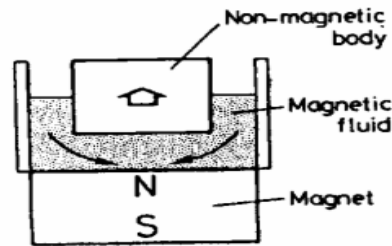


Figure 1.2.2 (In general) Schematic showing magneto-hydrodynamic behavior of magnetic fluid [Umehara and Kato, 1990]

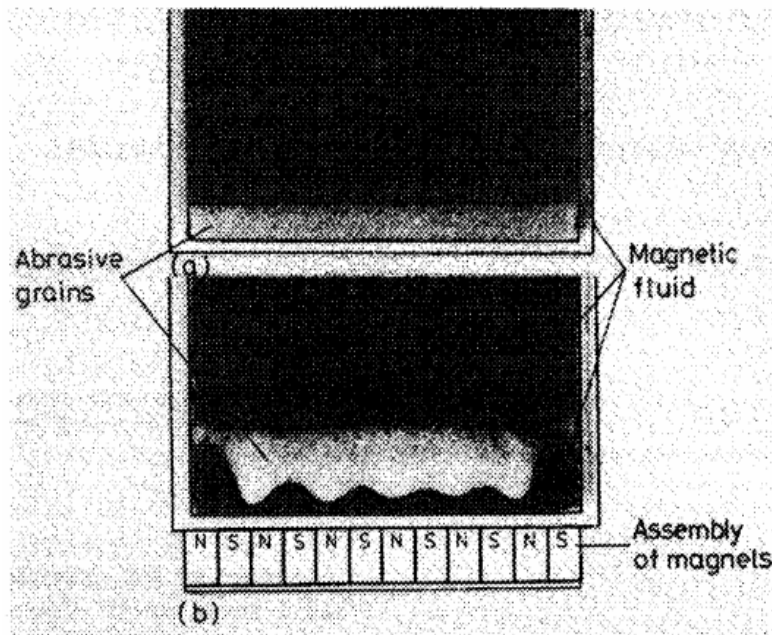


Figure 1.2.3 Schematic showing magneto-hydrodynamic behavior of magnetic fluid on non-magnetic abrasives. (a) Without the presence of magnets, the abrasives settle down to the bottom of the container. (b) With the presence of magnets, the abrasives are elevated from the bottom to a certain position of the container [Umehara and Kato, 1990]



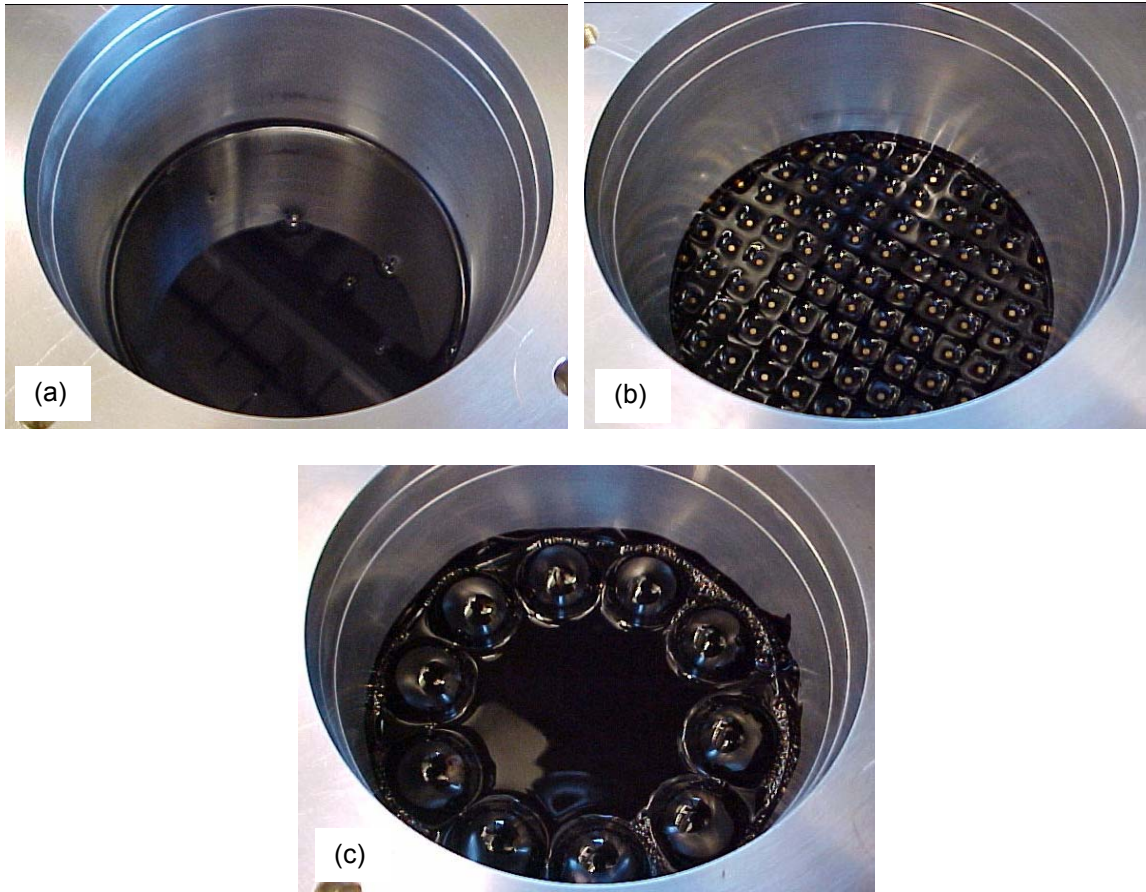


Figure 1.2.4 (a) The magnetic fluid profile (without the presence of magnetic field), (b) the magnetic fluid profile (in presence of a permanent magnet base), and (c) non-magnetic abrasives, acrylic float and Si<sub>3</sub>N<sub>4</sub> balls that are floated or elevated in the magnetic fluid by the magneto-hydrodynamic behavior of magnetic fluid (only the balls were shown).

Thus, in the MFP process, non-magnetic abrasives, acrylic float and Si<sub>3</sub>N<sub>4</sub> balls all float in the magnetic fluid, as shown in Figure 1.2.4. The drive shaft (also named polishing cup in this thesis) is fed down to apply the desired force (also named polishing load) on the balls. The balls are polishing by two-body abrasion under a three-point contact action, when the drive shaft rotates.

Low polishing loads (~ 1 N per ball), high polishing speeds (~ 2000 rpm), and commercially available abrasives, such as boron carbide ( $B_4C$ ), silicon carbide ( $SiC$ ), and cerium oxide ( $CeO_2$ ) are used. An actual polishing time of less than 24 hours is sufficiently to finish a batch of  $Si_3N_4$  balls from the as-received condition [Komanduri et al., 1999].

### 1.3 Abrasives – Boron Carbide, Silicon Carbide, Cerium Oxide

Figures 1.3.1 – 1.3.4 show the SEM micrograph of the abrasives, such as boron carbide ( $B_4C$ ), silicon carbide ( $SiC$ ), and cerium oxide ( $CeO_2$ ), that were used in this investigation. Their hardness values in Mohs and Knoop ( $kg/mm^2$ ) are listed in Table 1.3.1. Figures 1.3.1(a) and (b) show the coarser  $B_4C$  (500 grit) and  $SiC$  (600 grit) abrasives, respectively, which larger than ~ 10  $\mu m$ , and were used to obtain high material removal rate (MRR). Figures 1.3.2(a) and (b) show the finer  $B_4C$  (1500 grit) and  $SiC$  (1200 grit) abrasives, respectively, which are larger than ~ 5  $\mu m$ , and were used to obtain better roundness, surface finish, and control of MRR. Figure 1.3.3 shows extremely fine  $SiC$  (10,000 grit) abrasives, which are smaller than ~ 1  $\mu m$ , and to obtain good surface finish. Figure 1.3.4 show the  $CeO_2$  abrasive (larger than ~ 5  $\mu m$ ) to obtain superior finishing through, chemo-mechanical polishing effect.

Table 1.3.1 Abrasives used in this investigation [Jiang, 1998]

ABRASIVE	HARDNESS	
	Mohs	Knoop $kg/mm^2$
Diamond	10	7000
Boron Carbide ( $B_4C$ )	9.3	3200
Silicon Carbide ( $SiC$ )	9.2	2500
Cerium Oxide ( $CeO_2$ )	6	-

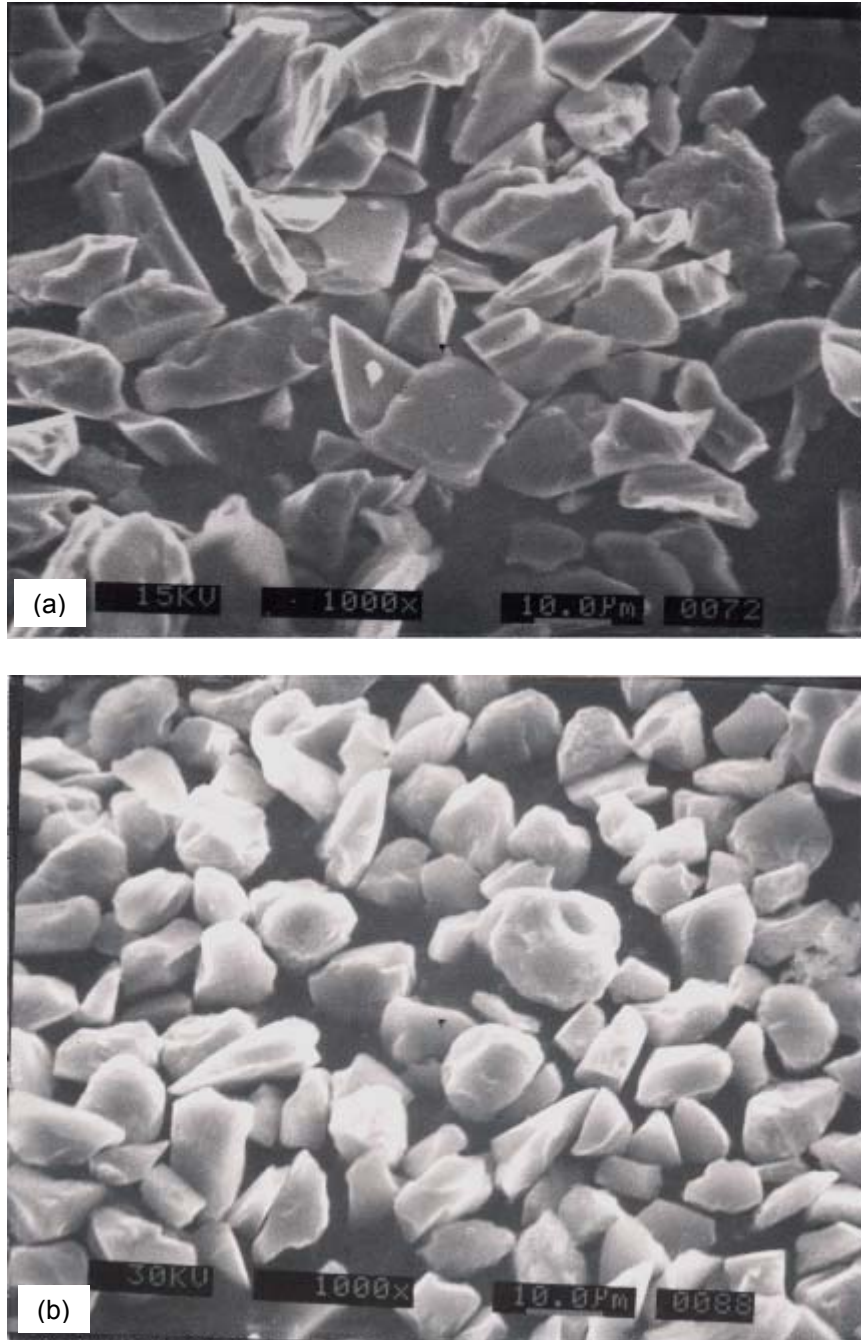


Figure 1.3.1 SEM micrographs of (a) B<sub>4</sub>C (500 grit) and (b) SiC (600 grit) abrasives, respectively.



Figure 1.3.2 SEM micrographs of (a) B<sub>4</sub>C (1500 grit) and (b) SiC (1200 grit) abrasives, respectively.

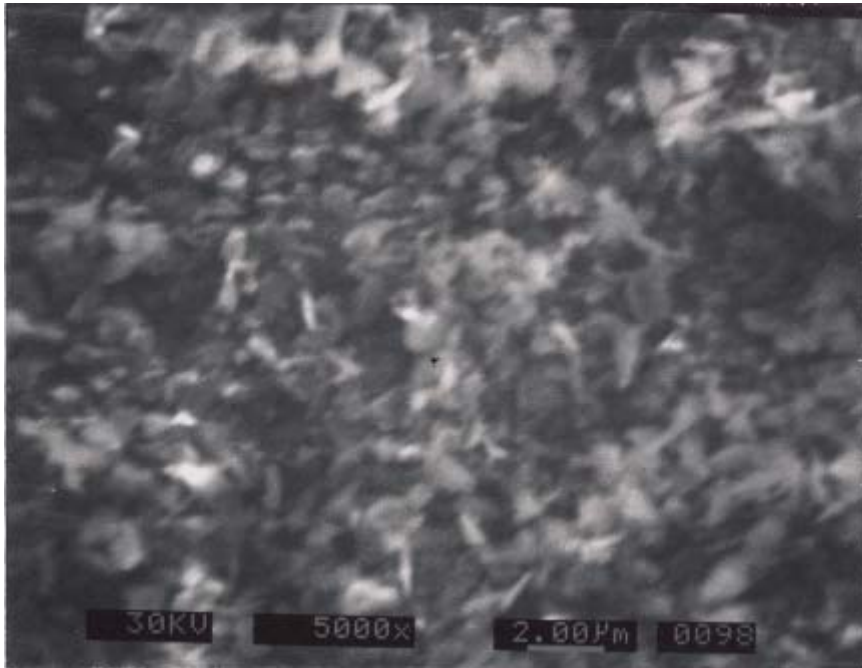


Figure 1.3.3 SEM micrographs of 10,000 grit SiC abrasive.

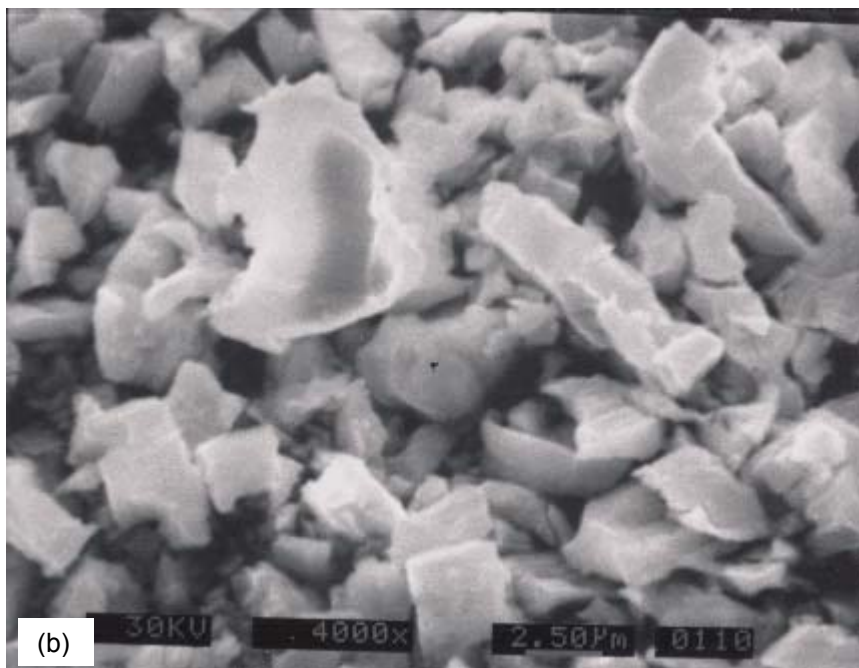
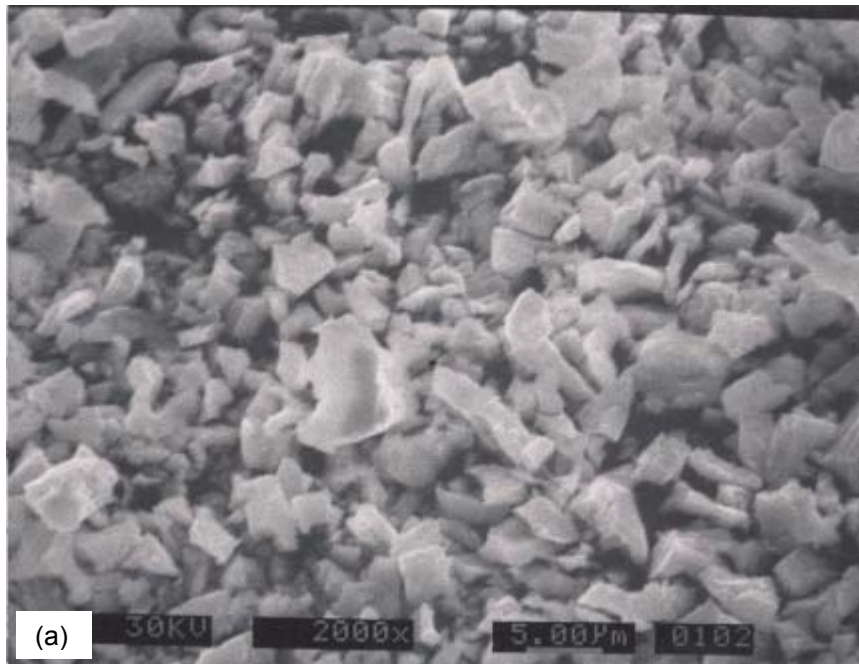


Figure 1.3.4 SEM micrographs of CeO<sub>2</sub> abrasives, (a) lower magnification (2000x) and (b) higher magnification (4000x).

## 1.4 Magnetic Fluid

The magnetic fluid is a stable colloidal suspension of extremely fine (100 to 150 Å) iron oxide particles, usually magnetite ( $\text{Fe}_3\text{O}_4$ ). Table 1.4.1 gives the characteristics of the water-base magnetic fluid (W-40) used in this investigation. The concept and manufacturing process of the magnetic fluid is described in [Rosensweig, 1985].

Table 1.4.1 Characteristics of the water-base magnetic fluid (W-40)\*  
[Kirtane, 2004]

Appearance	Black liquid
Density ( $\text{g/cm}^3$ ) at 25 °C	$1.4 \pm 0.02$
Viscosity (cp) at 25 °C	$25 \pm 7$
Magnetization (gauss) at 10 KOe	$380 \pm 30$
Boiling point (°C)	100
Flash point (°C)	nothing
Applicable thermal range (°C)	10 - 80
Base liquid	water

\* The W-40 magnetic fluid was obtained from Taiho Industries Co. Ltd., Japan

Chapter 2 reviews magnetic float polishing literature review.

Chapter 3 presents the problem statement.

Chapter 4 describes the approach of this investigation. The “Critical Polishing Condition” of MFP and a total of six experimental approaches are briefly described. Also, the alignment of the MFP apparatus is given.

Chapter 5 covers the results and discussion.

Chapter 6 gives the conclusions, mainly, the important roles and effects of the hidden polishing parameters in MPF process.

Chapter 7 suggests future work, namely, (1) modifying the existing polishing chamber with a water cooling system, (2) modifying the existing permanent magnets base with a grid (magnetic field insulator, such as copper) to separate each magnet, and (3) a SEM study of a ball's surface after each polishing stage or polishing condition.



## Chapter 2

### Magnetic Float Polishing Literature Review

Magnetic float polishing (MFP), also named previously as “Magnetic Fluid Grinding” was originally developed and studied by Imanaka et al. (1981) and Tani et al. (1984), according to [Umehara and Kato, 1990; Jiang and Komanduri, 1998; Jiang, 1998; Kirtane, 2004]. The experimental set-up is shown schematically in Figure 2.1. A workpiece was submerged and rotated in a layer of mixture (abrasives + magnetic fluid). It was believed that workpiece (e.g. acrylic) is polished by the free abrasive grains. However, the material removal rate was very low, and the control of shape was poor.

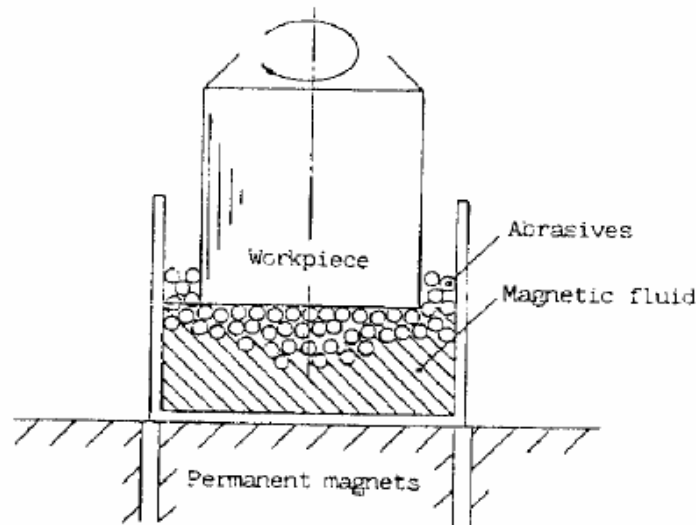


Figure 2.1 Diagram of the “Magnetic Fluid Grinding” apparatus [Tani and Kawata, 1984]

Later, the above experimental set-up of MFP technique was modified using the concept of a float by Umehara and Kato (1990), as shown in Figure 2.2. Due to the presence of a float in the MFP process, much higher polishing loads was easily obtained, as shown in Figure 2.3. Also, much better roundness of balls was found with longer polishing times, as shown in Figure 2.4. On the other hand, the roundness of balls (without a float) become worse with longer polishing time. Therefore, a batch of as-sintered  $\text{Si}_3\text{N}_4$  balls (11 balls of 7.7mm diameter) was successfully polished with this modified MFP set-up. The polishing result is shown in Table 2.1.

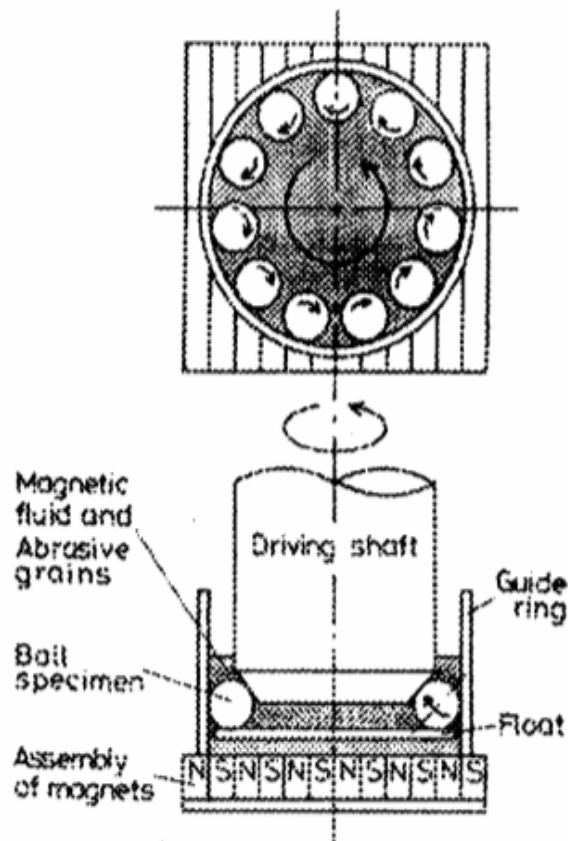


Figure 2.2 Schematic view of magnetic float polishing of  $\text{Si}_3\text{N}_4$  balls [Umehara and Kato, 1990]

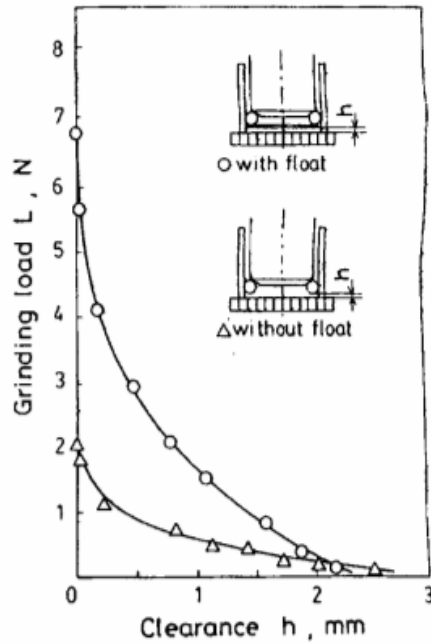


Figure 2.3 Variation of grinding loads with clearance showing the effective of the float [Umehara and Kato, 1990]

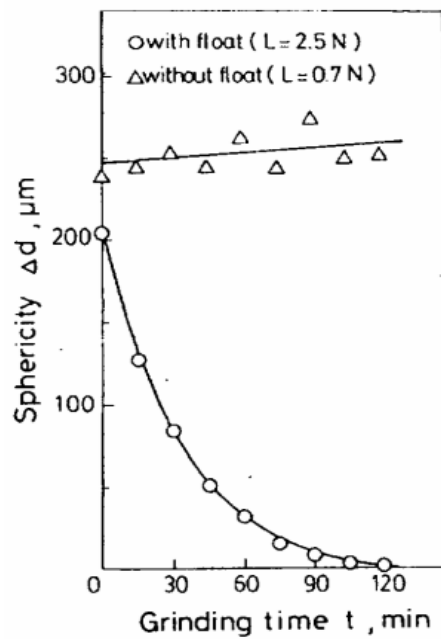




Figure 2.4 Variation of sphericity with grinding time showing improvement in sphericity using a float [Umehara and Kato, 1990]

Table 2.1 Polishing results of finished ball compared to the as-received ball [Umehara and Kato, 1990]

	As-received	Finished
Optical view		
Ball diameter	7.7 mm	7.1 mm
Roughness $R_{max}$	10 $\mu\text{m}$	0.1 $\mu\text{m}$
Sphericity	500 $\mu\text{m}$	0.14 $\mu\text{m}$
Grinding time ; 180 min		

Further, studies of the primary polishing parameters of the MFP process were first published by Umehara and Kato (1990). They are:

- Polishing time
- Polishing load
- Polishing speed
- Abrasives grain size
- Abrasives concentration

Figures 2.5 – 2.9 show the effects and roles of the primary polishing parameters played in MFP process. Figure 2.5 shows the effect of polishing time against the stock removal with and without a float. Higher stock removal ( $\mu\text{m}$ ) was found with longer polishing times (minutes). Figure 2.6 shows the effect of polishing load against the material removal rate (MRR) with and without a float. Higher MRR ( $\mu\text{m}/\text{min.}$ ) was found with a larger polishing load (N). Figure 2.7

shows the effect of polishing speed against the MRR, with and without a float. Higher MRR ( $\mu\text{m}/\text{min.}$ ) was found with higher polishing speed (rpm). Also, for even higher polishing speeds, such as  $> 10,000$  rpm, the MRR is slowed down and becomes constant (independent of polishing speed). Figure 2.8 shows the effect of abrasives grain size against the MRR, with and without a float. Higher MRR ( $\mu\text{m}/\text{min.}$ ) was found with coarser grains ( $\mu\text{m}$ ). Also, for even coarser abrasive grain,  $> 25 \mu\text{m}$ , the MRR becomes constant (independent of grain size). Figure 2.9 shows the effect of abrasive concentration against the MRR with and without a float. Higher MRR ( $\mu\text{m}/\text{min.}$ ) was found with higher abrasives concentration (vol. %). But, for higher concentration,  $> 10$  vol. %, the MRR is decreased.

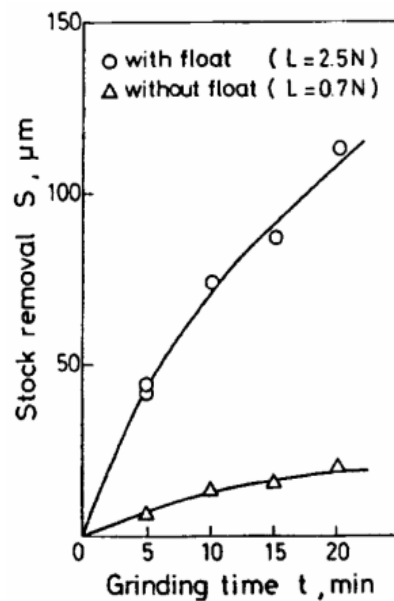


Figure 2.5 Effect of the stock removal with polishing time [Umehara and Kato, 1990]

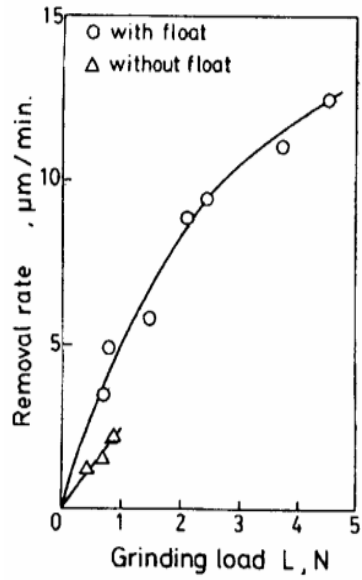


Figure 2.6 Effect of the material removal rate with polishing load [Umehara and Kato, 1990]

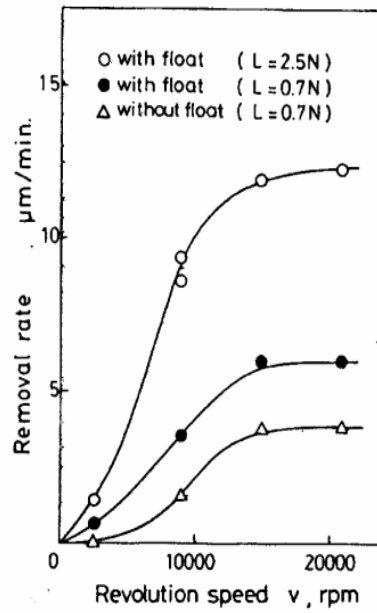


Figure 2.7 Effect of the material removal rate with polishing speed [Umehara and Kato, 1990]

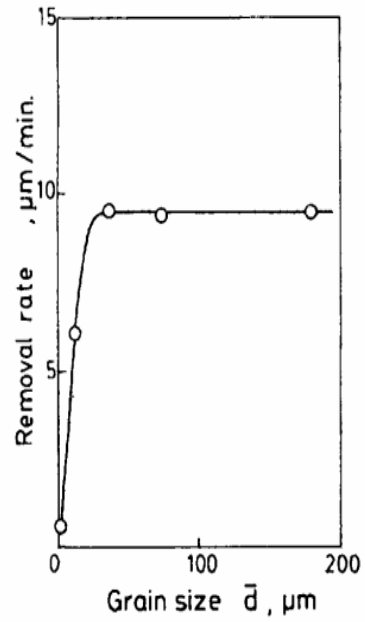


Figure 2.8 Variation of material removal rate with abrasives grain size [Umehara and Kato, 1990]

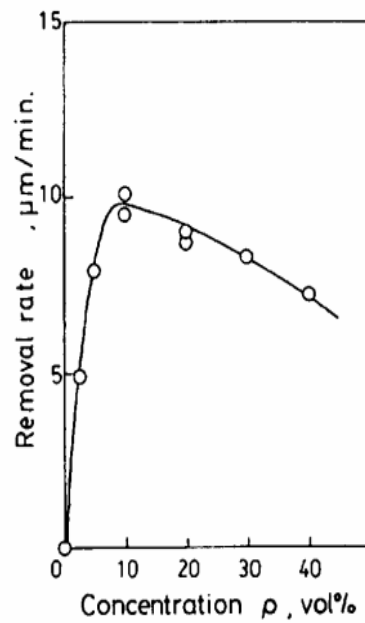


Figure 2.9 Effect of the material removal rate with abrasives concentration [Umehara and Kato, 1990]

For a better understanding of the MFP process, Childs *et al.* (1994) developed a model of MFP process, as shown in Figure 2.10(a). It was developed to calculate the sliding speed and was used to deduce an abrasive wear coefficient for the process. Therefore, an abrasive wear coefficient of  $0.007 \pm 0.02$  was observed. This allowed Childs *et al.* (1994) to indicate that the MFP process was dominated by two-body abrasion. Further, the high material removal rate that was caused by the large sliding speed, of several meters per second between the balls and polishing cup, was confirmed and understood.

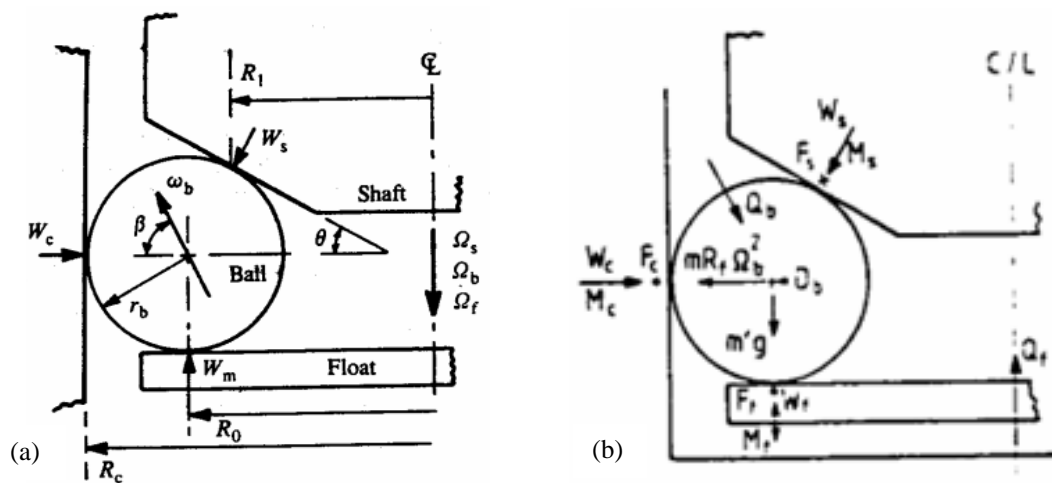


Figure 2.10 Schematic view of MFP model: (a) first model of MFP [Childs *et al.* 1994] and (b) modified model of MFP [Childs *et al.* and Zhang *et al.*, 1994]

Another complicated and modified model of the MFP process, shown in Figure 2.10(b), was also developed by Childs *et al.* (1994) and Zhang *et al.* (1994). The model included the serious considerations of:



- (i) The force and moment equilibrium of the balls with the polishing cup, and other surfaces.
- (ii) Other fluid drag forces and moments.
- (iii) Contact friction.

This modified model and the experimental results can be found in the paper [Childs *et al.* and Zhang *et al.*, 1994].

Umehara and Kato (1996), acknowledged that the previously polishing results (e.g. Umehara and Kato, 1988/1990; Childs *et al.*, 1994 and Raghunandan *et al.*, 1996) did not meet the ASTM standard specifications of Si<sub>3</sub>N<sub>4</sub> bearing balls, as shown in Table 2.2. The ASTM standard specifications of Si<sub>3</sub>N<sub>4</sub> bearing balls (which is indicated by letter “C” together with Grade number) for individual and lots of balls, are listed in Tables 2.3 and 2.4, respectively.

Table 2.2 Polishing results of Si<sub>3</sub>N<sub>4</sub> balls using MFP process by several researchers [Umehara and Kato, 1996]

	Removal rate ( $\mu\text{m min}^{-1}$ )	Sphericity ( $\mu\text{m}$ )	Surface roughness	Ball
Umehara and Kato [1,2] (1988/1990)	12.4 (GC, 38 $\mu\text{m}$ )	2.0 (GC, 38 $\mu\text{m}$ ) 0.14 (GC, 1.6 $\mu\text{m}$ )	0.50 $\mu\text{m}$ $R_{\text{max}}$ (GC, 38 $\mu\text{m}$ ) 0.12 $\mu\text{m}$ $R_{\text{max}}$ (GC, 1.6 $\mu\text{m}$ )	PLS-Si <sub>3</sub> N <sub>4</sub>
Childs et al. [4] (1994)	7.5 (D, 20–40 $\mu\text{m}$ )	0.7 (D, 20–40 $\mu\text{m}$ )	0.05 $\mu\text{m}$ $R_{\text{a}}$ (D, 2–4 $\mu\text{m}$ )	HIP-Si <sub>3</sub> N <sub>4</sub>
Raghunandan et al. [8] (1996)	0.13 (Cr <sub>2</sub> O <sub>3</sub> , 1–5 $\mu\text{m}$ )		< 0.01 $\mu\text{m}$ $R_{\text{a}}$ (Cr <sub>2</sub> O <sub>3</sub> , 1–5 $\mu\text{m}$ )	HIP-Si <sub>3</sub> N <sub>4</sub>

Table 2.3 ASTM standard specification for Si<sub>3</sub>N<sub>4</sub> bearing ball, μm (μin.) for individual ball [ASTM F 2094-03, 2004]

Grade	Allowable Ball Diameter Variation V <sub>D</sub>	Allowable Deviation from Spherical Form W	Maximum Surface Roughness Arithmetical Average Ra
2C	0.05 (2)	0.05 (2)	0.004 (0.15)
3C	0.08 (3)	0.08 (3)	0.004 (0.15)
5C	0.13 (5)	0.13 (5)	0.005 (0.20)
10C	0.25 (10)	0.25 (10)	0.006 (0.25)
16C	0.40 (16)	0.40 (16)	0.009 (0.35)
24C	0.61 (24)	0.61 (24)	0.013 (0.50)
48C	1.22 (48)	1.22 (48)	0.013 (0.50)

Table 2.4 ASTM standard specification for Si<sub>3</sub>N<sub>4</sub> bearing ball, μm (μin.) for lots of balls [ASTM F 2094-03, 2004]

Grade	Allowable Lot Diameter Variation	Nominal Diameter Tolerance	Allowable Ball Gage Deviation	
			High	Low
2C	0.08 (3)	± 0.51 (± 20)	+ 0.51 (+ 20)	- 0.51 (- 20)
3C	0.13 (5)	± 0.51 (± 20)	+ 0.51 (+ 20)	- 0.51 (- 20)
5C	0.25 (10)	± 0.76 (± 30)	+ 0.76 (+ 30)	- 0.76 (- 30)
10C	0.51 (20)	± 2.54 (± 100)	+ 1.27 (+ 50)	- 1.02 (- 40)
16C	0.80 (32)	± 2.54 (± 100)	+ 1.27 (+ 50)	- 1.02 (- 40)
24C	1.22 (48)	± 2.54 (± 100)	+ 2.54 (+ 100)	- 2.54 (- 100)
48C	2.44 (96)	N/A	N/A	N/A

A batch of Grade 10C Si<sub>3</sub>N<sub>4</sub> ball bearings (Roundness: 0.25 μm & Surface Finish: Ra = 6 nm) was not successfully finished by Umehara and Kato (1990) yielding a surface finish of Ra ~ 50 nm. Another example, a batch of Grade 24C Si<sub>3</sub>N<sub>4</sub> balls (Roundness: 0.61 μm & Surface Finish: Ra = 13 nm) was successfully finished by Rahgunandan et al. (1996). However, the Grade 24C of ball bearings were not adequate for the applications of high speed spindle and high precision machine tools. Therefore, some new ideas or alternative approaches to the MFP process for finishing a batch of Si<sub>3</sub>N<sub>4</sub> balls for ball bearings application were necessary.

As a response to the above statement, a new approach to the MFP process (named methodology of MFP process) was developed by Bhagavatula and Komanduri (1996); Komanduri *et al.* (1996); Jiang and Komanduri (1997); Jiang and Komanduri (1998); Raghunandan and Komanduri (1998); Jiang *et al.* (1998); Jiang, Wood and Komanduri (1998); Komanduri *et al.* (1999) at Oklahoma State University, Stillwater, Oklahoma, United States.

A systematic, efficient, and repeatable methodology of MFP process of finishing Si<sub>3</sub>N<sub>4</sub> ball bearings was successfully developed, as shown in Table 2.5. In general, the methodology consists of three stages of finishing a small batch of Si<sub>3</sub>N<sub>4</sub> balls (0.5 in. diameter). They are:

Stage 1: Roughing Stage, where the emphasis is on high MRR (to quickly reduce the diameter of the balls close to the desired diameter.)

Stage 2: Semi-Finishing Stage, where the emphasis is on roundness, surface finishing, and the desired diameter (all need to be closely monitored.)

Stage 3: Final Finishing Stage, where the emphasis is on superior finishing, final desired diameter, and good roundness. Details are given in Jiang's Ph.D. thesis [Jiang, 1998].

Table 2.5 Methodology for finishing Si<sub>3</sub>N<sub>4</sub> balls by MFP process [Jiang, 1998]

Stage	Abrasive			Abrasive, vol%	Speed, rpm	Load, N/ball	Time, min	Remarks
	Type	Grit Size	Size(μm)					
1	B <sub>4</sub> C	500	17	10%	2000	1.0	-	Roughing (High Material Removal)
	SiC	400	23	10%	2000	1.0	-	
2	SiC	1000	5	10%	2000	1.0	30	Semi-finishing (Sphericity and Roughness)
	SiC	1200	3	10%	2000	1.0	30	
3	SiC	8000	1	5%	4000	1.2	60	Final Finishing (Size, Sphericity, and Finish)
	CeO <sub>2</sub>		5	10%	2000	1.2	120	

With the introduction of this methodology in the MFP process, a batch of Grade 10C Si<sub>3</sub>N<sub>4</sub> bearing balls (Roundness: 0.25 μm & Surface Finish: Ra = 6 nm) was easily obtainable. Further, with care and consistent practice of this methodology, Grade 5C of Si<sub>3</sub>N<sub>4</sub> ball bearings (Roundness: 0.13 μm & Surface Finish: Ra = 5 nm) was possible. Some of the polishing results are included here, the TalyRond 250 roundness profile of as-received and finished Si<sub>3</sub>N<sub>4</sub> balls, the TalySurf 120 L surface roughness profile of finished Si<sub>3</sub>N<sub>4</sub> balls, and an SEM micrograph of finished Si<sub>3</sub>N<sub>4</sub> balls, as shown in Table 2.6, Figures 2.11, 2.12 and 2.13.

Table 2.6 Surface finish of Si<sub>3</sub>N<sub>4</sub> balls obtained using the methodology of MFP [Jiang, 1998]

Stage	Abrasive	Surface Finish (Ave.)		MRR per ball		Material Removal Mechanism
		Ra (nm)	Rt (μm)	mg/min	μm/min	
1	B <sub>4</sub> C 500	225	1.95	0.96	1.2	Microfracture
	SiC 400	170	1.40	0.64	0.8	Microfracture
2	SiC 1000	95	0.80	0.30	0.5	Submicrofracture
	SiC 1200	55	0.50	0.20	0.2	Submicrofracture
3	SiC 8000	15	0.15	0.04	-	Submicrofracture
	CeO <sub>2</sub>	4 nm	0.03 μm	0.01	-	Tribo-chemical

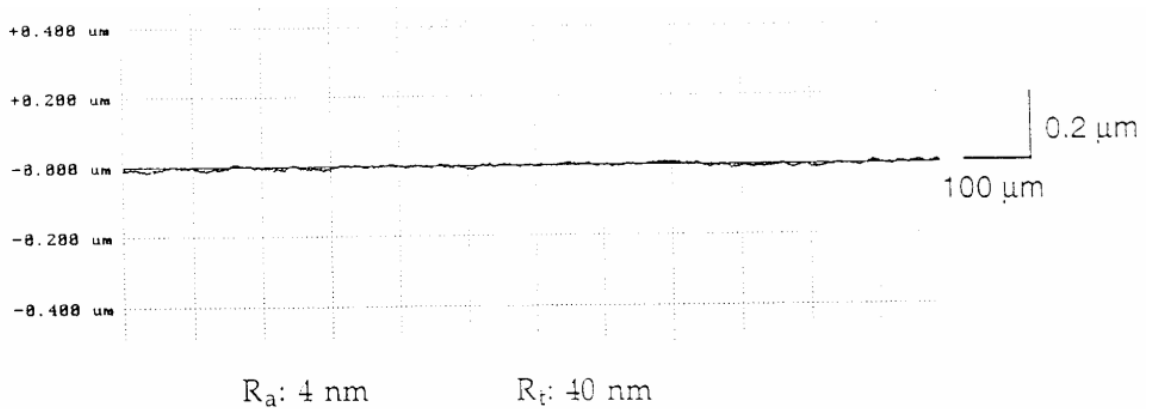


Figure 2.11 TalySurf 250 surface roughness profile of finished Si<sub>3</sub>N<sub>4</sub> balls surface [Jiang, 1998]

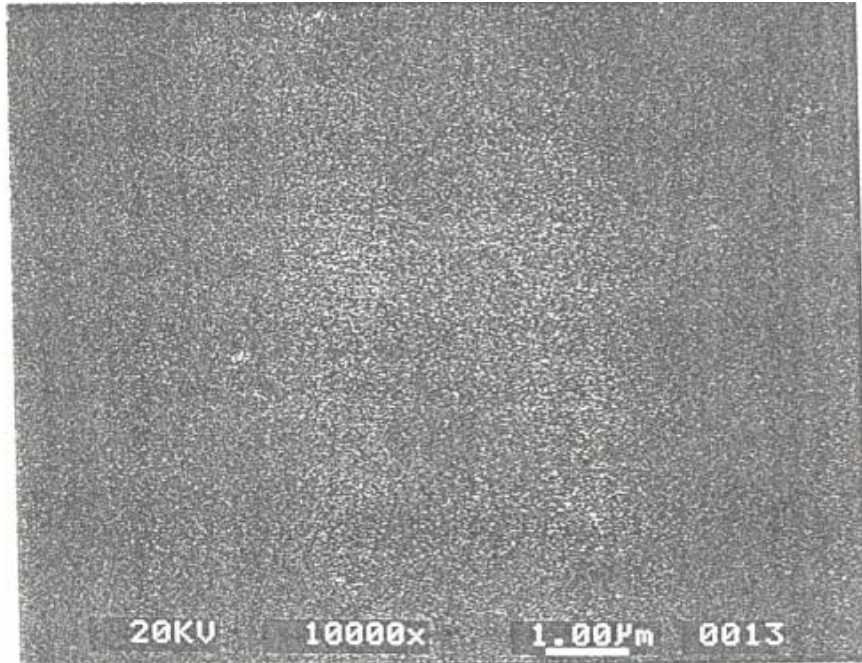


Figure 2.12 SEM micrograph of finished Si<sub>3</sub>N<sub>4</sub> balls surface [Jiang, 1998]

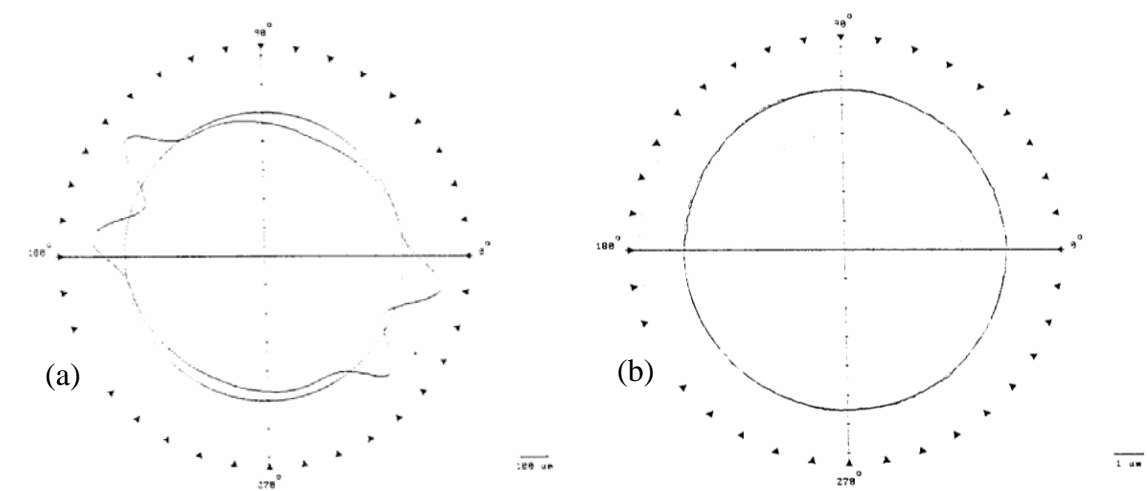


Figure 2.13 Roundness of Si<sub>3</sub>N<sub>4</sub> balls: (a) as-received: 200 µm and (b) final roundness: 0.15 µm [Jiang, 1998]

A vibration monitoring system, as shown in Figure 2.14, was added to the MFP apparatus by Rao (1999) to monitor the polishing run. This monitoring system was used to make sure that each MFP runs was operated under the optimum polishing condition. The optimum polishing condition was defined as a particular polishing run that would not damage the balls; instead it improved the quality of balls, such as roundness, surface finish, and final diameter. The main advantage of utilizing this monitoring system was to avoid damage to the, especially when the final diameter was very close.

Vibration frequency spectrums generated by the polishing run were recorded using two accelerometer pick-ups and a vibration monitoring system. Figure 2.15(a) shows two dominant frequencies and high vibration amplitude ( $0.6 \text{ m/s}^2$ ) that confirmed the polishing run is bad. Thus, roundness of  $10.3 \mu\text{m}$  was obtained. Figure 2.15(b) and (c) shows low vibration amplitude ( $0.12 \text{ m/s}^2$ ) and only one dominant frequency that confirmed the polishing run was good. Thus, roundness of  $0.35$  and  $0.25 \mu\text{m}$  were obtained, respectively [Rao, 1999].

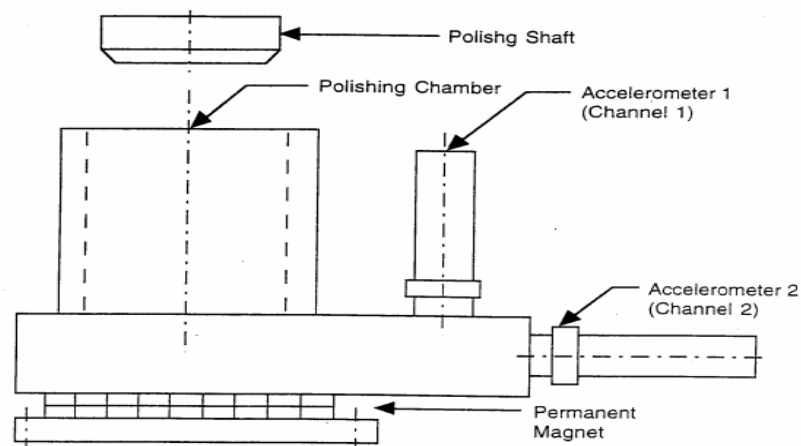


Figure 2.14 Vibration monitoring system attached to the polishing chamber [Rao, 1999]

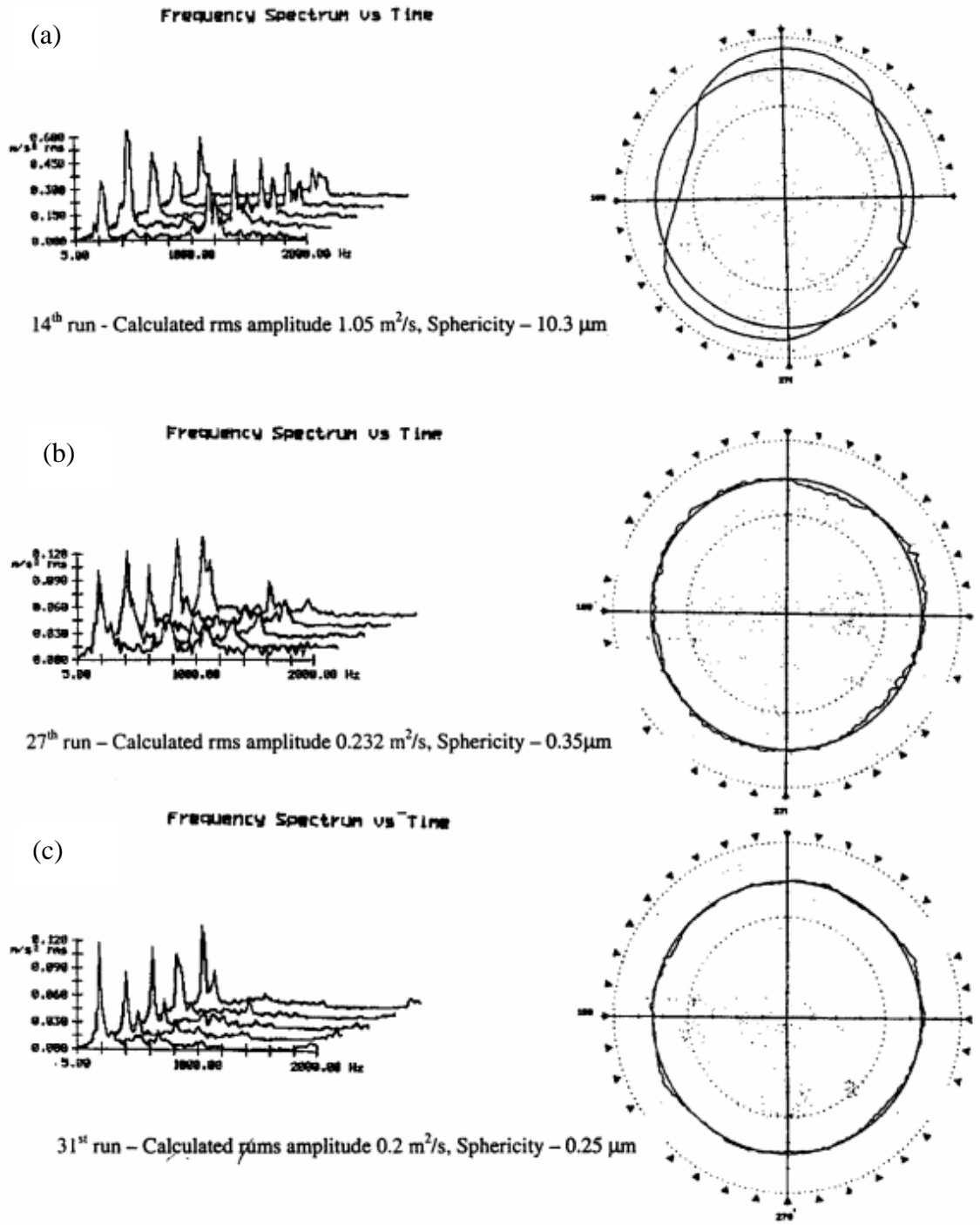


Figure 2.15 Variation of frequency spectrum against the time and corresponding roundness of Si<sub>3</sub>N<sub>4</sub> balls [Rao, 1999]



Gerlick (2004) and Kirtane (2004) used a self-alignment large batch polishing apparatus, as shown in Figure 2.16, 2.17 (a) and (b), to finish a batch of  $\text{Si}_3\text{N}_4$  balls (46 balls of 3/4 in. diameter). The detail of this new polishing apparatus and the studies can be found in Gerlick and Kirtane theses. The studies were conducted with the employment of the well-known concept of MFP technique, the well-studied polishing parameters of MFP, and the effective methodology of MFP process.

However, the polishing results of these larger  $\text{Si}_3\text{N}_4$  balls were not promising for the application of ball bearings, especially the roundness of balls. The average roundness of 46 balls was  $\sim 1 \mu\text{m}$  (0.35 - 1.78  $\mu\text{m}$ ).



Figure 2.16 Photograph of a self-aligned large batch polishing apparatus used to finish larger  $\text{Si}_3\text{N}_4$  balls (46 balls of 3/4 in. diameter) [Gerlick, 2004 and Kirtane, 2004]

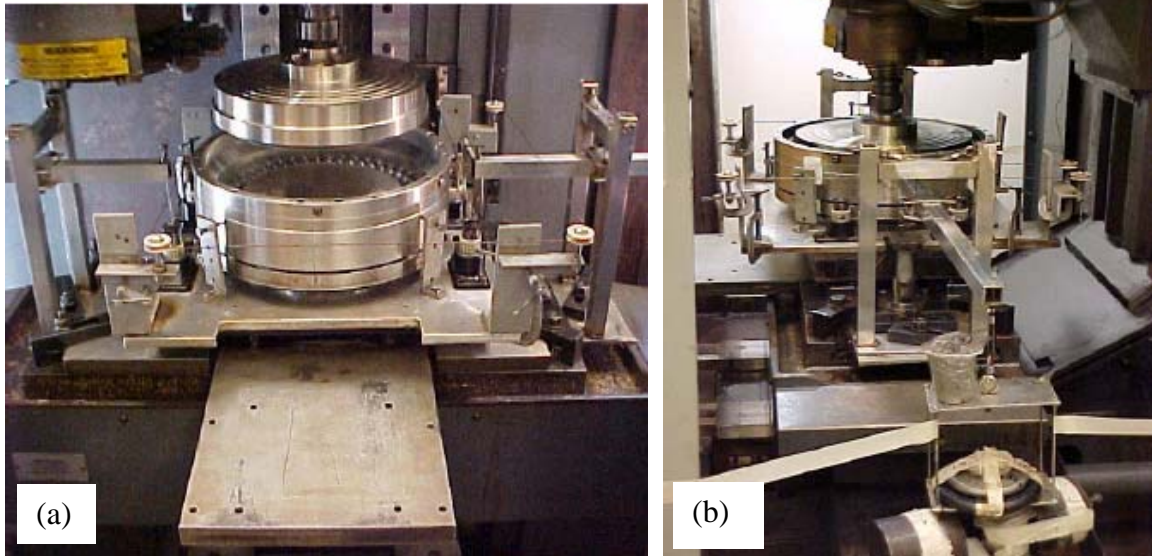


Figure 2.17 (a) Front view and (b) side view of the self-aligned large batch polishing apparatus [Gerlick, 2004 and Kirtane, 2004]

Later on, Kirtane (2004) had successfully finished a batch of  $\text{Si}_3\text{N}_4$  balls (46 balls of  $\frac{3}{4}$  in. diameter) with average roundness of  $0.27 \mu\text{m}$  and surface finish of  $R_a \sim 8 \text{ nm}$ , by applying one of the “hidden” polishing parameters that have been found and proven in this thesis. The “hidden” polishing parameters stated here is the groove that forms on the bevel of the polishing cup during previous run (details of the MFP process that takes this parameter into account can be found in Kirtane thesis).

From the above observations, there are additional polishing parameters that are worthy for further studies and investigating. Therefore, the objective of this thesis is to conduct a study on these parameters, the so-called “hidden” polishing parameters, which play an important role in improving the MFP process outcome.

## Chapter 3

### Problem Statement

As mentioned and discussed in the magnetic float polishing (MFP) literature review, the batch polishing technology has been successfully used for the finishing of silicon nitride ( $\text{Si}_3\text{N}_4$ ) balls of various sizes ( $\frac{1}{4}$  -  $\frac{3}{4}$  in. diameter) with small as well as large batch polishing apparatus. However, when the sizes of  $\text{Si}_3\text{N}_4$  balls become larger ( $> \frac{3}{4}$  in.), this MFP technology has difficulty to finish a batch of Grade 10C  $\text{Si}_3\text{N}_4$  balls for bearing applications, especially the roundness of the balls. It means the MFP technology is not fully understood. Further, the consumption of expensive magnetic fluid by this MFP technology needed to be greatly reduced, in order to have an impact on the commercial ball lapping process. Thus, the following tasks were undertaken in this thesis:

1. A new "Critical Polishing Condition" MFP apparatus was purposely designed and built for this investigation, in order to reveal and study hidden polishing parameters.
2. Two batches of  $\text{Si}_3\text{N}_4$  balls (10 balls of 0.9 in. diameter) were used.

3. A vibration monitoring system (Vibroport 41) was added to the newly built aluminum polishing chamber to clarify and study the hidden polishing parameters during polishing.
4. A total of 6 experimental approaches were planned and carried out to reveal and study the hidden polishing parameters that played an important role in MFP process.
5. A simple method of separating the after-polished abrasives and magnetic fluid was developed, in order to reduce the MFP cost through recycling the abrasives or use for other applications (if possible).
6. A Scanning Electron Microscope (SEM) study was undertaken to consider the shape/structure relationship between the fresh abrasives and the after-polishing abrasives, Boron Carbide (500 grit).
7. A study of optimization the magnetic field strength of the permanent magnets base (newly built for this investigation), in order to provide higher polishing load, especially for finishing larger  $\text{Si}_3\text{N}_4$  balls.

## Chapter 4

### Approach

#### 4.1 Design of the “Critical Polishing Condition” MFP apparatus

This section deals with the design of the “Critical Polishing Condition” MFP apparatus, which is purposely developed for this investigation in order to reveal and study the roles and effects of the hidden polishing parameters.

Figure 4.1.1(a) shows the “Critical Polishing Condition” apparatus developed and built for this investigation. It is defined as: using a small polishing chamber (4 in. inside diameter) to finish much larger  $\text{Si}_3\text{N}_4$  balls (10 balls of 0.9 in. diameter). It is apparent that this polishing condition was far from ideal or optimum polishing condition. Figure 4.1.1 (b) shows the newly built polishing chamber is more suitable for finishing a batch of smaller  $\text{Si}_3\text{N}_4$  balls (20 balls of  $\frac{1}{2}$  in. diameter).

In other words, this MFP process is analogue to the commercial ball bearing. With a specific size or diameter of the balls, there is a pre-defined inner and outer diameter of the bearing sleeve, which is purposely designed for better ball rolling motion for that particular size of ball bearing. If this designated specification is not met, that particular commercial ball bearing would not perform satisfactorily. As a result, that ball bearing will fail earlier or not perform at the require specification. This is similar to the MFP process. A bad

polishing result will be expected if this “Critical Polishing Condition” of MFP is used in this investigation. However, the purpose is not to prove this polishing condition is bad for MFP process. The purpose is to study and reveal the effect of the “hidden” polishing parameters of the MFP process.

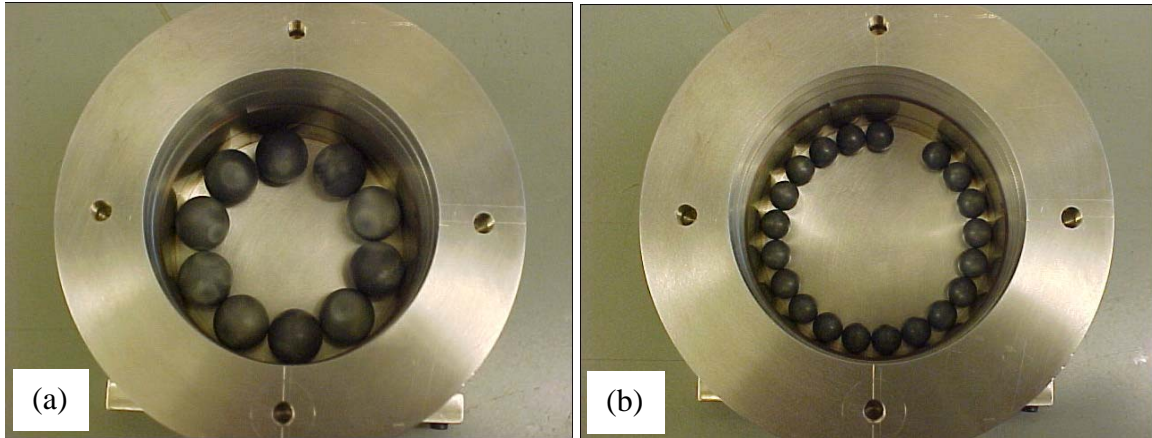


Figure 4.1.1 (a) Newly built MFP chamber designed and developed for this investigation to reveal the roles and effects of the hidden polishing parameters, named, the “Critical Polishing Condition” chamber for finishing larger  $\text{Si}_3\text{N}_4$  balls (10 balls of 0.9 in. diameter). Instead, it was more suitable for finishing a batch of smaller  $\text{Si}_3\text{N}_4$  balls (20 balls of  $\frac{1}{2}$  in. diameter) as shown in (b).

To compensate the “Critical Polishing Condition” chamber, a new non-magnetic stainless steel polishing cup and a new permanent magnet base were built, as shown in Figure 4.1.2. Also, a vibration monitoring system was added to the polishing chamber to study the vibration behavior of polishing. Figure 4.3 shows the overview of the MFP apparatus used in this thesis.

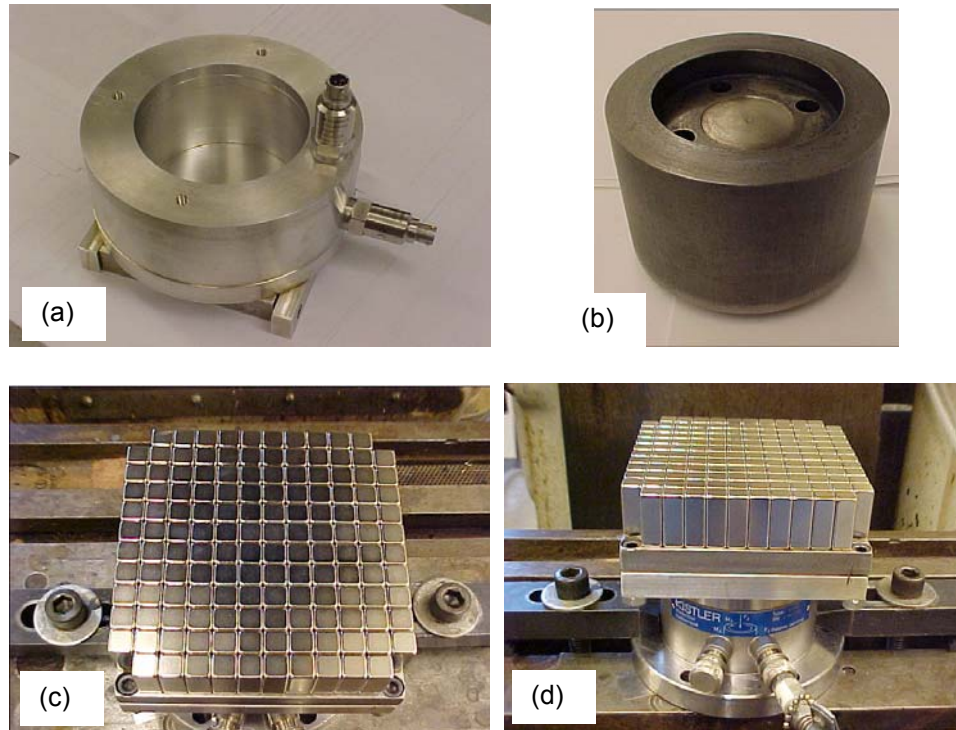


Figure 4.1.2 (a) Newly made polishing chamber with two accelerometers attached, (b) the polishing cup, (c) top-view and (d) front-view of the permanent magnet base.



Figure 4.1.3 Overview of the MFP apparatus used in this thesis

## 4.2 Alignment of MFP apparatus

The MFP set-up of each polishing run is very important, especially the alignment of the MFP apparatus that (mainly) consists of drive shaft and the spindle, polishing cup, polishing chamber, and permanent magnet base. There are two critical alignments, namely, (1) the alignment of polishing cup to drive shaft and (2) the alignment of polishing cup to polishing chamber. In order to obtain consistent and useful experiment results, care and patience are needed while performing these alignments procedures.

Figure 4.2.1 shows the alignment system that consists of (1) Pneumo-Centric 5500 system, (2) Pick-up probe, and (3) home-made coupling. The Pneumo-Centric 5500 was actually a roundness profiler (an older model of TalyRond 250 that was used in this investigation).

Figures 4.2.2 (a) – (f) illustrate the procedures for the first alignment of the polishing apparatus. The details are listed below:

1. Secure (not tightly) the polishing cup to the driving shaft of the spindle with 4 nuts, as shown in Figure 4.2.2 (a).
2. Plug the pick-up probe at the back of the Pnuemo-Centric system and turn on the power, as shown in Figure 4.2.2 (b).
3. Select the sensitivity of the system, 12.5  $\mu\text{m}$  per division.
4. Then, properly locate the tip of the pick-up probe to the side of the polishing cup with the help of portable magnetic stand, as shown in Figure 4.2.2 (c).



5. Apply some pressure to the tip of the pick-up probe through contact against the side polishing cup, as shown in Figure 4.2.2 (d).
6. Later, slowly rotate the driving shaft by hand and now observe the deflection through the meter of the system.
7. Adjust the 4 nuts until the polishing cup is properly aligned to the driving shaft, the deflection of one fully revolution of driving shaft is within 2 divisions.
8. After that, relocate the tip of the pick-up probe to the bevel of the polishing cup and repeat steps 5 - 7, as shown in Figure 4.2.2 (e)& (f).
9. Finally, tighten the nuts.



Figure 4.2.1 Alignment system of MFP apparatus for the present study

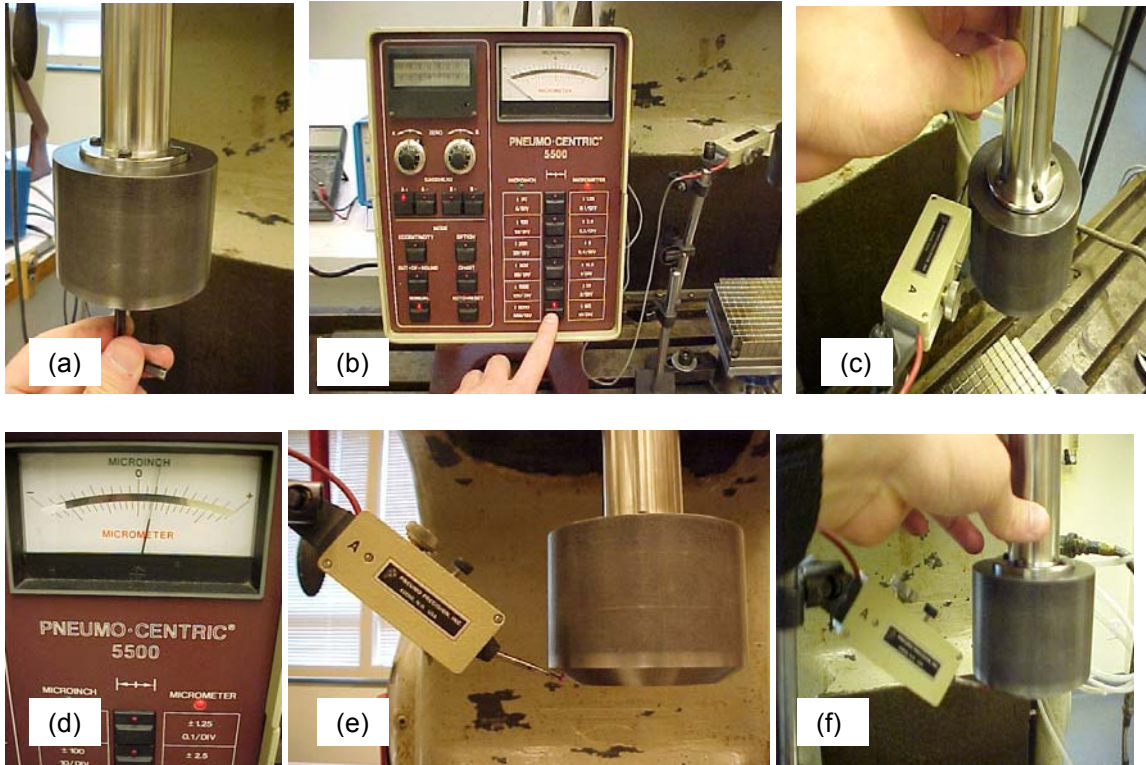


Figure 4.2.2 (a) – (f) First alignment of the polishing apparatus

After the first alignment, Figures 4.2.3 (a) – (f) show the procedures for the second alignment of the polishing apparatus. The details are listed below:

1. Secure the polishing chamber tightly on the permanent magnets base.
2. Attach the pick-up probe to the polishing cup with the home-made coupling, as shown in Figure 4.2.3 (a).
3. Raise the polishing chamber through raising the XYZ-milling table until the tip of the pick-up probe is very close to the location where the balls will circulate around the chamber, as shown in Figure 4.2.3 (b).
4. Apply some pressure to the tip of the pick-up probe, through contact against the wall of the polishing chamber.

5. Adjust the XY-direction of the milling table until the deflection of the “front and back” and the “left and right” measured positions is the same, as shown in Figure 4.2.3 (c) and (d).

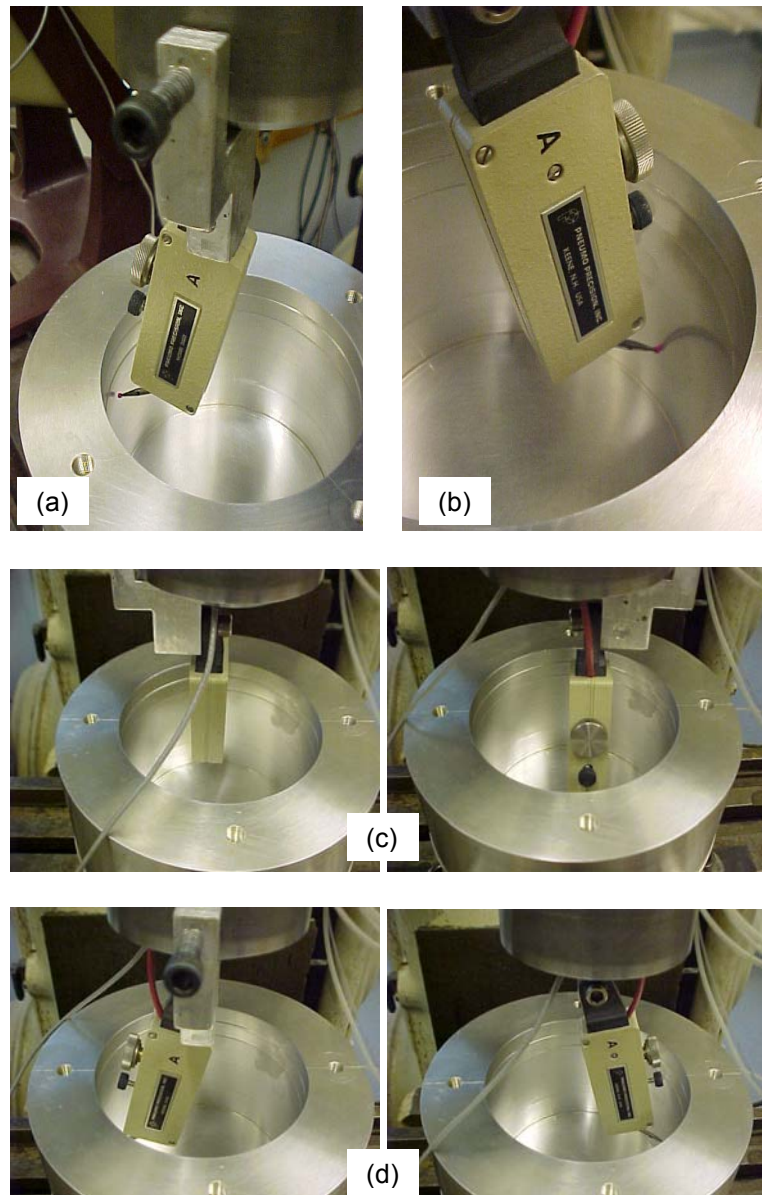


Figure 4.2.3 (a) – (d) Second alignment of the polishing apparatus

### **4.3 Six experimental approaches**

Figures 4.3.1 – 4.3.6 show the six experimental approaches used in this investigation, to reveal and study the hidden polishing parameters.

Figure 4.3.1 shows the first experimental approach used to reveal the roles and effects of the groove formed on the bevel of the polishing cup during polishing, in order to improve the average roundness of the balls.

Figure 4.3.2 shows the second experimental approach used to clarify the formation of the two distinctive magnetic fluid patterns during the MFP process. For a better understanding, a vibration monitoring system (Vibroport 41) was installed to the polishing chamber to aid the study of this experimental approach.

Figure 4.3.3 shows the third experimental approach used to study the roles of gap/spacing among the balls during the MFP process, in order to further improve the average roundness and (more important) the uniform roundness of a single ball.

Figure 4.3.4 shows the fourth experimental approach used to demonstrate poor or non-uniform roundness of a single  $\text{Si}_3\text{N}_4$  ball, due to non-uniformity in workmaterial.

Figure 4.3.5 shows the fifth experimental approach, which is used to reveal and study the roles and effects of the prevention of magnetic fluid during the MFP process, in order to reduce the consumption of expensive magnetic fluid.

Figure 4.3.6 shows the sixth experimental approach used to reveal and study the microstructures of the after-polished abrasives using SEM, in order to bring down the overall cost of MFP process.

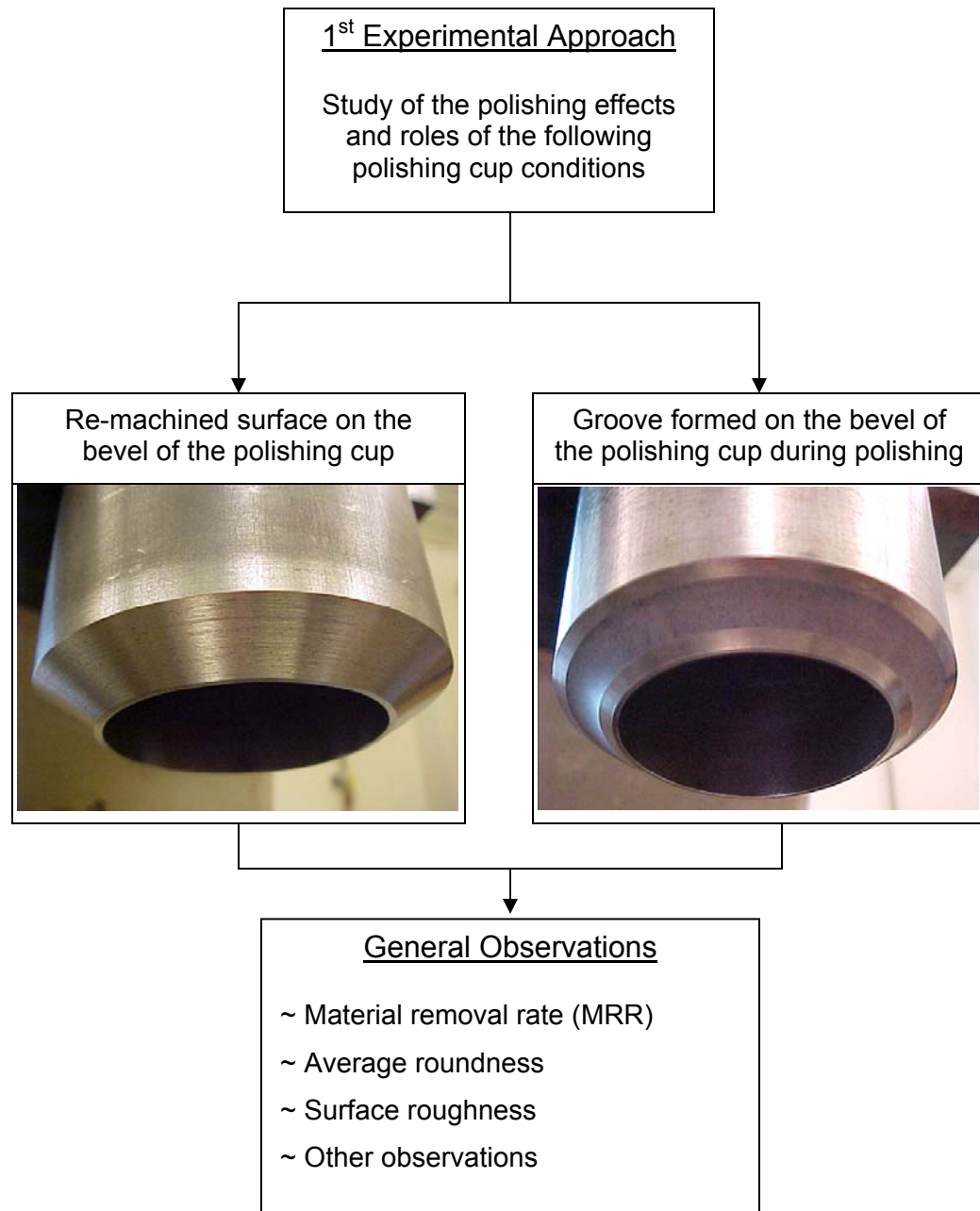


Figure 4.3.1 First experimental approach, used to reveal and study the roles and effects of the groove formed on the bevel of the polishing cup during polishing.

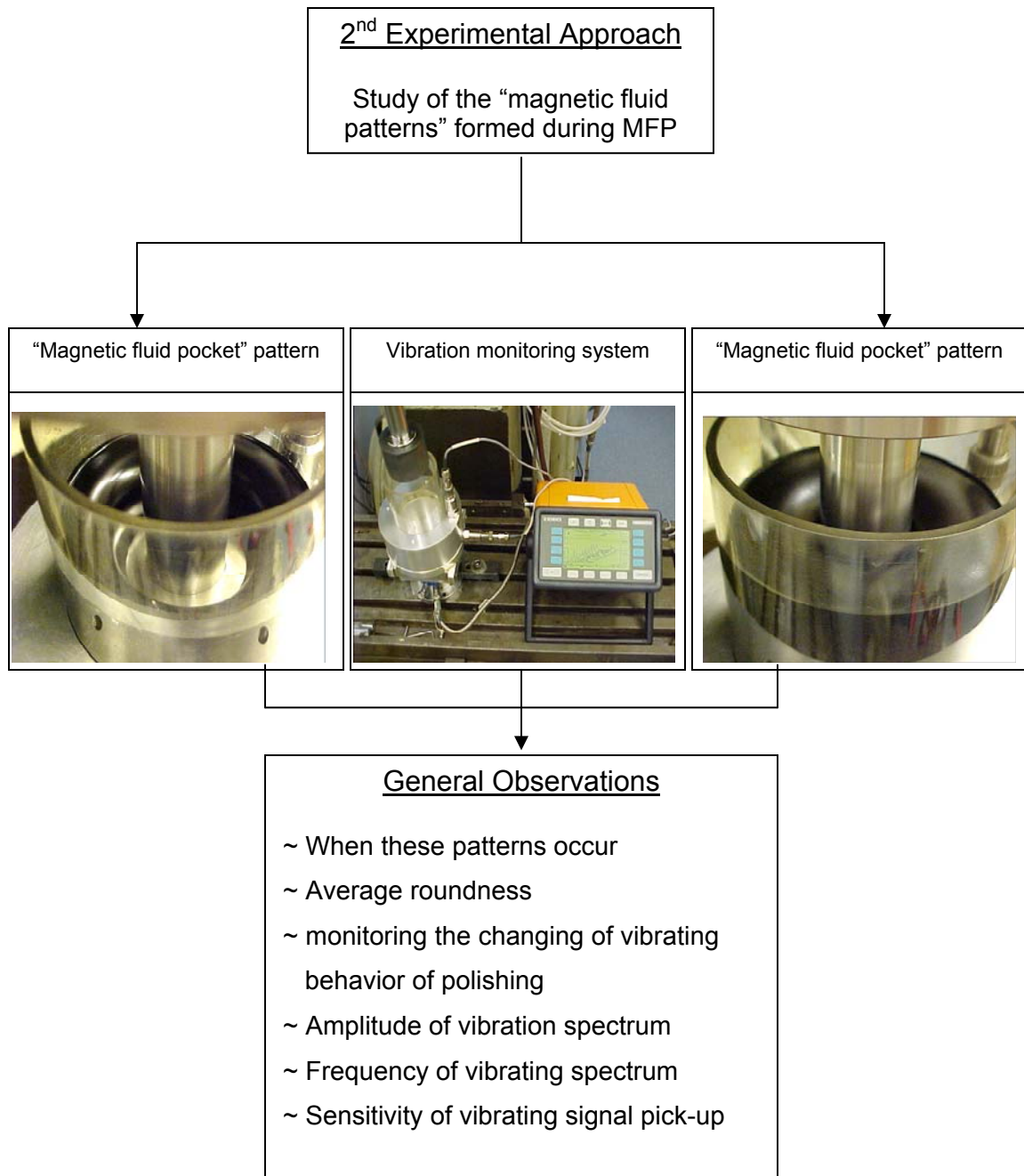


Figure 4.3.2 Second experimental approach, used to clarify the magnetic fluid patterns formation that observed in the first experimental approach.

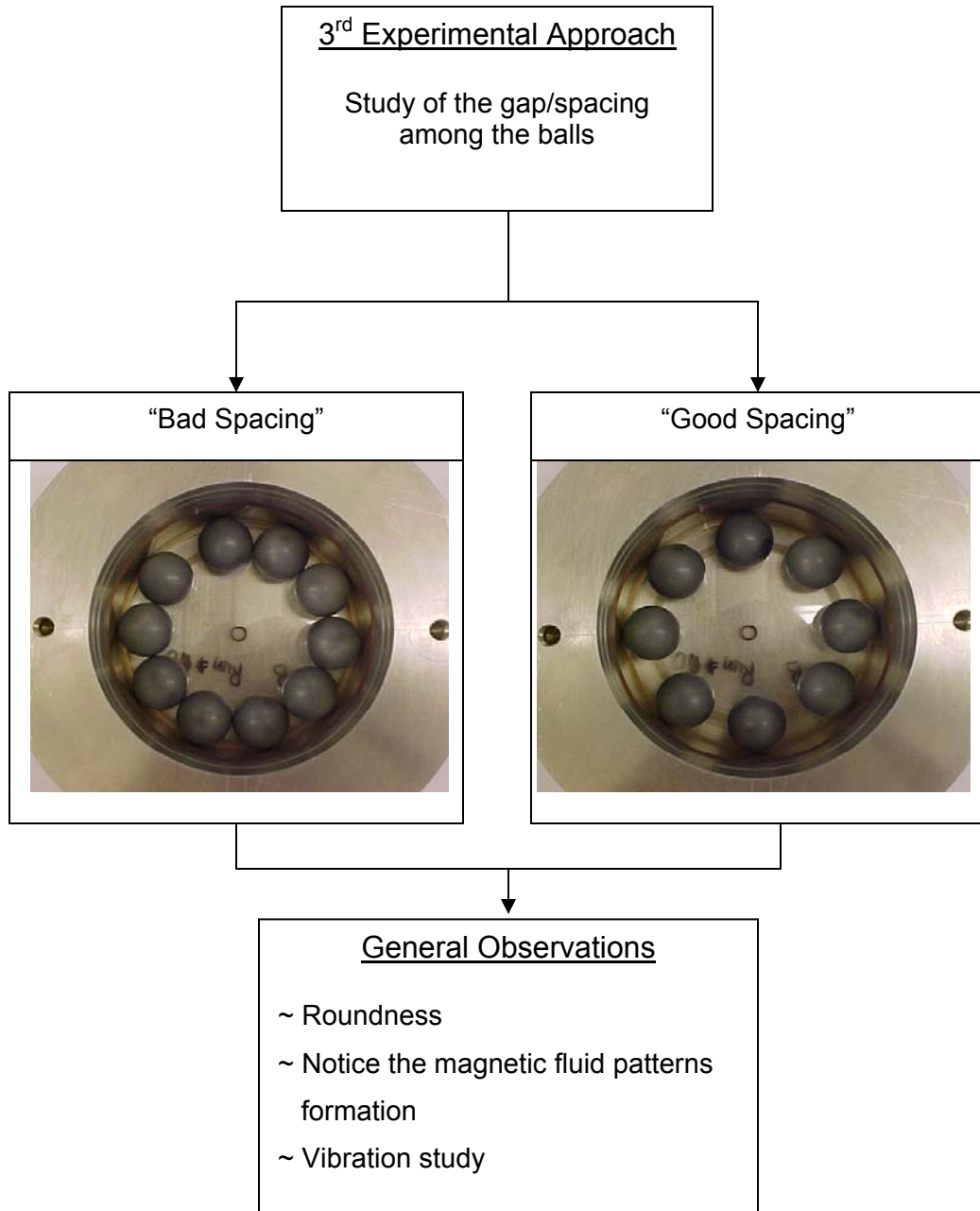


Figure 4.3.3 Third experimental approach, used to further improve the average roundness of the  $\text{Si}_3\text{N}_4$  balls and the uniform roundness of a single ball, namely, the gap/spacing among the balls during MFP process.

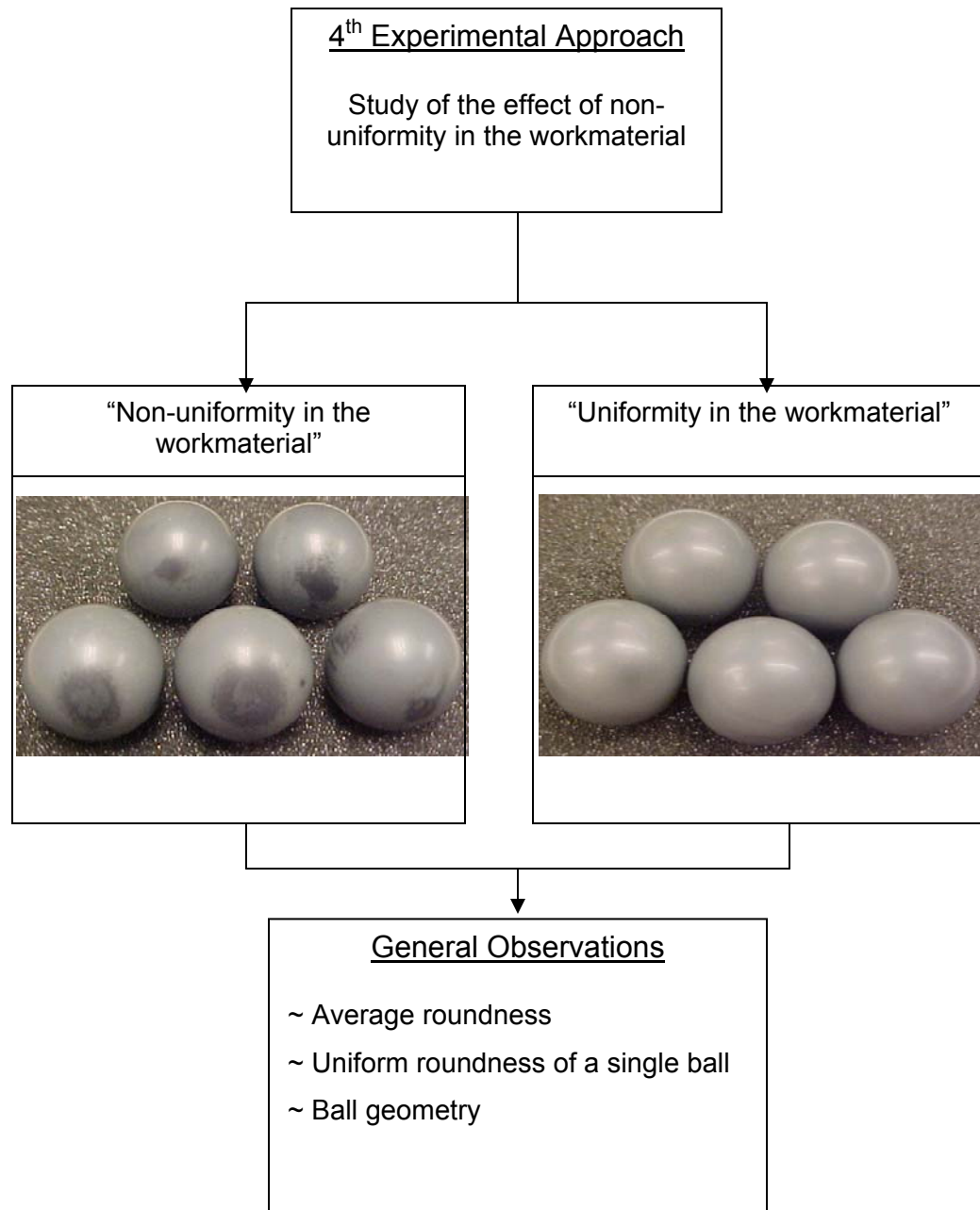


Figure 4.4.4 Fourth experimental approach, used to find the non-uniform roundness of a single non-uniform workmaterial (the  $\text{Si}_3\text{N}_4$  balls).



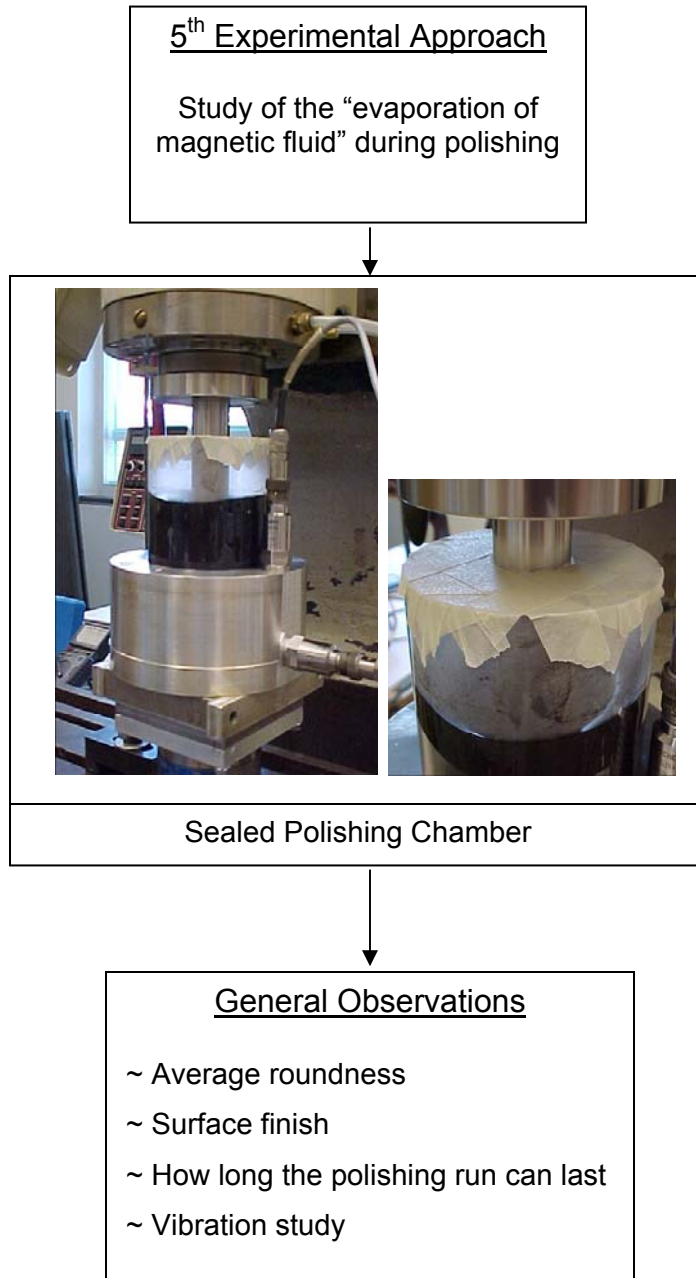


Figure 4.3.5 Fifth experimental approach, used to study the possibility of saving or reduced the consumption of the expensive magnetic fluid in MFP process.

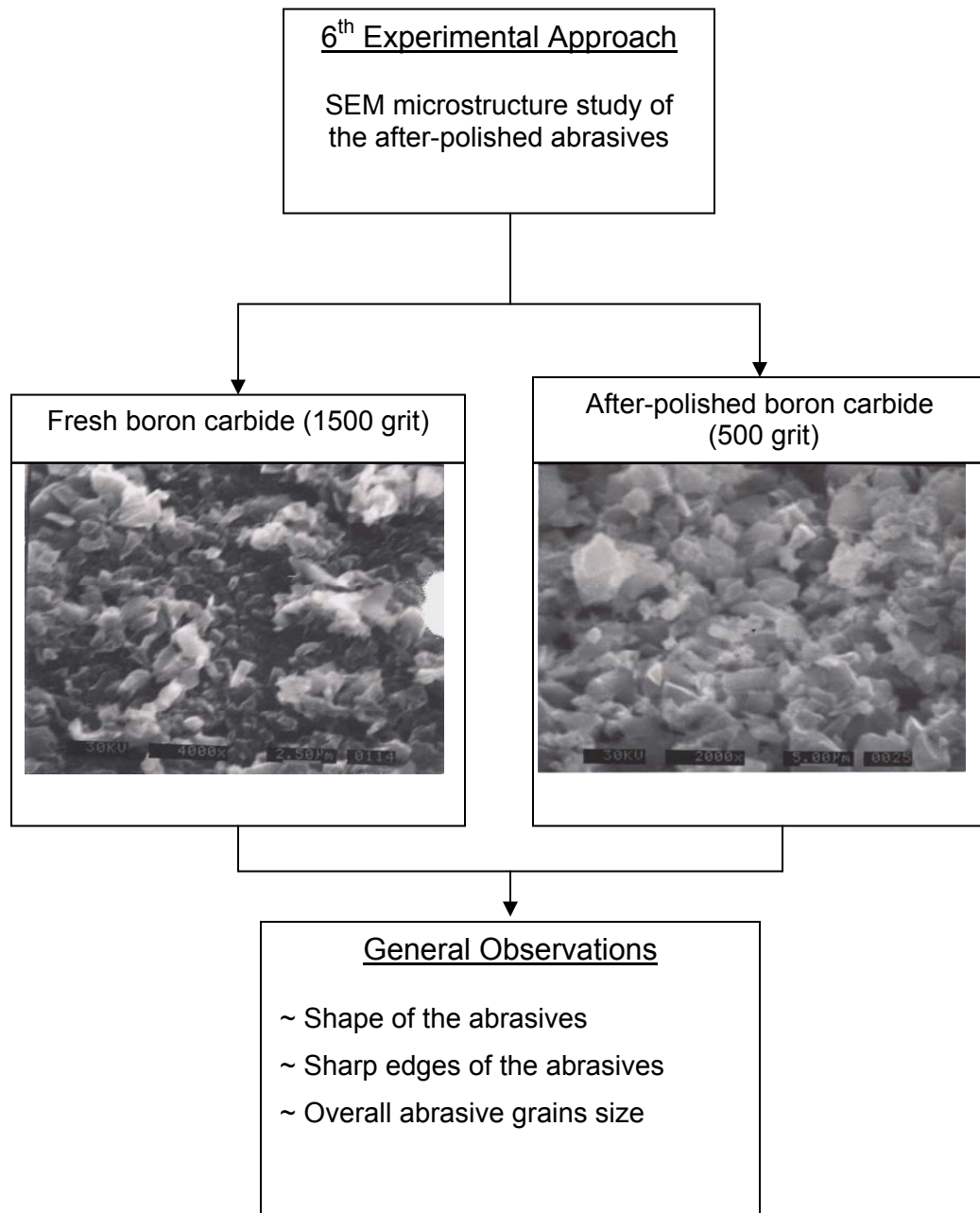


Figure 4.3.6 Sixth experimental approach, used to study the possibility of recycling and used it as (1500 grit) abrasives or for other applications, in order to bring down the overall cost of MFP process.

#### **4.4 List of the balls' characterization instruments**

Section 4.4 contains a list of instruments for characterizing the  $\text{Si}_3\text{N}_4$  balls. Details of each instrument are not covered in this thesis and they have been described in number of theses [Jiang, 1998, Rao, 1999, and Kirtane, 2004].

Following is a list of equipments used to characterize the polished balls:

- TalyRond 250, for roundness measurement
- TalySurf 120L, for surface roughness measurement
- Micrometer
- Scanning Electron Microscope (SEM)

## Chapter 5

### Results and Discussion

The “Critical Polishing Condition” MFP set-up developed in this investigation as described in Chapter 4 (Approach), had successfully revealed the roles and effects of the hidden polishing parameters in MFP process. Also, 6 experimental approaches were used to clarify the roles and effects of each hidden polishing parameter.

#### **5.1 First experimental approach: Reveal and study the roles of Groove formed on the bevel of the polishing cup during MFP process**

At the roughing stage, a re-machined surface on the bevel of the polishing cup is used initially to improve the roundness and diameter of a batch of  $\text{Si}_3\text{N}_4$  balls (10 balls of 0.9 in. diameter) with initial average roundness of  $26.59 \mu\text{m}$  ( $16.52 - 40.22 \mu\text{m}$ ) and average ball diameter of 0.9075 in. ( $0.9060 - 0.9092$  in.). The groove formed on the bevel of the polishing cup is removed after each polishing run. Figure 5.1.1 shows the poor average roundness of  $1.43 \mu\text{m}$  ( $0.78 - 2.72 \mu\text{m}$ ) was found, after four polishing runs (Run 1 – 4). On the other hand, Figure 5.1.2 shows the uniform geometry of balls (0.9013 in. diameter) was already obtained. Details of the polishing conditions are given in Table 5.1, Run 1 to 4.

Table 5.1 Details of the polishing conditions from Run 1 to Run 4 (prior each polishing run the groove formed on the bevel of the polishing cup was removed).

Polishing Conditions	Run 1	Run 2	Run 3	Run 4
Polishing Speed (rpm)	2000	2000	2000	2000
Polishing Load (N/ball)	1.5	1.5	1.5	1.5
Polishing Time (minutes)	240	240	240	240
Amount of Magnetic Fluid used (ml)	180	180	180	180
Abrasives (Boron Carbide, 500 grit)	same	same	same	same
Abrasive Concentration (% vol.)	20	20	20	20

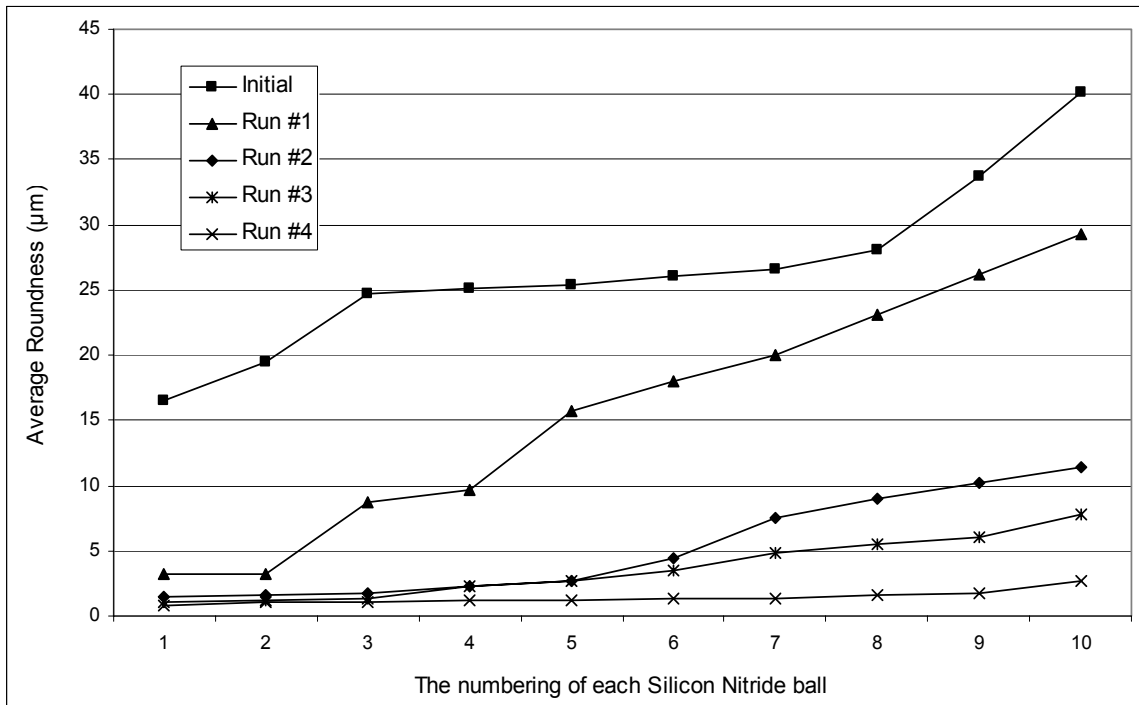


Figure 5.1.1 Average roundness improvement of a batch of Si<sub>3</sub>N<sub>4</sub> balls (10 balls of 0.9 in. diameter) after 4 polishing runs.

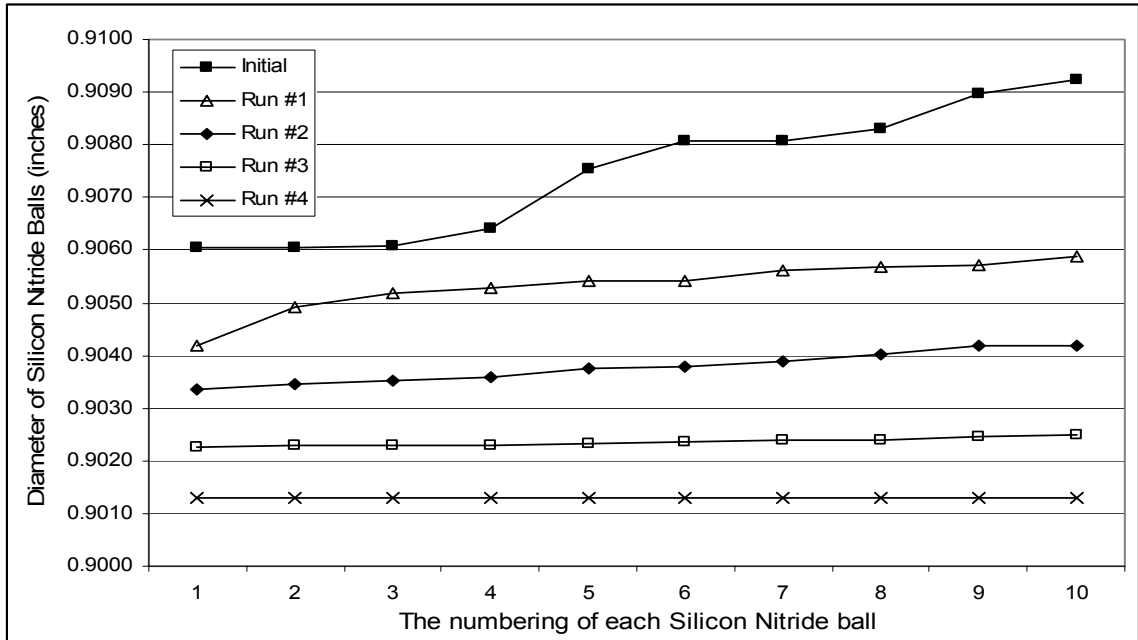


Figure 5.1.2 Ball diameter reduction and shape improvement of a batch of  $\text{Si}_3\text{N}_4$  balls (10 balls of 0.9 in. diameter) after 4 polishing runs.

Then, a groove formed on the bevel of the polishing cup during polishing (in Run 4) was maintained and used in Run 5. Figure 5.1.3 shows an average roundness of the balls was greatly improved from  $1.43 \mu\text{m}$  ( $0.78 - 2.72 \mu\text{m}$ ) to  $0.94 \mu\text{m}$  ( $0.70 - 1.12 \mu\text{m}$ ) and the uniform geometry of balls ( $0.8996$  in. diameter) was also maintained. Hence, a properly formed groove on the bevel of the polishing cup during polishing plays an important role in improving the roundness of the balls. The details of the polishing conditions are shown in Table 5.2, Run 4 and 5.

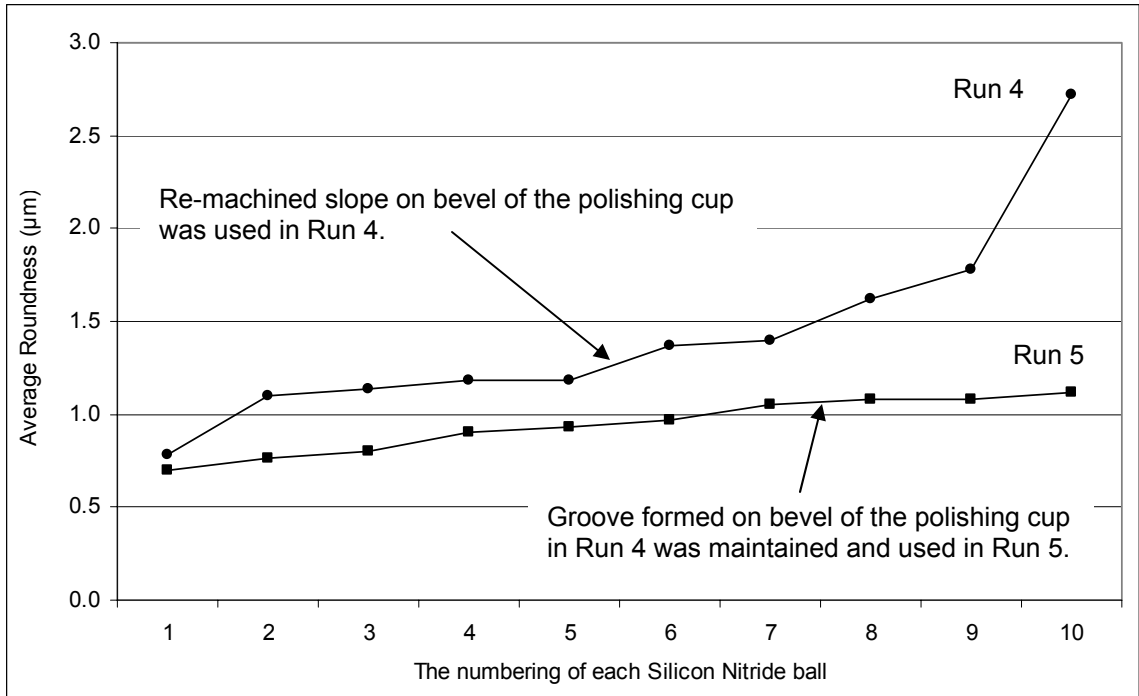


Figure 5.1.3 Variation of average roundness for different balls with the groove (Run 5) and re-machined groove (Run 4) on the polishing cup.

Table 5.2 Detail of polishing conditions in Run 4 and 5

Polishing Conditions	Run 4	Run 5
Polishing Speed (rpm)	2000	2000
Polishing Load (N/ball)	1.5	1.5
Polishing Time (min)	240	240
Amount of Magnetic Fluid used (ml)	180	180
Abrasives	Boron Carbide, 500 grit	Boron Carbide, 500 grit
Abrasive Concentration (% vol.)	20	20

Again, in Run 6, the groove formed on the bevel of the polishing cup during Run 5 was removed. The same polishing conditions of Run 5 were used in Run 6. Surprisingly, Figure 5.1.4 shows a slightly better average roundness of 0.86 µm (0.63 – 1.15 µm) was obtained.

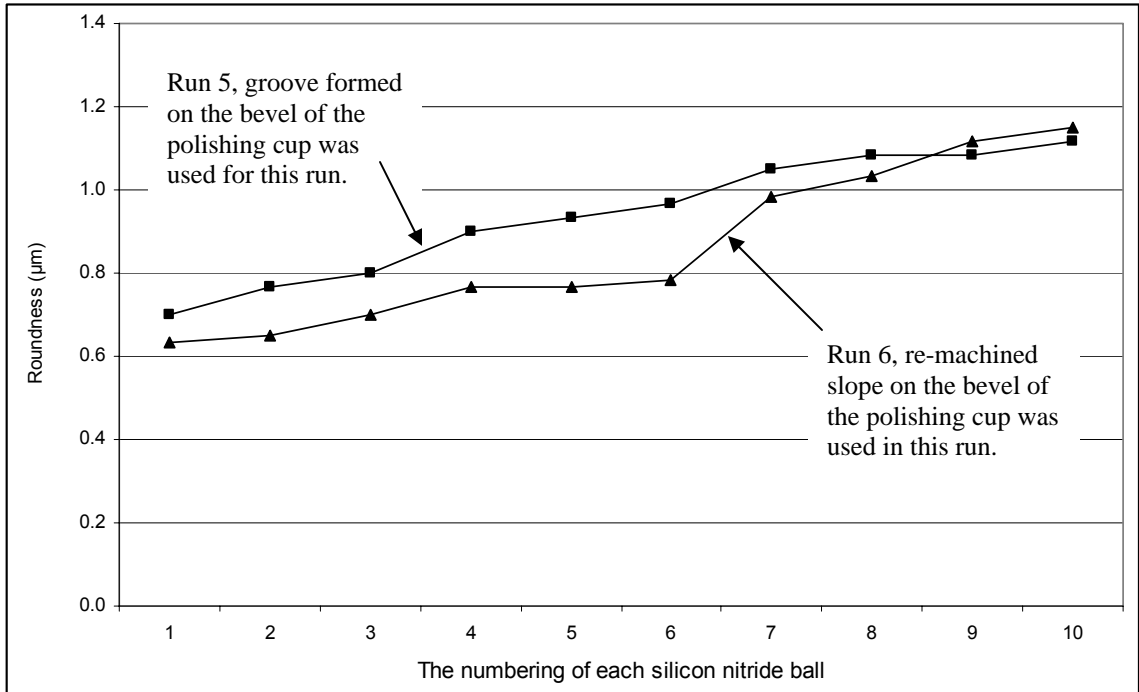


Figure 5.1.4 Variation of average roundness for different balls with the re-machined groove (Run 6) and groove (Run 5) on the polishing cup.

Therefore, from the previous observations, without groove or properly groove formed on the bevel of the polishing cup, poor average roundness should be found. But, it is not what happened in Run 6. Hence, another important hidden polishing parameters of MFP process that is not easily revealed and studied by the ordinary MFP apparatus, was found and confirmed. It was found that the MFP process would only improve the roundness and diameter of the balls, as long as other polishing parameters (e.g. optimum polishing speed, load and time) and polishing set-up (e.g. the alignment of polishing apparatus) are maintained. The groove formed on the bevel of the polishing cup was only required to further improve the roundness of the balls.



Here, another new batch of  $\text{Si}_3\text{N}_4$  balls (10 balls of 0.9 in. diameter) was used to conduct another study of the groove formed on the polishing cup during polishing. The groove formed on the bevel of the polishing cup in Run 1, was maintained throughout the runs at roughing stage and semi-finishing stage, the average roundness of balls was further improved.

At the roughing stage, Figures 5.1.5(a) and (b) show the average roundness was greatly improved from  $29.30 \mu\text{m}$  to  $0.87 \mu\text{m}$  ( $0.53 - 0.90 \mu\text{m}$ ), after 7 polishing runs. The details of polishing conditions are shown in Table 5.3, Run 1 to 7.

Table 5.3 Details of the polishing conditions for Runs 1 to 7

<b>Polishing Conditions</b>	<b>Run 1</b>	<b>Run 2</b>	<b>Run 3</b>	<b>Run 4</b>	<b>Run 5</b>	<b>Run 6</b>	<b>Run 7</b>
Polishing Speed (rpm)	2000	2000	2000	2000	2000	2000	2000
Polishing Load (N/ball)	2.0	2.0	2.0	2.0	2.0	2.0	2.0
Polishing Time (minutes)	240	240	300	300	300	300	300
Amount of Magnetic Fluid used (ml)	180	180	200	200	200	200	200
Abrasives (Silicon Carbide, 600 grit)	same	same	same	same	same	same	same
Abrasive Concentration (% vol.)	10	10	10	10	10	10	10

Table 5.4 Details of the polishing conditions for Runs 8 to 11

<b>Polishing Conditions</b>	<b>Run 8</b>	<b>Run 9</b>	<b>Run 10</b>	<b>Run 11</b>
Polishing Speed (rpm)	2000	2000	2000	2000
Polishing Load (N/ball)	2.0	2.0	2.0	2.0
Polishing Time (minutes)	300	300	300	300
Amount of Magnetic Fluid used (ml)	200	200	200	200
Abrasives (Silicon Carbide, 10,000 grit)	same	same	same	same
Abrasive Concentration (% vol.)	10	10	10	10

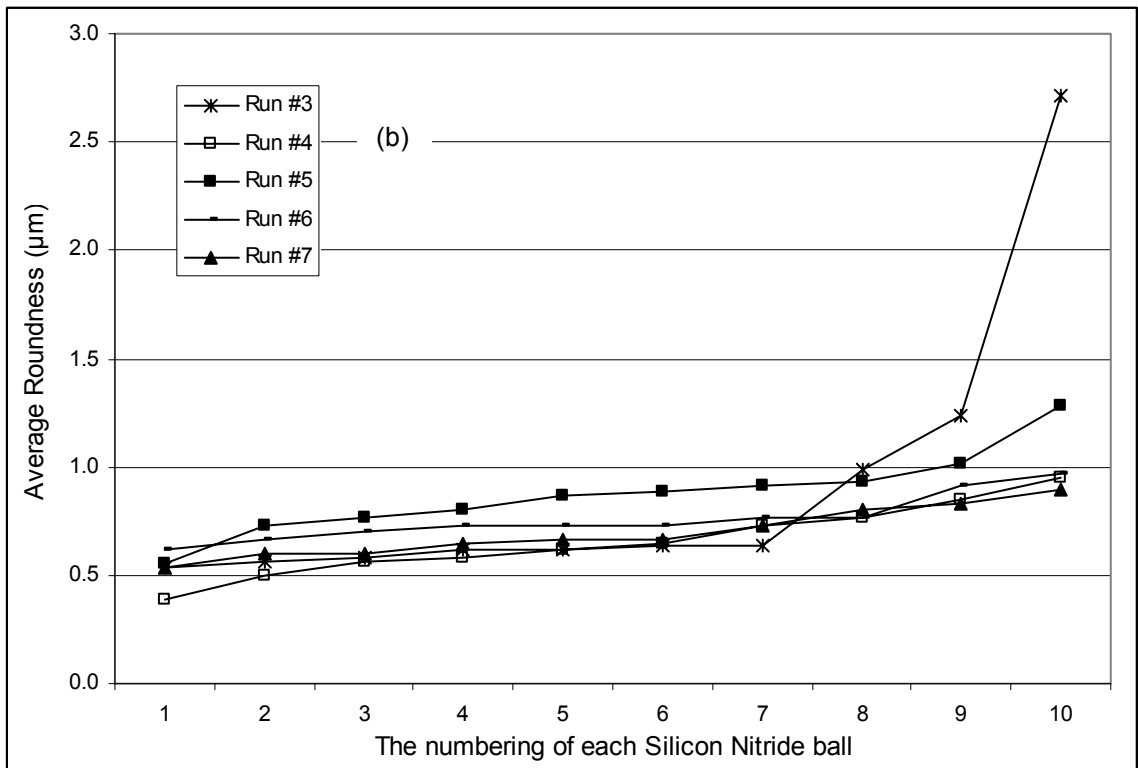
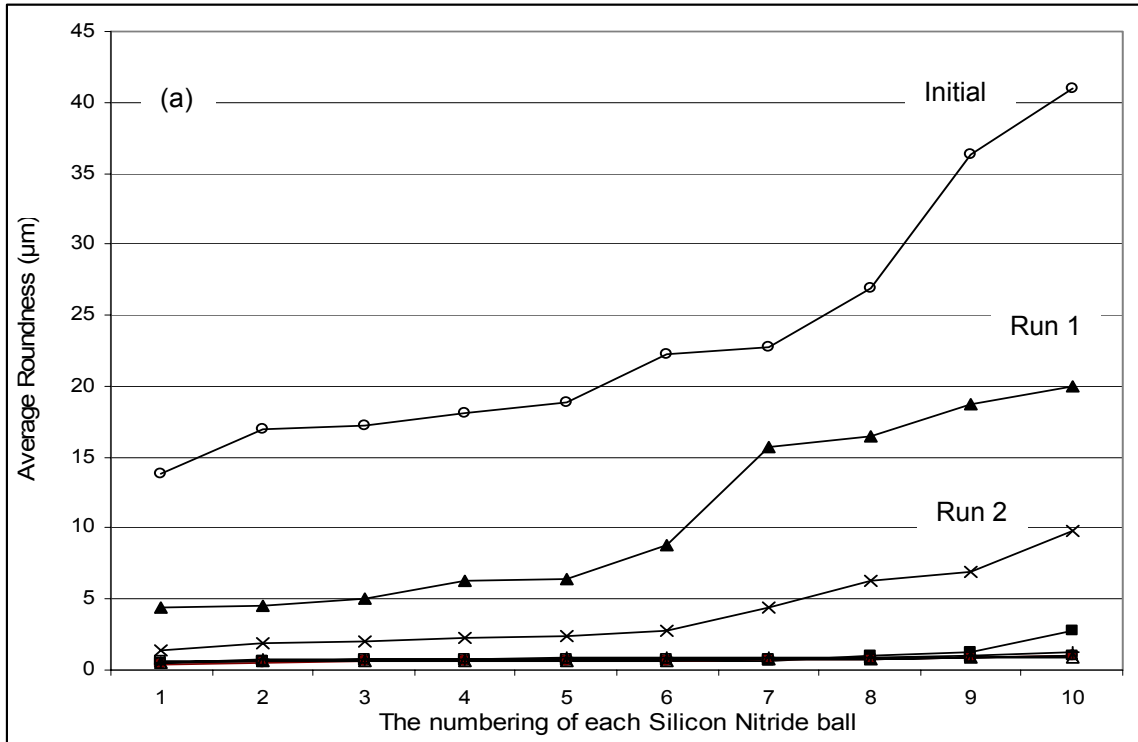


Figure 5.1.5 (At roughing stage, Runs 1 - 7) the average roundness of the balls was greatly improved by maintaining the groove throughout the runs.

At the semi-finishing stage, Figure 5.1.6 shows the average roundness was further improved to 0.58  $\mu\text{m}$  (0.43 – 0.75  $\mu\text{m}$ ). In order to provide the correct results or information, only 8  $\text{Si}_3\text{N}_4$  balls were plotted in Figure 5.1.6. This is because of two non-uniform workmaterial ( $\text{Si}_3\text{N}_4$  balls) were found, and the roundness that measured across the non-uniform area of the balls surface were very poor, as shown in Figures 5.1.7(b) and (c). Table 5.4 shows the details of polishing runs, Runs 8 to 11.

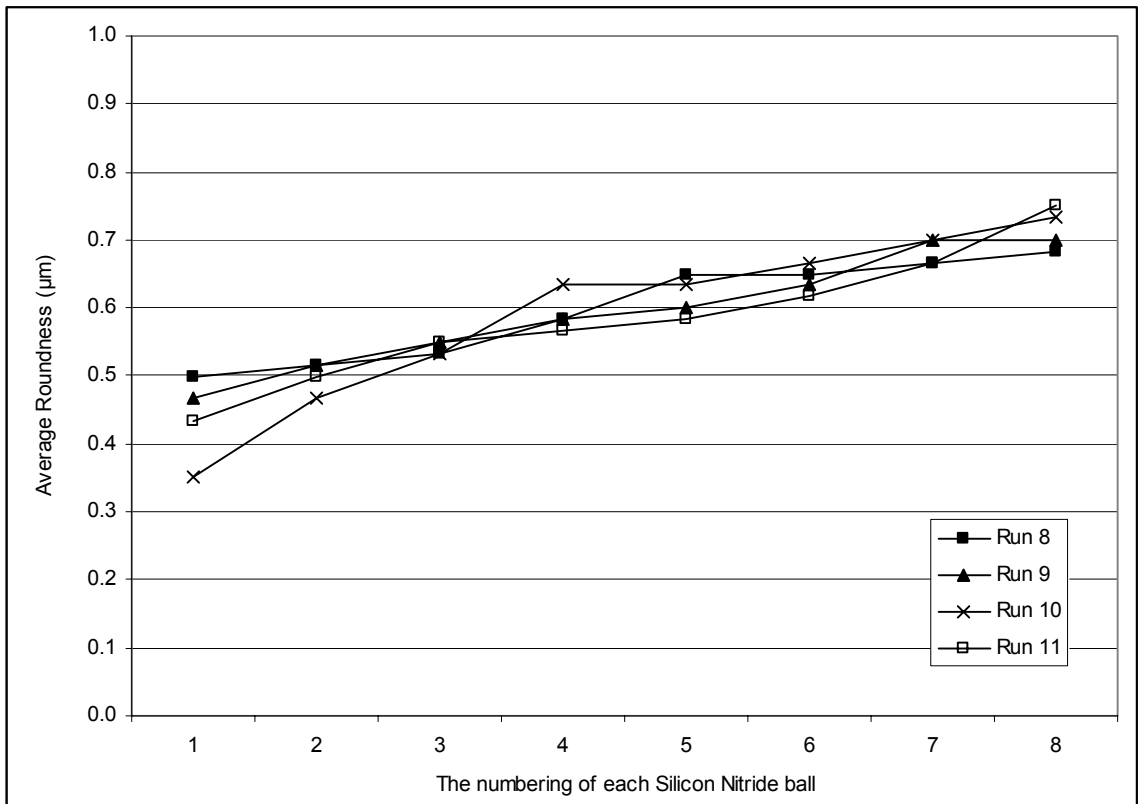
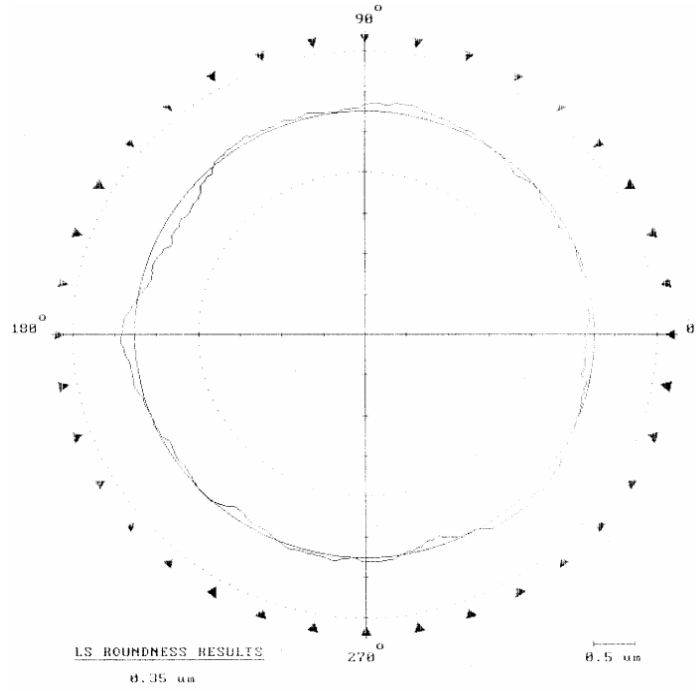
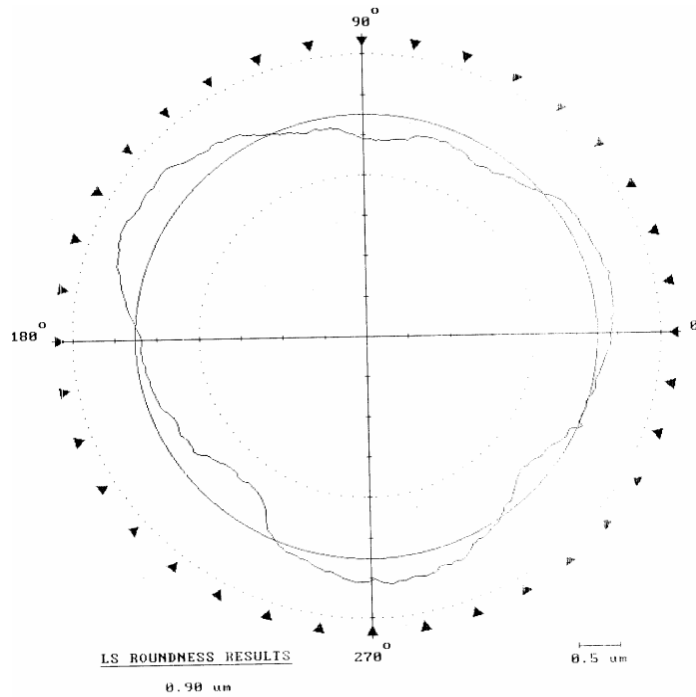


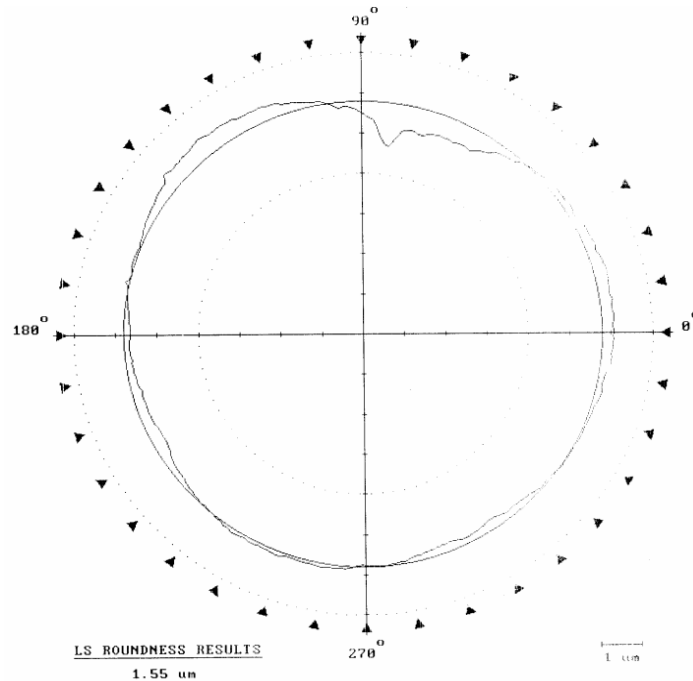
Figure 5.1.6 (At semi-finishing stage, Runs 8 - 11) the average roundness of the balls was further improved by maintaining the groove throughout the runs.



(Roundness:  $0.35 \mu\text{m}$ )  
 (a) 1<sup>st</sup> – axis measurement of roundness  
 (not crossing the non-uniform area of ball surface)



(Roundness:  $0.90 \mu\text{m}$ )  
 (b) 2<sup>nd</sup> – axis measurement of roundness  
 (near the non-uniform area of ball surface)



(Roundness: 1.55  $\mu\text{m}$ )  
(c) 3<sup>rd</sup> – axis measurement of roundness  
(crossing the non-uniform area of ball surface)

Figure 5.1.7 (a) – (c) TalyRond roundness profile of a single non-uniform workpiece ( $\text{Si}_3\text{N}_4$  ball) at three different axis measurements ( $90^\circ$  apart).

With the understanding of the above hidden polishing parameters, groove formed on the bevel of the polishing cup will further improve the roundness of the balls. Also, it is believed that with or without a groove on the bevel of polishing cup, it will not damage the roundness of the balls, as long as other polishing parameters (e.g. optimum polishing speed, load and time) and polishing set-up (e.g. the alignment of polishing apparatus) are maintained. Further, any non-uniform of workmaterial that show on the ball surface, the roundness of the particular ball is very poor and the range of the roundness is very large.

Another study of the roles and effects of the groove formed on the bevel of the polishing cup was conducted. It was the comparison of material removal rate (MRR) between the re-machined surface and groove formed on the bevel of the polishing cup. Figure 5.1.8 shows MRR was greatly reduced if the groove formed on the bevel of the polishing cup was used in Run B. The MRR was  $\sim 0.196 \mu\text{m}/\text{min}$ . On the other hand, in Run A, high MRR was found ( $\sim 0.38 \mu\text{m}/\text{min}$ ) if a re-machined surface on the bevel of the polishing cup was used. The details of the polishing conditions of Run A and B are shown in Table 5.5.

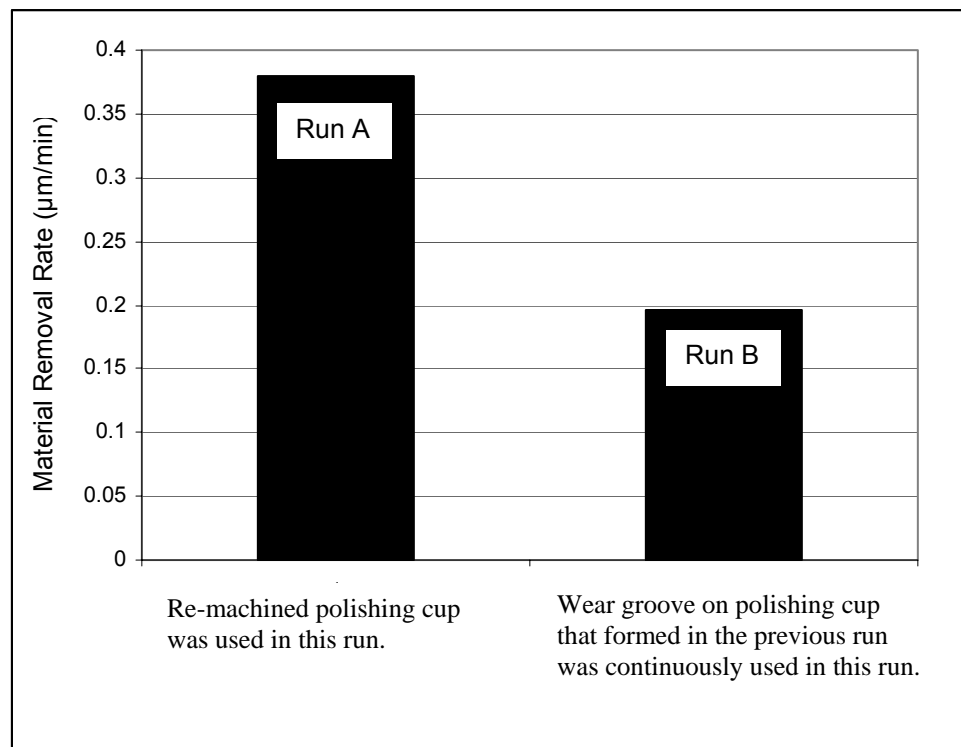


Figure 5.1.8 MRR comparison between the groove formed on the bevel of the polishing cup and re-machined surface on the bevel on the polishing cup.

Table 5.5 Polishing conditions of Run A and B

Polishing Conditions	Run A	Run B
Polishing Speed (rpm)	2000	2000
Polishing Load (N/ball)	2.0	2.0
Polishing Time (minutes)	180	300
Amount of Magnetic Fluid used (ml)	200	200
Abrasives (Boron Carbide, 500 grit)	same	same
Abrasive Concentration (% vol.)	10	10

Another abnormal observation (the surface finish of  $\text{Si}_3\text{N}_4$  balls) was found. At the roughing stage of MFP ( $\text{B}_4\text{C}$ , 500 grit), the surface finish of  $\text{Si}_3\text{N}_4$  balls that was polished with and without the presence of the groove formed on the bevel of the polishing cup were similar, with  $R_a \sim 138.4$  nm (without groove) and  $R_a \sim 138.3$  nm (with groove).

However, at the final stage of MFP ( $\text{SiC}$ , 10,000 grit), the surface finish of  $\text{Si}_3\text{N}_4$  balls that was polished, with and without the presence of the groove formed on the bevel of the polishing cup, was very different, as shown in Figure 5.1.9 (a) and (b). The surface finish was very rough ( $R_a \sim 0.47$   $\mu\text{m}$ ) with the presence of the groove formed on the bevel of the polishing cup, as shown in Figure 5.1.9(a). Also, a rough surface finish ( $R_a \sim 0.52$   $\mu\text{m}$ ) was observed with the presence of the groove formed on the bevel of the polishing cup in (Kirtane, 2004). On the other hand, if the groove was removed from the polishing cup, a very smooth surface finish ( $R_a \sim 13$  nm) was found, as shown in Figure 5.1.9 (b). Thus, it was believed that those two different surface finish profiles were caused by two different polishing mechanisms, namely, rolling (with groove) and sliding (without groove).



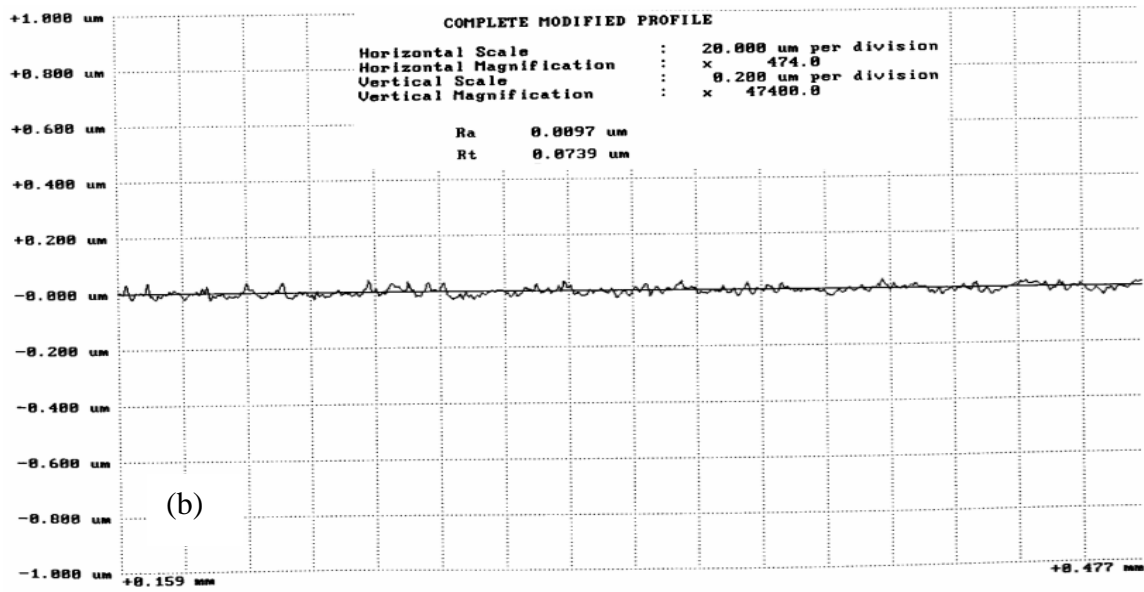
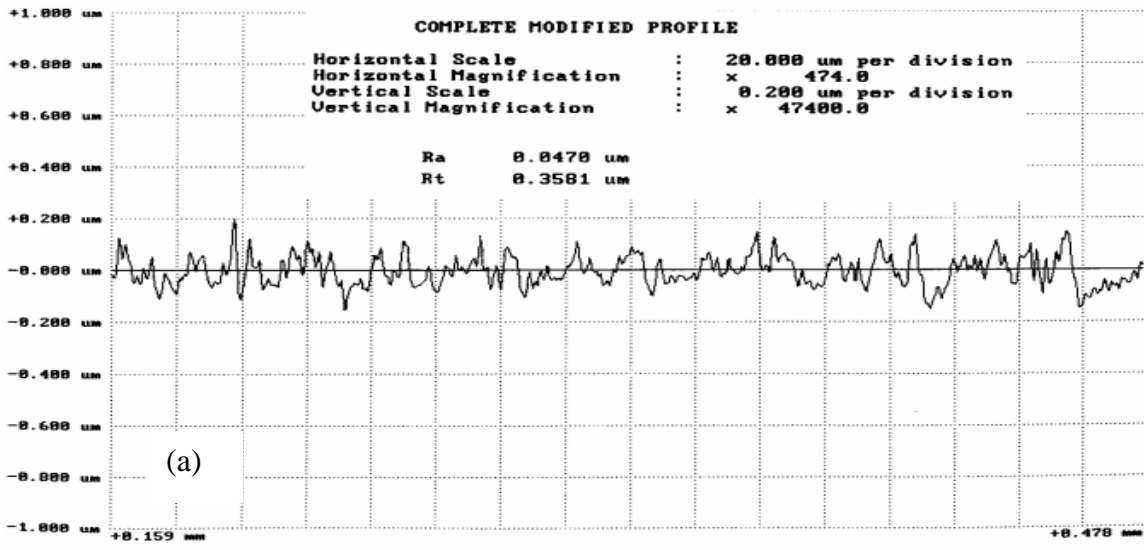


Figure 5.1.9 (a) With the presence of the groove formed on the bevel of the polishing cup, rougher surface finish of the balls was observed with SiC (10,000 grid), Ra ~ 0.47  $\mu\text{m}$  and Rt ~ 0.3501  $\mu\text{m}$ . (b) Without the presence of groove, very smooth surface finish was found, Ra ~ 9.7 nm and Rt ~ 739 nm.

## 5.2 Second experimental approach: Clarify the formation of the two distinctive magnetic fluid patterns during MFP process

Another, helpful hidden polishing parameter which was found very useful and easy to apply in MFP process, is the two distinctive magnetic fluid patterns formed during polishing (magnetic fluid pocket and magnetic fluid bubbles), as shown in Figure 5.2.1(a) and (b).

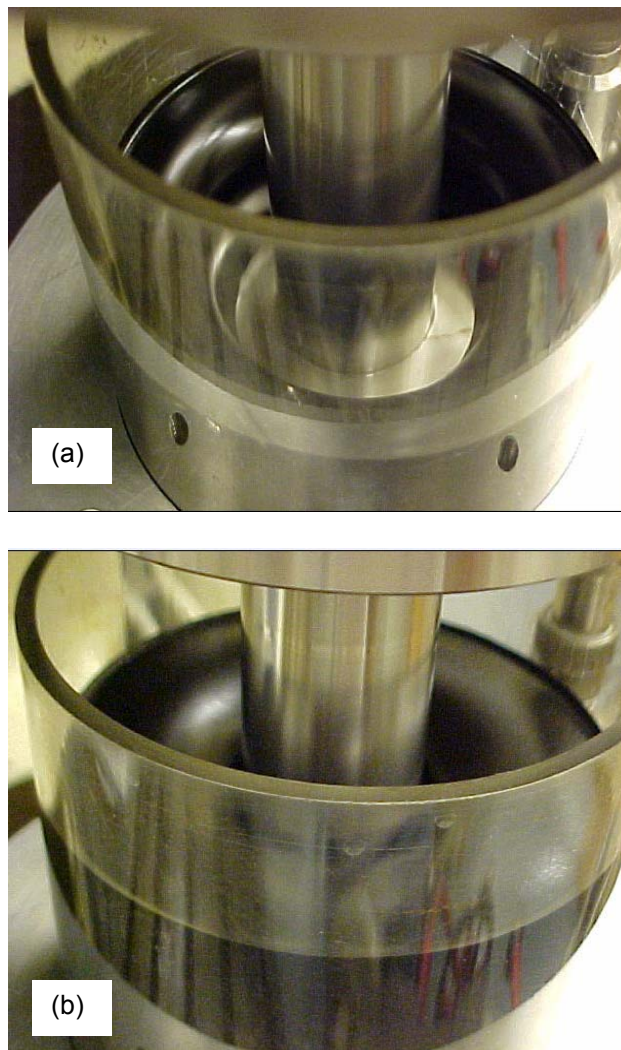


Figure 5.2.1 Two different type of magnetic fluid patterns formation during polishing, namely, (a) “magnetic fluid pocket” and (b) “magnetic fluid bubbles” patterns.

In this experimental approach, as shown in Figure 4.4, a vibration monitoring system (Vibroport 41) was added to the newly built polishing chamber to clarify the “doubt” why there were two different magnetic fluid patterns formed during polishing and only the “magnetic fluid bubbles” pattern would guarantee a better roundness of the balls. As shown in Figure 5.2.2, it was found that the “magnetic fluid bubbles” pattern generated low vibration amplitude at ~ 200 Hz excitation frequency ( $\sim 0.06 \text{ m/s}^2$ ) and only one dominant frequency spectrum was observed.

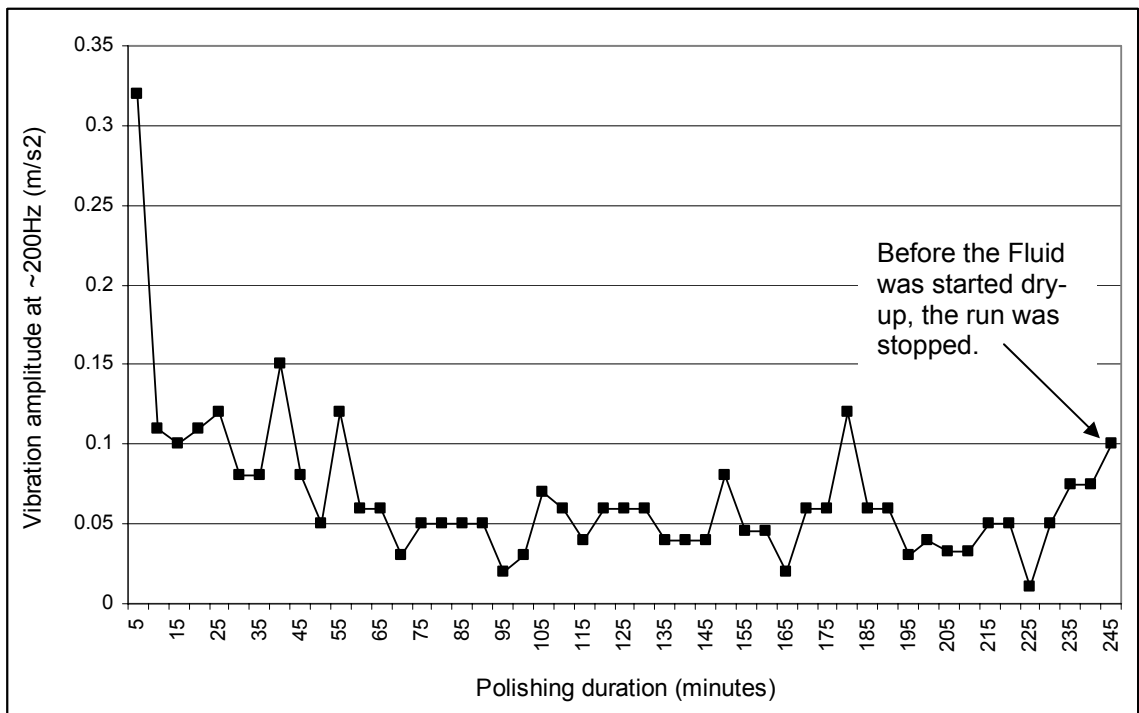


Figure 5.2.2 Average vibration amplitude of the “magnetic fluid bubbles” pattern at ~ 200 Hz excitation frequency, was  $\sim 0.06 \text{ m/s}^2$ .

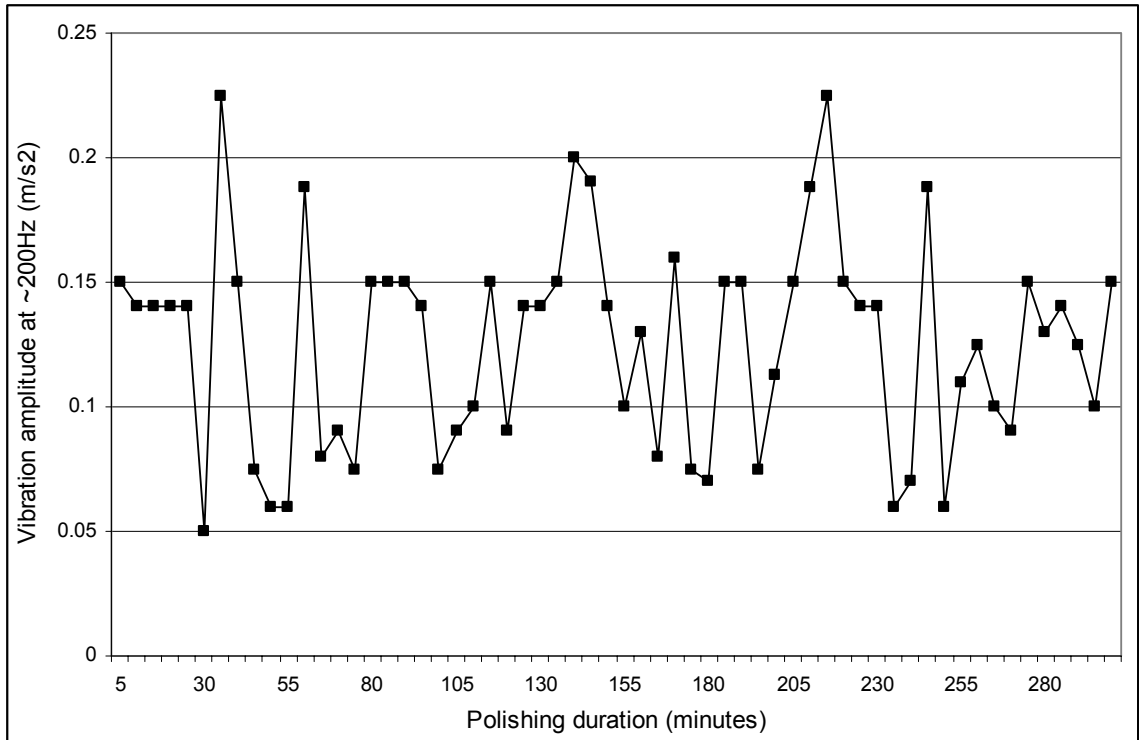
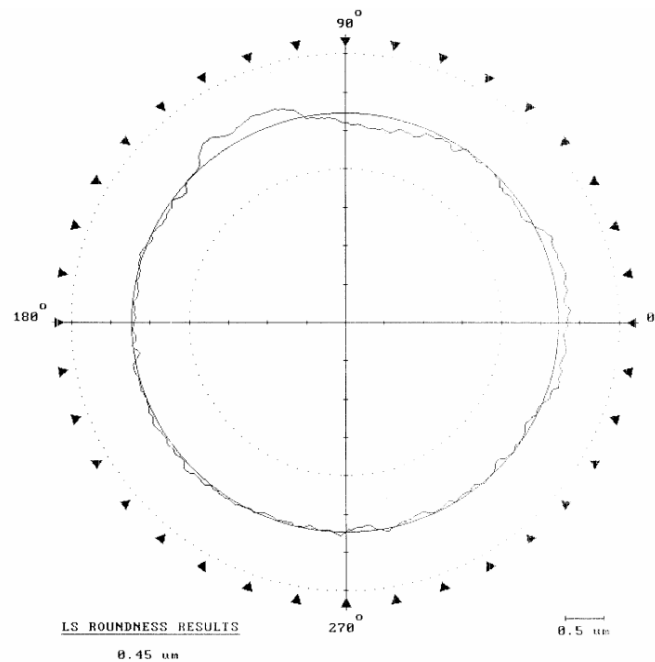


Figure 5.2.3 Average vibration amplitude of the “magnetic fluid pocket” pattern at ~ 200 Hz excitation frequency, was ~ 0.13 m/s<sup>2</sup>.

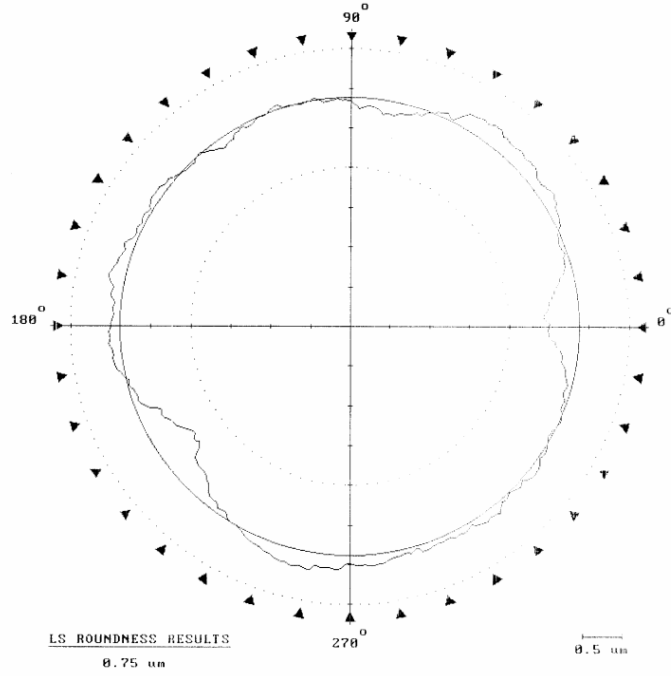
On the other hand, Figure 5.2.3 shows the “magnetic fluid pocket” pattern generated higher vibration amplitude at ~ 200Hz excitation frequency (~ 0.13 m/s<sup>2</sup>). Hence, the low amplitude of the excitation frequency (~ 200 Hz), which is analogue to the vibrating behavior of a good commercial ball bearing, indicated the “magnetic fluid bubbles” pattern during MFP process as a positive sign. It means an effective polishing run is taking place. Hence, roundness of < 1 μm is resulted. The formation of the “magnetic fluid pocket” pattern during polishing is a bad sign of MFP process. It means an ineffective polishing run is taking place.

### 5.3 Third experimental approach: Reveal and study the roles of gap/spacing among the balls during MFP process

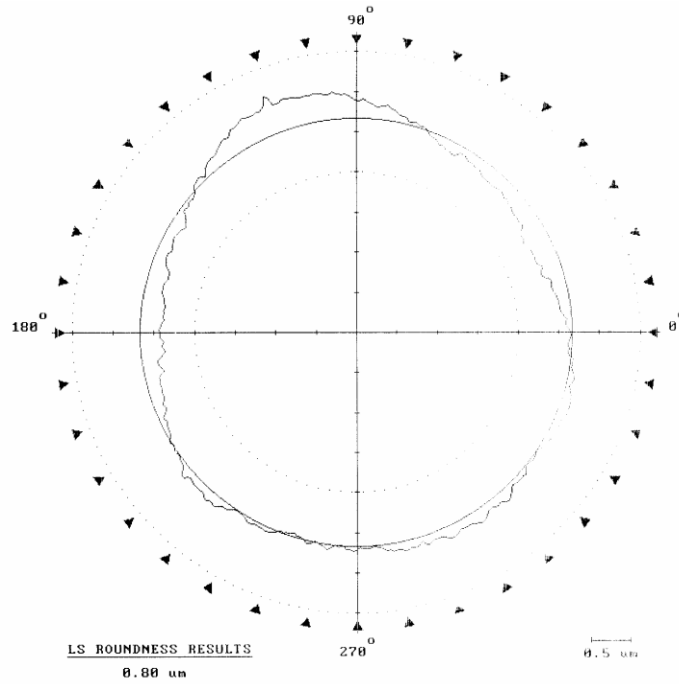
Uniform roundness of a single  $\text{Si}_3\text{N}_4$  ball is difficult to obtain when the size of the balls is larger (0.9 in.), as shown in Figure 5.3.1(a) and (b). A total of 3 measurements were taken per ball with each measurement was  $90^\circ$  apart to give the average roundness of a single ball.



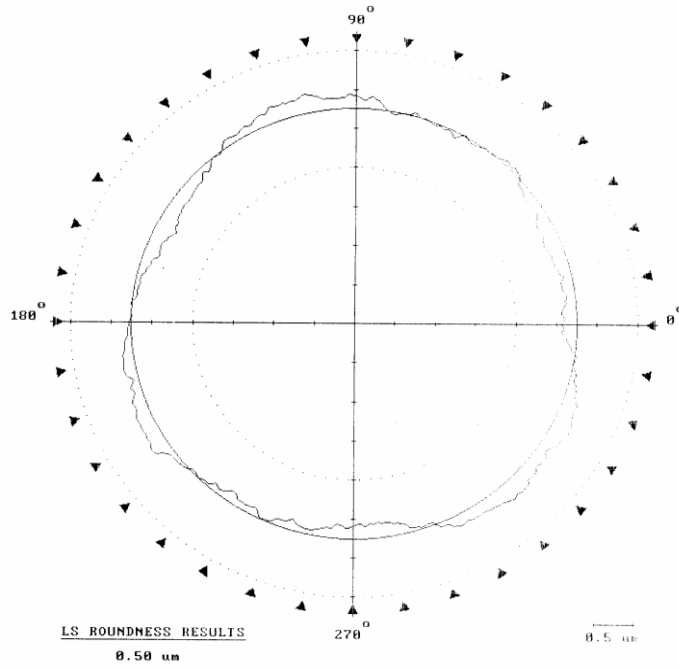
(Roundness: 0.45  $\mu\text{m}$ )  
1<sup>st</sup> – axis measurement of roundness  
(Example 1)



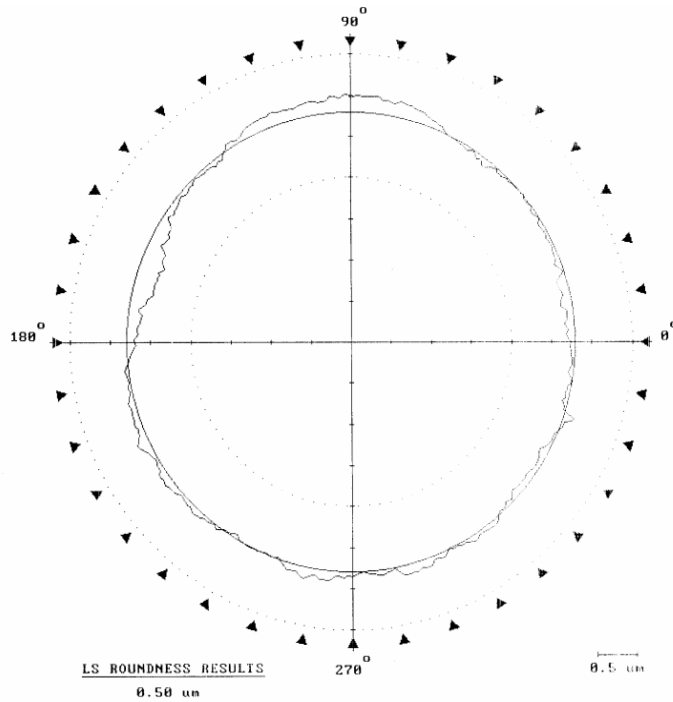
(Roundness: 0.75 μm)  
2<sup>nd</sup> – axis measurement of roundness  
(Example 1)



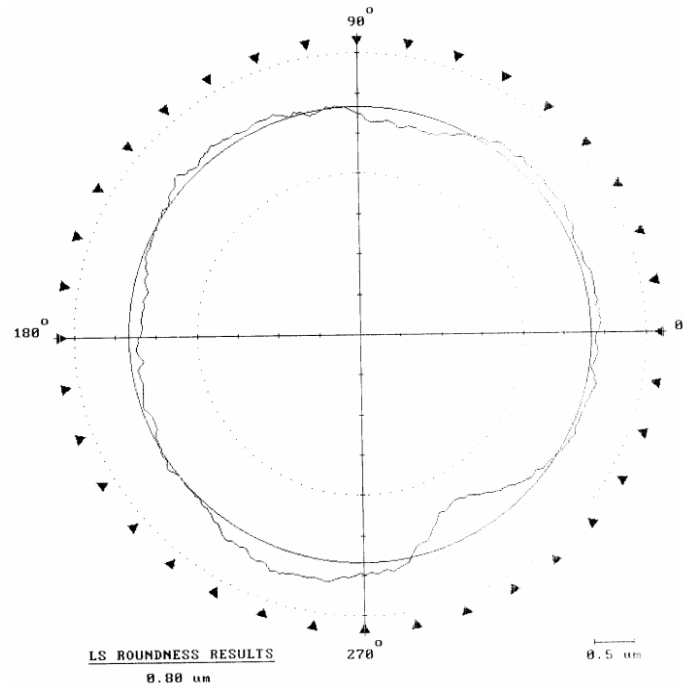
(Roundness: 0.80 μm)  
3<sup>rd</sup> – axis measurement of roundness  
(Example 1)



(Roundness: 0.50  $\mu\text{m}$ )  
 1<sup>st</sup> – axis measurement of roundness  
 (Example 2)



(Roundness: 0.50  $\mu\text{m}$ )  
 2<sup>nd</sup> – axis measurement of roundness  
 (Example 2)



(Roundness: 0.80  $\mu\text{m}$ )  
 3<sup>rd</sup> – axis measurement of roundness  
 (Example 2)

Figure 5.3.1 Non-uniform roundness of a single  $\text{Si}_3\text{N}_4$  ball, Example 1 and 2.

In order to achieve uniform roundness of a single  $\text{Si}_3\text{N}_4$  ball of 0.9 in. diameter, a batch of  $\text{Si}_3\text{N}_4$  ball (8 balls of 0.9 in. diameter) instead of (10 balls of 0.9 in. diameter) was used. This means the gap/spacing between the balls is increased, as shown in Figure 5.3.2(a) and (b). Thus, the balls can roll around the polishing chamber freely and rotate more efficiently. Figure 5.3.3 shows the low-amplitude vibration behavior (was  $\sim 0.06 \text{ m/s}^2$  at  $\sim 200 \text{ Hz}$  excitation frequency throughout the polishing run) of a batch of 8  $\text{Si}_3\text{N}_4$  balls.



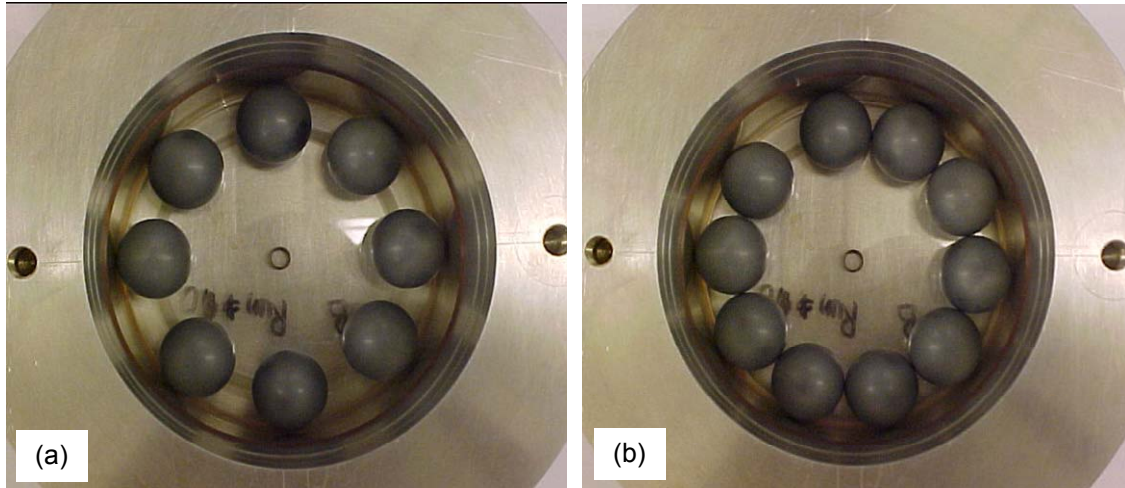


Figure 5.3.2 (a) Good gap/spacing among the balls (a batch of 8 Si<sub>3</sub>N<sub>4</sub> balls) and (b) Poor gap/spacing among the balls (a batch of 10 Si<sub>3</sub>N<sub>4</sub> balls).

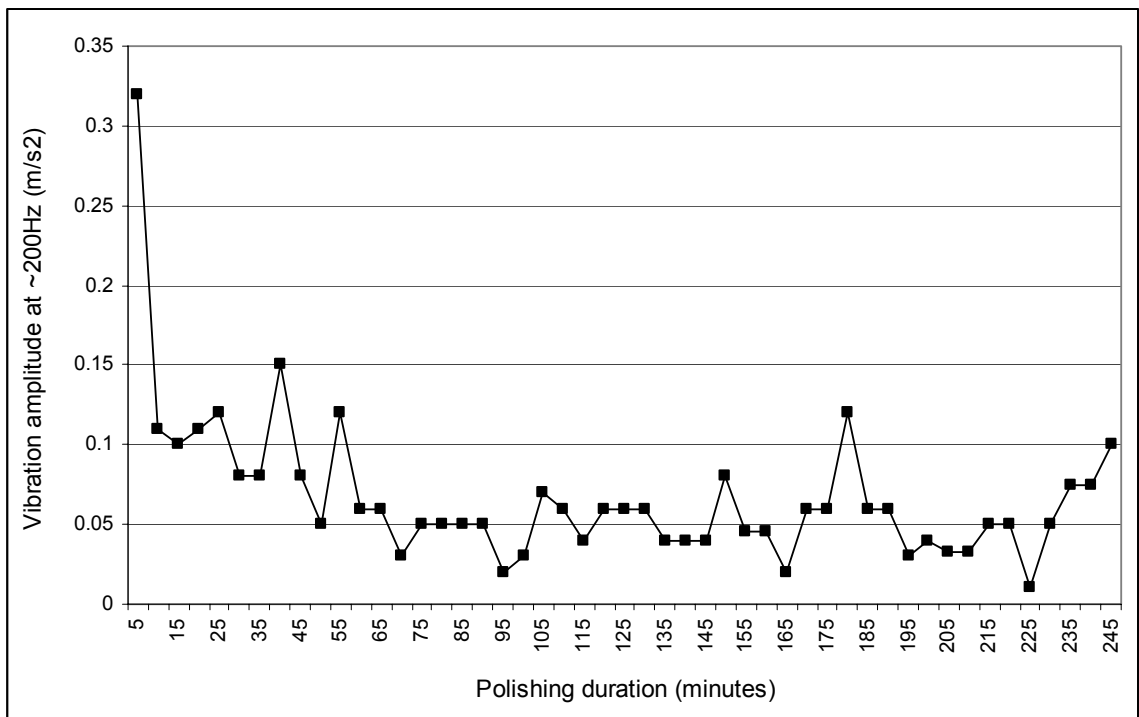


Figure 5.3.3 Low-amplitude vibration of a “good gap/spacing among the balls” polishing run. The average amplitude was ~ 0.06 m/s<sup>2</sup> at ~ 200 Hz excitation frequency throughout the polishing run.

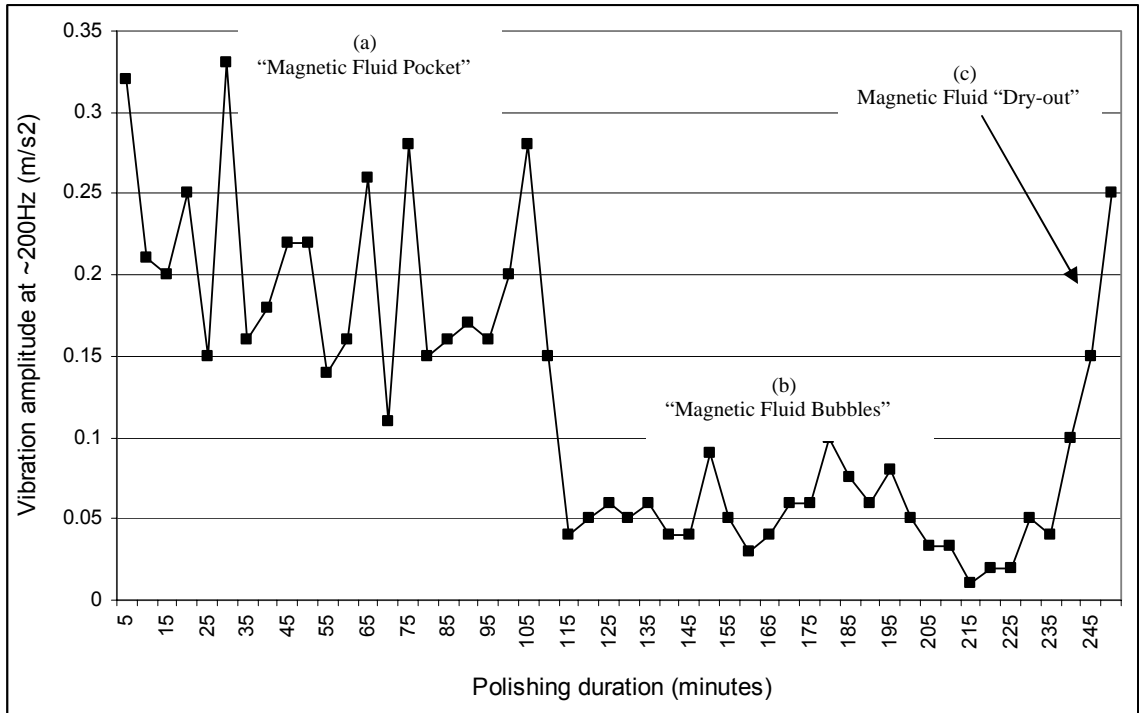


Figure 5.3.4 Vibration behavior (at ~ 200 Hz excitation frequency) of a batch of a “poor gap/spacing among the balls” polishing run. (a) High amplitude (also means the formation of the “magnetic fluid pocket” pattern) was observed, ~ 0.20 m/s<sup>2</sup> for the first 2 - 2½ hours of the run. (b) Low amplitude (also means the formation of the “magnetic fluid bubbles” pattern) was observed, ~0.06 m/s<sup>2</sup> till the end of the run. (c) Gradually increased amplitude (~ 0.25 m/s<sup>2</sup> or higher) was observed, if the polishing run was not stopped before the magnetic fluid started drying-up.

On the other hand, Figure 5.3.4 shows the “two-amplitude” vibration behavior of a batch of 10 Si<sub>3</sub>N<sub>4</sub> balls. At the beginning of the polishing run, a high vibration amplitude at ~ 200 Hz excitation frequency was observed, ~ 0.20 m/s<sup>2</sup>. After 2 to 2½ hours of the polishing time, the amplitude dropped suddenly to a lower ~ 0.06 m/s<sup>2</sup> and was maintained till the end of the run. If the polishing run was not stopped before the magnetic fluid started drying-up, the gradually increased amplitude (~ 0.25 m/s<sup>2</sup> or higher) was observed. As shown in Figure 5.3.5, at the end of each polishing run, the particular run must be stopped before

the magnetic fluid was severely dry-out. Increased of roundness was observed [Raghunandan, 1998].

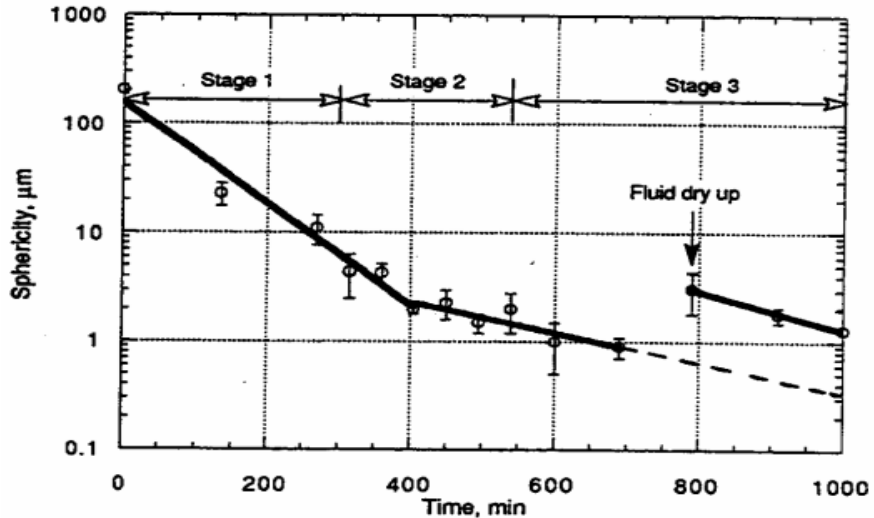
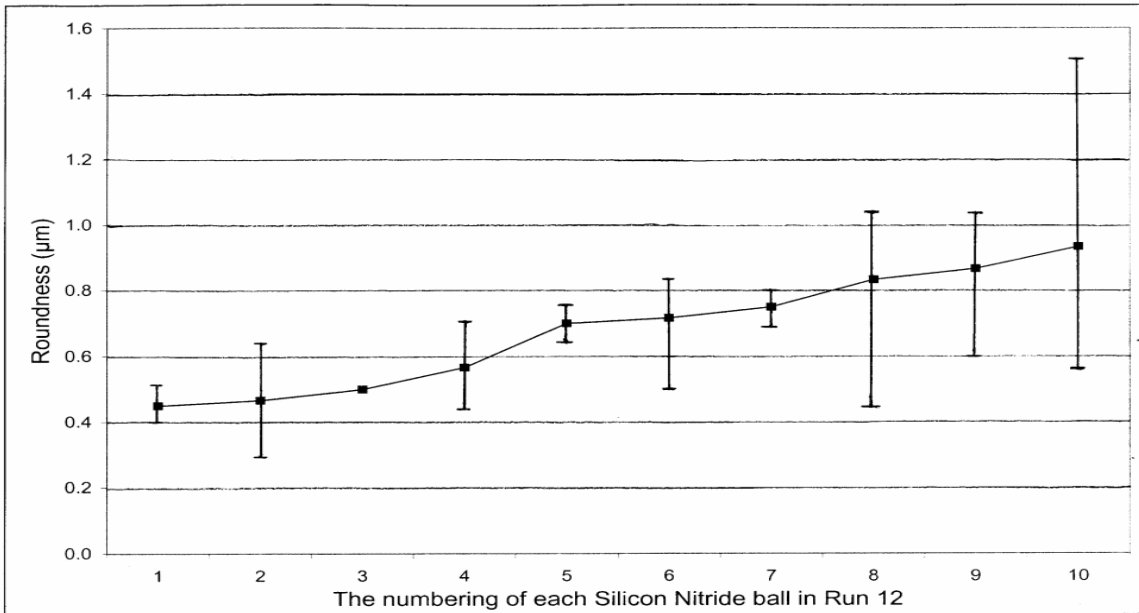
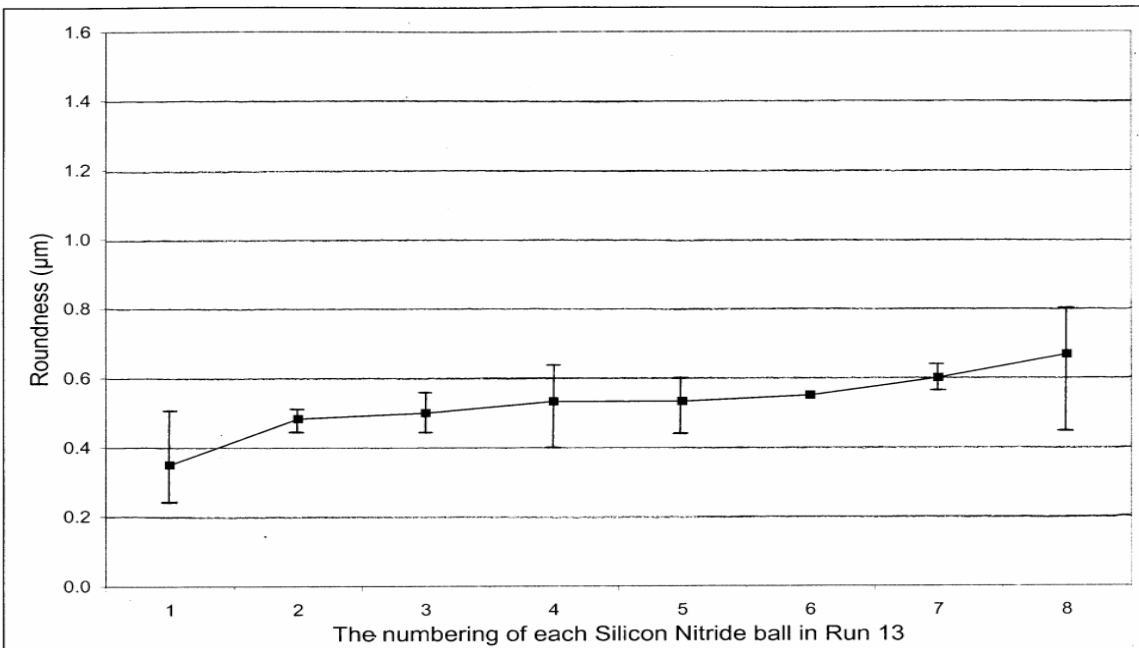


Figure 5.3.5 Poor roundness was observed, if the magnetic fluid was severely dry-out at the end of the run [Raghunandan, 1998].

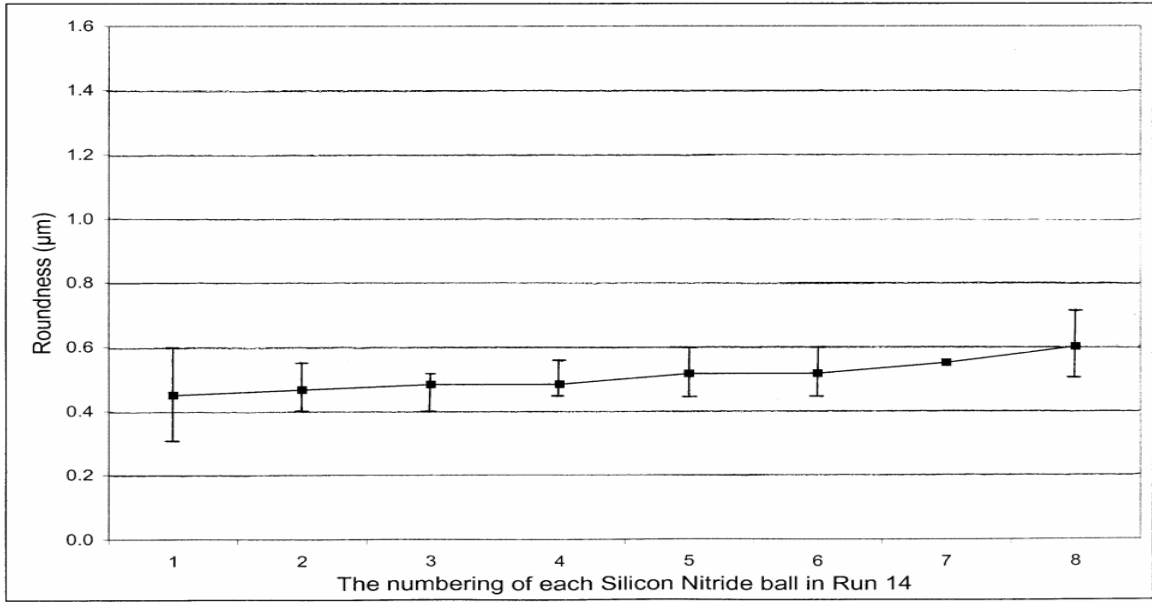
From the observations of the second experimental approach, low vibration amplitude (also means the formation of “Magnetic Fluid Bubbles” pattern) polishing run would guarantee good roundness. Hence, Figures 5.3.6(a) – (c) show a polishing run that running with a batch of 8  $\text{Si}_3\text{N}_4$  balls was more efficient than a batch of 10  $\text{Si}_3\text{N}_4$  balls. In this way, each ball was uniformly polished. At the same time, the average roundness of a batch of 8  $\text{Si}_3\text{N}_4$  balls was further greatly improved. The average roundness was  $0.51 \mu\text{m}$  ( $0.45 - 0.60 \mu\text{m}$ ), after Run 14.



(a) Poor uniform roundness of  $\text{Si}_3\text{N}_4$  balls after Run 12  
(10  $\text{Si}_3\text{N}_4$  balls)



(b) Good uniform roundness of  $\text{Si}_3\text{N}_4$  balls after Run 13  
(8  $\text{Si}_3\text{N}_4$  balls)



(b) Good uniform roundness of Si<sub>3</sub>N<sub>4</sub> balls after Run 14 (8 Si<sub>3</sub>N<sub>4</sub> balls)

Figure 5.3.6 (a) Poor uniform roundness of Si<sub>3</sub>N<sub>4</sub> balls, after Run 12 with 10 balls. (b) – (c) Good uniform roundness of Si<sub>3</sub>N<sub>4</sub> balls, after Run 13 and 14, respectively, with 8 balls.

#### 5.4 Fourth experimental approach: Found poor uniform roundness of a single Si<sub>3</sub>N<sub>4</sub> ball due to the non-uniform workmaterial

Figure 4.4.4 shows non-uniformity in the workmaterial (Si<sub>3</sub>N<sub>4</sub> balls). The non-uniformity in the workmaterial (only appear near the ball surface) is due to the residue products of the hot isostatically pressed (HIP) process, which is used to fabricate commercial Si<sub>3</sub>N<sub>4</sub> balls.

TalyRond 120L and a micrometer were used to study the shape/geometry of the non-uniform area on the uniform roundness and ball diameter of a single ball. From section 5.1(First Experimental Approach), Figure 5.1.7 shows the non-uniform area has the bad effect of getting uniform roundness of a single ball.

Poor roundness was found across or near the non-uniform area. Figures 5.4.1 (a) and (b) show the non-uniform area also has bad effect of getting uniform diameter of a single ball. Two geometry measurements with micrometer were carried out on a non-uniform workmaterial. Measurement was made away from the non-uniform area; the ball diameter was 0.8997 in. Another measurement was taken right on top of the non-uniform area; the ball diameter was 0.0001 in. smaller (0.8996 in.)

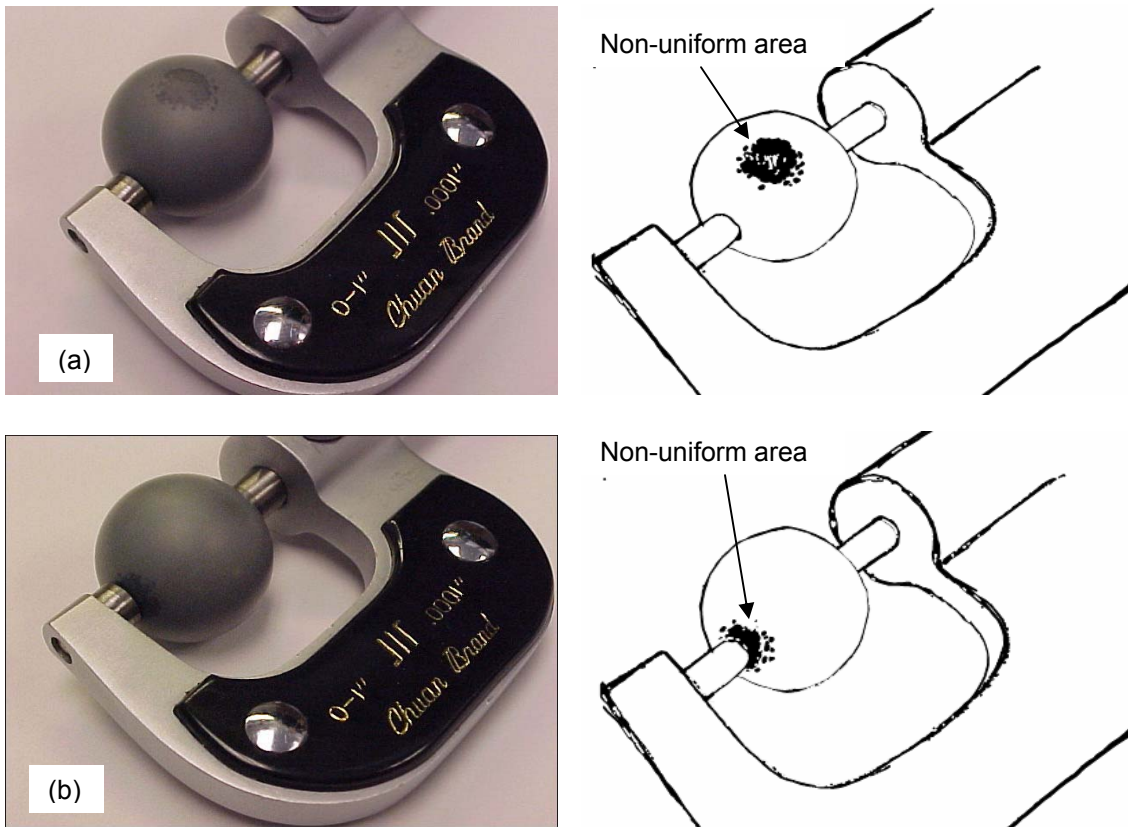


Figure 5.4.1 Two geometry measurements with micrometer were carried out on a non-uniform workmaterial. (a) Away from the non-uniform area and (b) right on the non-uniform area.

This non-uniformity in the workmaterial ( $\text{Si}_3\text{N}_4$  balls) can be effectively polished by MFP process through further reducing the diameter of the balls (if the final diameter is allowed).

### **5.5 Fifth experimental approach: Reveal and study the roles and effects of the prevention of magnetic fluid during MFP process**

In order to reduce the consumption of expensive magnetic fluid (water-based, W-40), as shown in Figure 5.5.1, a sealed-polishing chamber (simply tapped-off the top opening of the newly built chamber) was used to study the effects during the MFP process.

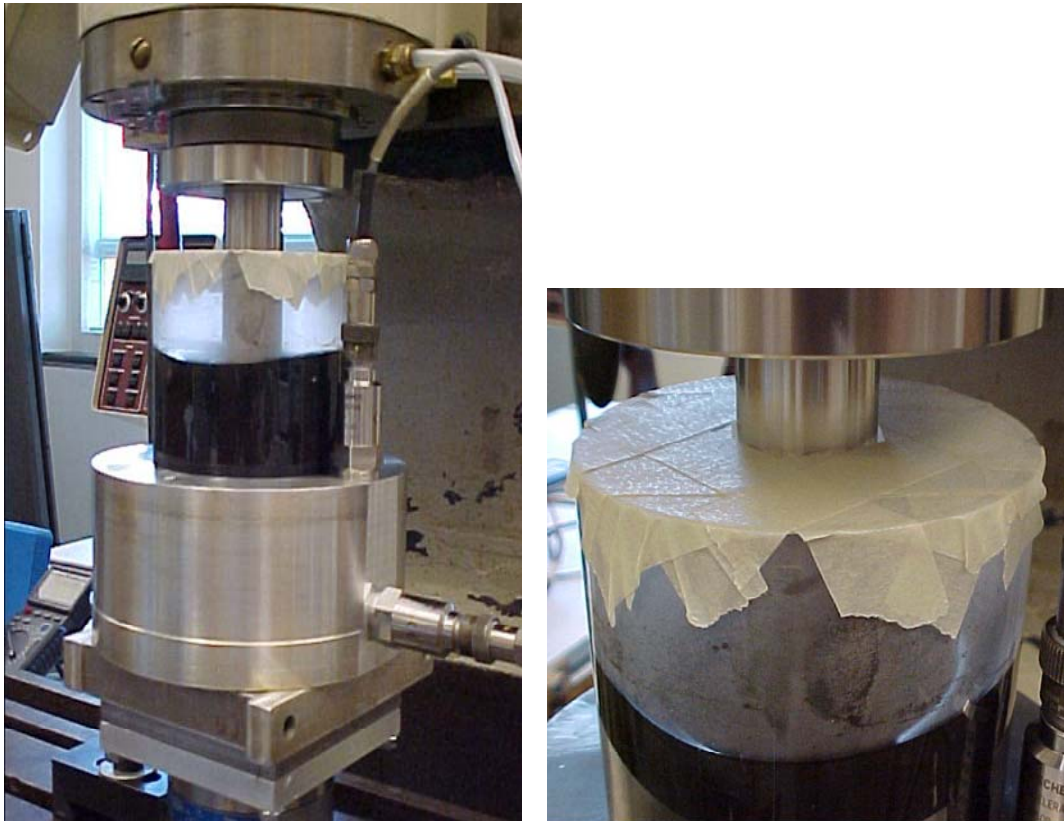


Figure 5.5.1 Photographs of sealed-polishing chamber.

After 8 hours of a single polishing run, no sign of magnetic fluid “dry-out”. It was believed that this polishing set-up would allow a single run to extend the polishing time up to 24 hours or more. Figures 5.5.2(a) – (d) show loss of water content from the heated magnetic fluid during polishing through evaporation would back to the chamber by condensation. However, the average roundness of the balls was damaged. Hence, this polishing condition is only suitable for the roughing stage where higher material removal rate is the only concern. Furthermore, surprisingly, the average roundness of the balls was damaged, which was also matched the “bad sign” of polishing; only the “magnetic fluid pocket” pattern was observed that was revealed and studied in second experimental approach.



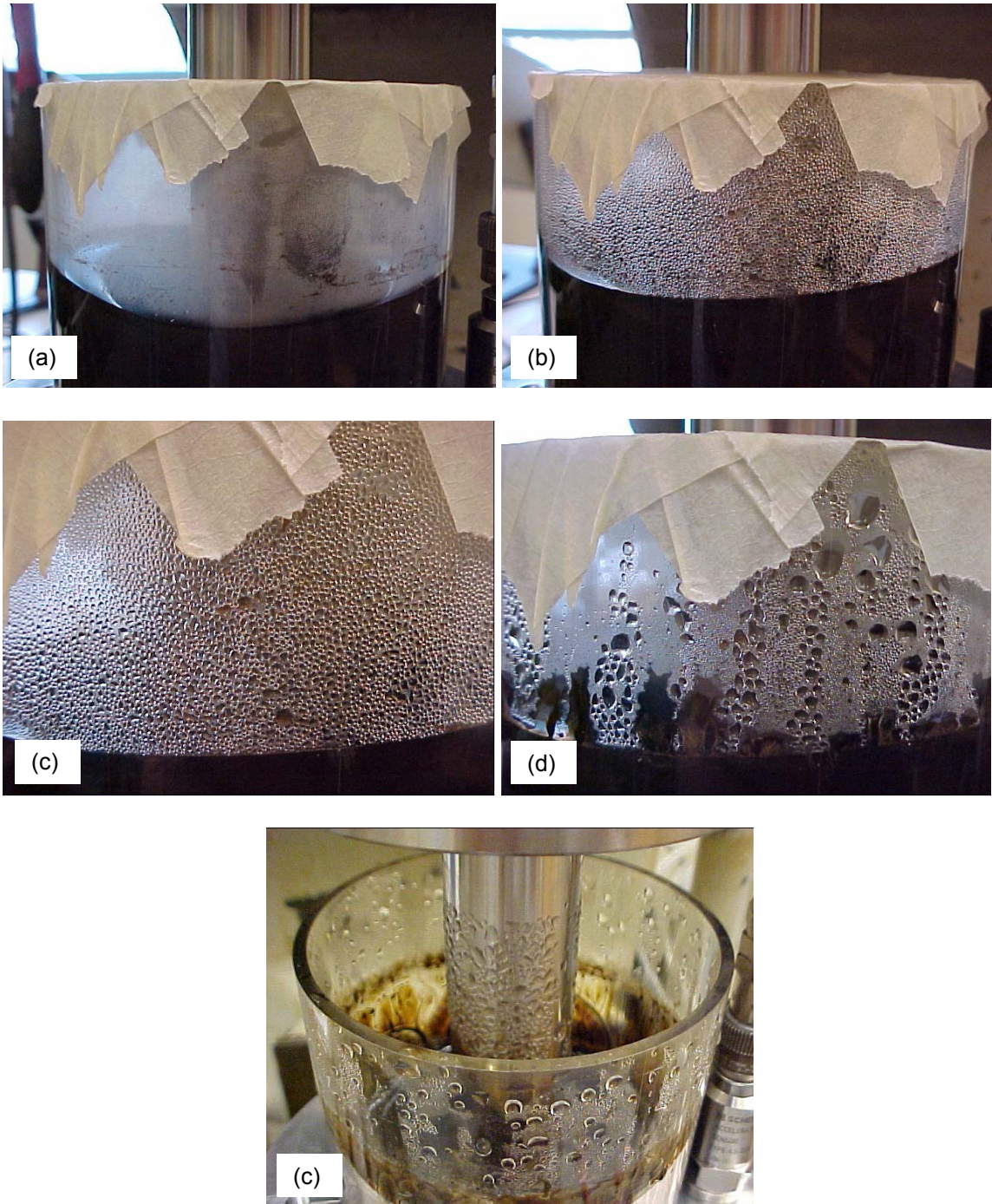


Figure 5.5.2 (a) – (b) Photographs showing evaporation and condensation of magnetic fluid during polishing. (c) A view at the end of a sealed-chamber polishing run.

## 5.6 Sixth experimental approach: Reveal and study the benefit of the after-polishing abrasives

Figure 5.6.1(a) shows the SEM image of the microstructure of the after-polished 500 grit boron carbide. It was found that the shape and the sharp edges of the abrasives were still maintained. As shown in Figure 5.6.1(b), if compare the after-polished 500 grit B<sub>4</sub>C abrasives with the fresh 1500 grit B<sub>4</sub>C abrasives, except the size of the abrasive grains, they are similar.

Thus, it is believed that, if the after-polished 500 grit B<sub>4</sub>C abrasives were collected and successfully separated from the magnetic fluid, and it can be used as fresh 1500 grit B<sub>4</sub>C abrasives for the following polishing stage or for other applications, the overall cost of the MFP process can be reduced. In this study, the after-polishing abrasives was successfully separated from the magnetic fluid through (time consuming method) settling the more dense abrasives at the bottom of a container that consist of huge amount of water.

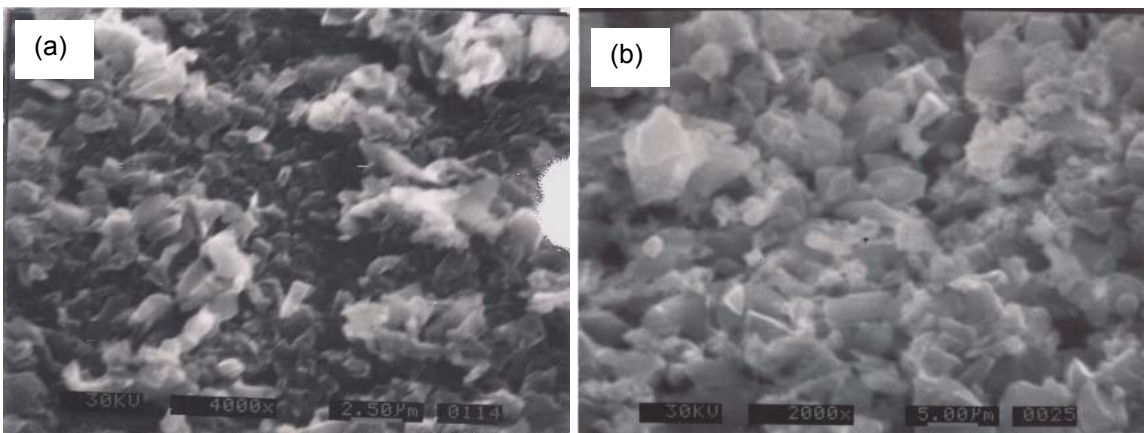


Figure 5.6.1 SEM images of: (a) After-polished 500 grit B<sub>4</sub>C abrasives and (b) fresh 1500 grit B<sub>4</sub>C abrasives.

## Chapter 6

### Conclusions

1. The emphasis of this thesis was to reveal and study the “hidden” polishing parameters in MFP process.
2. The “Critical Polishing Condition” apparatus was developed and built for this investigation. It was simply defined as: using a small polishing chamber (4 in. inside diameter) to finish much larger  $\text{Si}_3\text{N}_4$  balls (10 balls of 0.9 in. diameter).
3. Six experimental approaches were used to reveal, study, and clarify the roles and effects of the “hidden” polishing parameters in MFP process.
4. The “Critical Polishing Condition” and the 6 experimental approaches had successfully revealed the “hidden” polishing parameters in MFP process.
5. A properly formed groove on the bevel of the polishing cup during polishing plays an important role in improving the roundness of the balls. The roundness of the balls was greatly improved from  $1.43\ \mu\text{m}$  ( $0.78 - 2.72\ \mu\text{m}$ ) to  $0.94\ \mu\text{m}$  ( $0.70 - 1.12\ \mu\text{m}$ ) with the use of the groove.
6. Once the roundness of the balls was good (less than  $1\ \mu\text{m}$ ); without using the groove formed on the polishing cup, the roundness of the balls was not damaged, on the other hand, it was slightly improved. The roundness of  $0.86\ \mu\text{m}$  ( $0.63 - 1.15\ \mu\text{m}$ ) was obtained.

7. It was found that the MFP process would only improve the roundness and diameter of the balls, as long as other polishing parameters (e.g. optimum polishing speed, load and time) and polishing set-up (e.g. the alignment of polishing apparatus) are maintained. The groove formed on the bevel of the polishing cup was only required to further improve the roundness of the balls.
8. The groove formed on the bevel of the polishing cup in Run 1, was maintained throughout the runs at roughing and semi-finishing stage, the average roundness of balls was further improved. This means the proper size (optimum condition) of the groove formed on the bevel of the polishing cup was needed to obtain better roundness. The average roundness was further improved to  $0.58\ \mu\text{m}$  ( $0.43 - 0.75\ \mu\text{m}$ ).
9. Higher MRR ( $\sim 0.38\ \mu\text{m}/\text{min}$ ) was found in the run that used re-machined surface on the bevel of the polishing cup than the run that used the groove formed on the bevel of the polishing cup ( $\sim 0.196\ \mu\text{m}/\text{min}$ ).
10. The surface finish of  $\text{Si}_3\text{N}_4$  balls (at the final stage of MFP that using SiC abrasives, 10,000 grit) that was polished with and without the presence of the groove formed on the bevel of the polishing cup was very different. The surface finish was very rough ( $R_a \sim 0.47\ \mu\text{m}$ ) with the presence of the groove formed on the bevel of the polishing cup. On the other hand, if the groove was removed from the polishing cup, a very smooth surface finish ( $R_a \sim 13\ \text{nm}$ ) was found. It was believed that those two different surface

finish profiles were caused by two different polishing mechanisms, namely, rolling (with groove) and sliding (without groove).

11. Two distinctive magnetic fluid patterns were formed during polishing (magnetic fluid pocket and magnetic fluid bubbles). The “magnetic fluid bubbles” pattern was considered as a positive sign, which means an effective polishing run is taking place. Hence, roundness of  $< 1 \mu\text{m}$  was resulted. However, the “magnetic fluid pocket” was a bad sign of MFP process.
12. A vibration monitoring system (Vibroport 41) was added to the newly built polishing chamber to clarify the formation of the two different magnetic fluid patterns formation during polishing and only the “magnetic fluid bubbles” pattern would guarantee a better roundness of the balls. It was found that the “magnetic fluid bubbles” pattern generated low vibration amplitude at  $\sim 200 \text{ Hz}$  excitation frequency ( $0.06 \text{ m/s}^2$ ), which analogues to the vibrating behavior of a good commercial ball bearing.
13. Uniform roundness of a single  $\text{Si}_3\text{N}_4$  ball is difficult to obtain when the size of the balls considered is large. In order to achieve uniform roundness of a single  $\text{Si}_3\text{N}_4$  ball of 0.9 in. diameter, a batch of  $\text{Si}_3\text{N}_4$  ball (8 balls of 0.9 in. diameter) instead of (10 balls of 0.9 in. diameter) was used. This means the gap/spacing among the balls is increased. The uniform roundness of a single  $\text{Si}_3\text{N}_4$  ball was greatly improved and the average roundness was also improved to  $0.51 \mu\text{m}$  ( $0.45 - 0.60 \mu\text{m}$ ).

14. The non-uniformity in the workmaterial ( $\text{Si}_3\text{N}_4$  balls) has a detrimental effect on obtaining uniform roundness and diameter of a single ball. Thus, material has to be removed in order to improve uniformity and size of the balls (if the final diameter is allowed).
15. In order to reduce the consumption of expensive magnetic fluid (water-based, W-40), a sealed-polishing chamber (simply tapped-off the top opening of the newly built chamber) was used. An 8-hour of a single polishing run was carried out and no sign of magnetic fluid “dry-out” was observed. It is believed that this polishing set-up would allow the polishing time of a single run to extend up to 24 hours or more. However, the average roundness of the balls was damaged.
16. The SEM image of the after-polished 500 grit boron carbide shows that the shape and the sharp edges of the abrasives were still maintained, except the size of the abrasive grains. It was believed that it can be used as 1500 grit  $\text{B}_4\text{C}$  abrasive for the following polishing stage or for other applications, in order to reduce the overall cost of the MFP process.

## **Chapter 7**

### **Future Work**

Number of “hidden” polishing parameters that played important roles in MFP process were successfully revealed and understood through the efforts of this investigation. However, it was believed that there may be other “hidden” polishing parameters yet to be found. There can be identified as (1) modification of the existing polishing chamber with a water cooling system, (2) modification of the existing permanent magnets base with a grid (magnetic field insulator, such as copper) to separate each magnet, and (3) SEM study of the ball’s surface after each polishing stage or polishing condition.

#### **7.1 Modified the existing polishing chamber with a water cooling system**

In order to reduce the consumption of the expensive magnetic fluid, an improved cooling system (other than the sealed-polishing chamber used in the fifth experimental approach) needs to be considered. Figure 7.1.1 shows a simple modification and inexpensive design of a cooling system to the newly built polishing chamber that is used in this investigation. A slot or channel is machined on the polishing chamber and two holes for water in and out were made. In order to prevent the water flows over the chamber, acrylic plate can be easily made to

seal the slot. Then, other functions, such as thermometer and flow meter, can be included to have better control of the cooling system. It is understood that this cooling system design is not as efficient as commercial cooling systems, such as coil-cooling system and fins-cooling system. However, it is a good start to study the effects of this cooling system in MFP process. If the study reveals the cooling system is not affecting the polishing results and instead prolong the polishing time and reduce the consumption of magnetic fluid; then, a better design of cooling system will be the next task of developing a more economic MFP process.

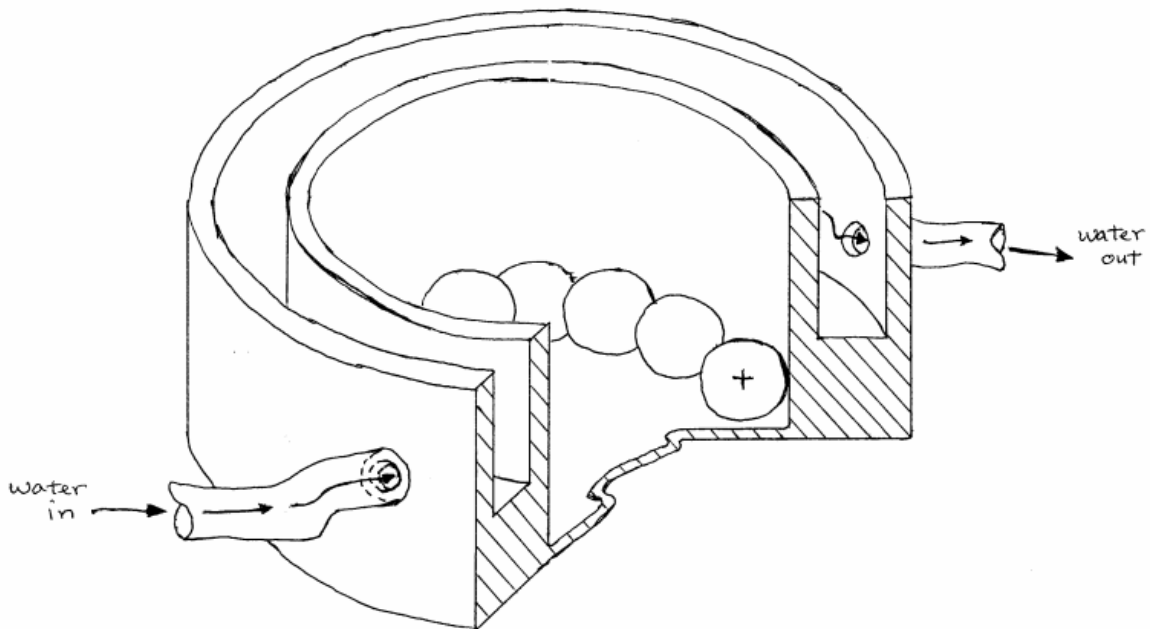


Figure 7.1.1 A simple modification and inexpensive design of cooling system to the newly built polishing chamber that used in this thesis.



## **7.2 Modified the existing permanent magnets base with a copper grid**

It is known that a stronger magnetic field can be created through separating each permanent magnet with a copper grid (magnetic field insulator). Thus, the newly made permanent magnets base could be modified with the copper grid, in order to offset some of the lose magnetic strength due to the 1 mm thickness of aluminum base of polishing chamber. With a stronger magnetic field, the stability of magnetic fluid that is a function of temperature can be greatly improved. Not to forget, the stability of the magnetic fluid is another important parameter of MFP process. Some simple experiments were conducted to determine the thickness of the copper grid, in order to obtain maximum magnetic field. A thickness of 1 to 2 mm (roughly) increased the magnetic field from 0.525 to 0.68 Tesla. Thus, a more accurate experimental set-up is needed to find the optimum thickness of the grid.

## **7.3 SEM study of the ball's surface after each polishing stage or polishing condition**

A preliminary SEM study of the ball's surface at roughing stage with and without groove formed on the bevel of the polishing cup using boron carbide abrasives (500 grit) was conducted. Interesting features were found. Thus, it is worth to conduct a thoroughly study, in order to understand the polishing mechanism of MFP process.

## References

- ASTM F 2094-03, "Standard specification for silicon nitride bearing balls," Annual Book of ASTM Standards, 01.08 (2004) 497-504.
- Akazawa, M., Kato, K. and Umeya, K., "Wear properties of silicon nitride in rolling contact," *Wear* 110 (1986) 285-293.
- Baghavatula, R. S. and Komanduri, R. "On chemomechanical polishing of  $\text{Si}_3\text{N}_4$  with  $\text{Cr}_2\text{O}_3$ ," *Philosophical Magazine A*, 74 (1996) 1003-1017.
- Bengisu, M., "Engineering ceramics," Springer, New York (2001).
- Budinski, K. G. and Budinski, M. K., "Engineering materials – Properties and selection," Prentice Hall, 7<sup>th</sup> Edition, New Jersey (2002).
- Chiang, Y. M., Birnie, D. and Kingery, W. D., "Physical ceramics – Principles for ceramic science and engineering," John Wiley & Sons, Inc., New York (1997).
- Childs, T. H. C., Jone, D. A., Mahmood, S., Kato, K., Zhang, B., and Umehara, N., "Magnetic fluid grinding mechanics," *Wear* 175 (1994) 189-198.
- Childs, T. H. C., Mahmood, S., and Yoon H. J., "The material removal mechanism in magnetic fluid grinding of ceramic ball bearings," *Proceedings of the I. Mech. E Part B*, London, 208 (1994) 47-59.
- Childs, T. H. C., Mahmood, S. and Yoon, H. J., "Magnetic fluid grinding of ceramic balls," *Tribology International*, 28 (1995) 341-348.

- Hou, Z. B. and Komanduri, R., "Magnetic field assisted finishing of ceramics – Part I: Thermal model," Transaction of the ASME, Journal of Tribology, 120 (1998) 645-651.
- Hou, Z. B. and Komanduri, R., "Magnetic field assisted finishing of ceramics – Part II: On the thermal aspects of magnetic float polishing (MFP) of ceramics balls," Transaction of the ASME, Journal of Tribology, 120 (1998) 652-659.
- Hou, Z. B. and Komanduri, R., "Magnetic field assisted finishing of ceramics – Part III: On the thermal aspects of magnetic abrasive finishing (MAF) of ceramics rollers," Transaction of the ASME, Journal of Tribology, 120 (1998) 660-667.
- Jiang, M. and Komanduri, R., "Application of taguchi method for optimization of finishing conditions in magnetic float polishing (MFP)," Wear 213 (1997) 59-71.
- Jiang, M. and Komanduri, R., "On the finishing of  $\text{Si}_3\text{N}_4$  balls for bearing applications," Wear 215 (1998) 267-278.
- Jiang, M., Wood N. O. and Komanduri, R., "On the chemo-mechanical polishing (CMP) of  $\text{Si}_3\text{N}_4$  bearing balls with water based  $\text{CeO}_2$  slurry," Trans of the ASME, Journal of Engineering Materials and Technology 120 (1998) 304-312.
- Jiang, M., Wood N. O. and Komanduri, R., "On chemo-mechanical polishing (CMP) of silicon nitride  $\text{Si}_3\text{N}_4$  workmaterial with various abrasives," Wear 220 (1998) 59-71.

- Jiang, M., "Finishing of advanced ceramic balls for bearing applications by magnetic float polishing (MFP) involving fine polishing followed by chemo-mechanical polishing (CMP)," Ph.D. Thesis, Oklahoma State University (1998).
- Kato, K., "Tribology of ceramics," *Wear* 136 (1990) 117-133.
- Kirtane T. S., "Finishing of silicon nitride ( $\text{Si}_3\text{N}_4$ ) balls for advanced bearing applications by large batch magnetic float polishing (MFP) apparatus," M.S. Thesis, Mechanical & Aerospace Engineering, Oklahoma State University (2004).
- Komanduri, R. and Jiang, M., "Magnetic float polishing processes and materials therefore," US Patent No. 5931718 (1999).
- Komanduri, R. and Jiang, M., "Magnetic float polishing of magnetic materials," US Patent No. 5957753 (1999).
- Komanduri, R., Umehara, N. and Raghunandan, M., "On the possibility of chemo-mechanical action in magnetic float polishing of silicon nitride," *Transaction of the ASME, Journal of Tribology*, 118 (1996) 721-727.
- Komanduri, R., Hou, Z. B., Umehara, N., Raghunandan, M., Jiang, M., Bhagavatula, S. R., Noori-Khajavi, A. and Wood, N. O., "A 'Gentle' method for finishing  $\text{Si}_3\text{N}_4$  balls for hybrid bearing applications," *Tribology Letters*, 7 (1999) 39-49.
- Lee, W. E. and Rainforth, W. M., "Ceramic microstructures – Property control by processing," Chapman & Hall, 1<sup>st</sup> Edition, New York (1994).

- Raghunandan, M., "Magnetic float polishing of silicon nitride balls," Ph.D. Thesis, Mechanical & Aerospace Engineering, Oklahoma State University (1997).
- Raghunandan, M. and Komanduri, R., "Finishing of silicon nitride balls for high-speed bearing applications," Transaction of the ASME, Journal of Manufacturing Science and Engineering, 120 (1998) 376-386.
- Rao, S.R., "Finishing of ceramic balls by magnetic float polishing with online vibration monitoring and control," M.S. Thesis, Mechanical & Aerospace engineering, Oklahoma State University (1999).
- Rosensweig, R. E., "Ferrohydrodynamics," Cambridge University Press, New York (1985).
- Saito, S., "Advanced ceramics," Oxford University Press, Great Britain (1988).
- Tani, Y. and Kawata, K., "Development of high-efficient fine finishing process using magnetic fluid," Annals of the CIRP, 33 (1984) 217-220.
- Umehara, N. and Kato, K., "Hydro-magnetic grinding properties of magnetic fluid containing grains at high speeds," Journal of Magnetism and Magnetic Materials, 65 (1987) 397-400.
- Umehara, N. and Kato, K., "Principles of magnetic fluid grinding of ceramic balls," Applied Electromagnetics in Materials, 1 (1990) 37-43.
- Umehara, N. Hayashi, T. and Kato, K., "In situ observation of the behavior of abrasives in magnetic fluid grinding," Journal of Magnetism and Magnetic Materials, 149 (1995) 181-184.
- Umehara, N. and Kato, K., "Magnetic fluid grinding of advanced ceramic balls," Wear, 200 (1996) 148-153.

Umehara, N. and Komanduri, R., "Magnetic fluid grinding of HIP-Si<sub>3</sub>N<sub>4</sub> rollers,"  
Wear, 196 (1996) 85-93.

# VITA

**Kok-Loong Lee**

**Candidate for the Degree of**

**Master of Science**

Thesis: INVESTIGATION OF "HIDDEN" POLISHING PARAMETERS IN  
MAGNETIC FLOAT POLISHING (MFP) OF SILICON NITRIDE ( $\text{Si}_3\text{N}_4$ )  
BALLS

Major Field: Mechanical Engineering

Biographical:

Personal Data: Born in Kuala Pilah, Negeri Sembilam, Malaysia, on April 15, 1976, the son of Mr. Kim-Choy Lee and Mrs. Nyok-Lin Chong

Education: Received Bachelor of Engineering degree in Mechanical and Aerospace Engineering from Oklahoma State University, Stillwater, Oklahoma, in May 2000. Completed the requirements for the Master of Science degree with a major in Mechanical Engineering at Oklahoma State University, Stillwater, Oklahoma in May 2005

Experience:

- Graduate Research Assistant in Mechanical and Aerospace Engineering Department, Oklahoma State University, Stillwater, Oklahoma, August 2001 – May 2005.
- Mechanical Engineer in Sundowner Trailers, Inc., Coleman, Oklahoma, February 2001 – June 2001.
- Food Service in Wilham Dining, Oklahoma State University, Stillwater, January 1998 – May 2000.

Name: Kok-Loong Lee

Date of Degree: May, 2005

Institution: Oklahoma State University

Location: Stillwater, Oklahoma

Title of Study: INVESTIGATION OF "HIDDEN" POLISHING PARAMETERS IN  
MAGNETIC FLOAT POLISHING (MFP) OF SILICON NITRIDE  
( $\text{Si}_3\text{N}_4$ ) BALLS

Pages in Study: 95

Candidate for the Degree of Master of Science

Major Field: Mechanical Engineering

**Scope and Methodology of Study:** Magnetic float polishing (MFP) is well-known as the most efficient batch polishing process for finishing a batch (10 to 100 balls) of industrial standard silicon nitride ( $\text{Si}_3\text{N}_4$ ) bearing balls (Grade 10C) for hybrid bearing applications within 24 hours and low capital investment. This investigation was conducted to improve the MFP process through finding the "hidden" polishing parameters that also play an important role in MFP process. In order to reveal and identify the roles or effects of the "hidden" polishing parameters, original polishing apparatus is not adequate, a "Critical Polishing Condition" polishing apparatus was developed and different experimental approaches were investigated.

**Findings and Conclusions:** (1) Proper groove formed on the bevel of the polishing cup and maintaining it through the end of roughing stage and in semi-finishing stage results in significant improvement in the roundness and better control of MFP process, (2) Machining the groove (in final finishing stage) is necessary for obtaining superior surface finish, (3) Proper gap/spacing between the balls during polishing is essential for obtaining uniform roundness of a single ball and improving the average roundness of the balls further, (4) Study of prevention of magnetic fluid from evaporation or displacement during polishing was conducted and no sign of "dry-out" was found after an 8-hour of run. This investigation provides a better appreciation of the MFP process for finishing  $\text{Si}_3\text{N}_4$  balls. Also, by preventing loss of magnetic fluid, overall cost can be reduced and the process can competes with the conventional industrial lapping process.

ADVISOR'S APPROVAL: Dr. Ranga Komanduri